

Adaptive prognostics for remaining useful life of composite structures

Eleftheroglou, N.

DOI

[10.4233/uuid:538558fb-ac9a-414d-8a59-4b523d8ff74c](https://doi.org/10.4233/uuid:538558fb-ac9a-414d-8a59-4b523d8ff74c)

Publication date

2020

Document Version

Final published version

Citation (APA)

Eleftheroglou, N. (2020). *Adaptive prognostics for remaining useful life of composite structures*. [Dissertation (TU Delft), Delft University of Technology]. <https://doi.org/10.4233/uuid:538558fb-ac9a-414d-8a59-4b523d8ff74c>

Important note

To cite this publication, please use the final published version (if applicable).
Please check the document version above.

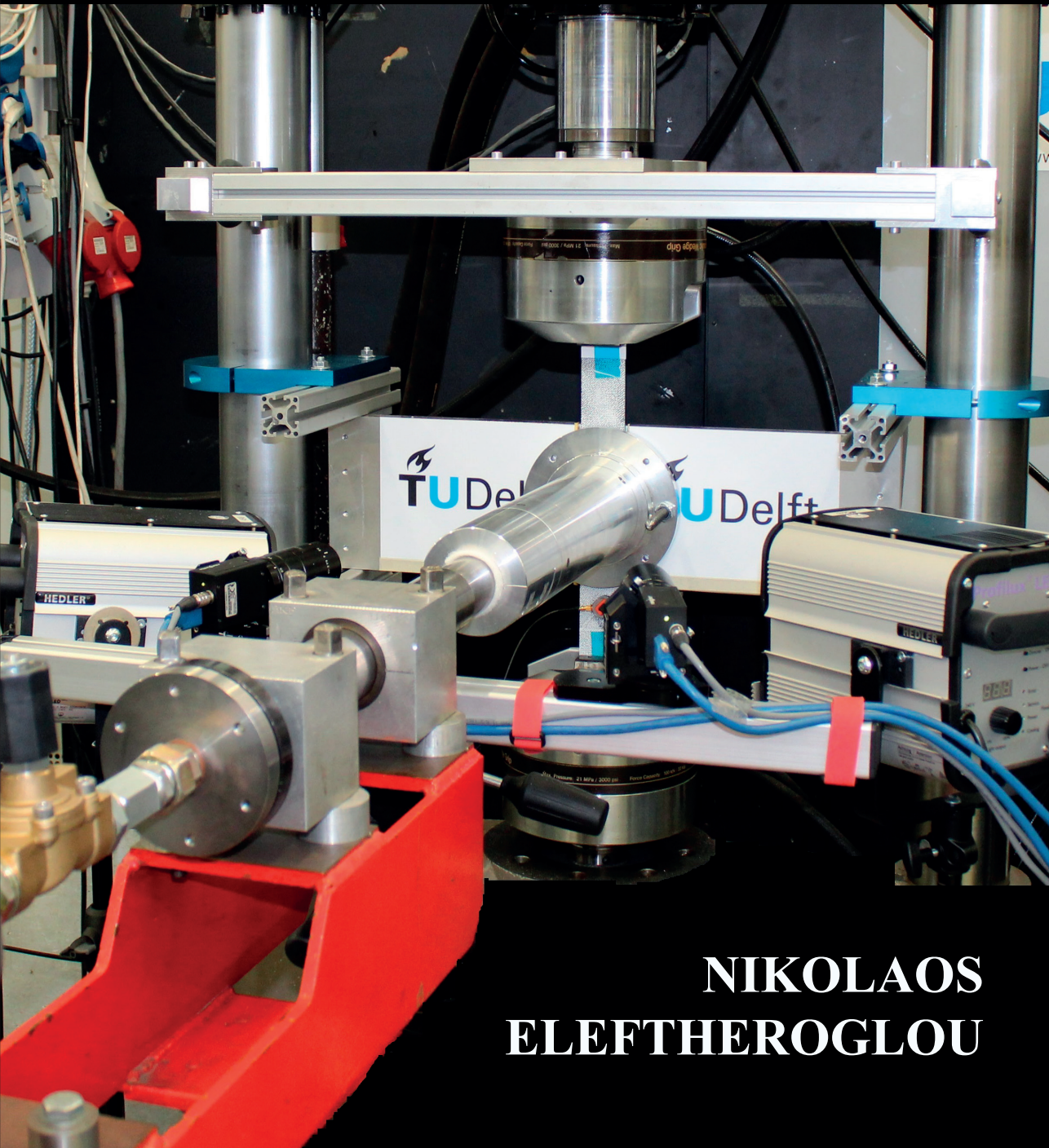
Copyright

Other than for strictly personal use, it is not permitted to download, forward or distribute the text or part of it, without the consent of the author(s) and/or copyright holder(s), unless the work is under an open content license such as Creative Commons.

Takedown policy

Please contact us and provide details if you believe this document breaches copyrights.
We will remove access to the work immediately and investigate your claim.

ADAPTIVE PROGNOSTICS FOR REMAINING USEFUL LIFE OF COMPOSITE STRUCTURES



**NIKOLAOS
ELEFTHEROGLOU**

ADAPTIVE PROGNOSTICS FOR REMAINING USEFUL
LIFE OF COMPOSITE STRUCTURES

ADAPTIVE PROGNOSTICS FOR REMAINING USEFUL LIFE OF COMPOSITE STRUCTURES

Dissertation

for the purpose of obtaining the degree of doctor
at Delft University of Technology,
by the authority of the Rector Magnificus Prof. dr. ir. T.H.J.J. van der Hagen,
chair of the Board of Doctorates,
to be defended publicly on
Monday, 12th October 2020 at 15:00 o'clock

by

Nikolaos ELEFTHEROGLOU

Diploma in Mechanical Engineering and Aeronautics
Department of Mechanical Engineering and Aeronautics
School of Engineering, University of Patras, Greece
born in Amarousio, Greece

This dissertation has been approved by the promotor.

Composition of the doctoral committee:

Rector Magnificus	Chairman
Prof. dr. ir. R. Benedictus	Delft University of Technology, promotor
Dr. D. Zarouchas	Delft University of Technology, copromotor
Prof. dr. T.H. Loutas	University of Patras, Greece

Independent members:

Prof. dr. ir. G. Jongbloed	Delft University of Technology
Prof. dr. M. Meo	University of Bath, United Kingdom
Prof. dr. E. Chatzi	Eidgenössische Technische Hochschule Zürich, Switzerland
Prof. dr. C. Sbarufatti	Politecnico di Milano, Italy
Prof. dr. ir. C.J. Simao Ferreira	Delft University of Technology, reserve member



Keywords: structural health monitoring, prognostics, remaining useful life, outlier analysis, adaptive prognostics, data-driven model, condition monitoring

Printed by: Ipskamp Printing (www.ipskampprinting.nl)

Front and back covers: Experimental set-up and prognostic results.

Copyright © 2020 by N. Eleftheroglou

All rights reserved. No part of this publication may be reproduced, stored in a retrieval system or transmitted in any form or by any means, electronic, mechanical, photocopying, recording or otherwise, without the prior written permission of the author.

This research was supported by the Department of Aerospace Structures & Materials of the Aerospace Engineering Faculty, Delft University of Technology.

ISBN 978-94-028-2151-2

An electronic version of this dissertation is available at
<http://repository.tudelft.nl/>.

*In memory of my uncle,
Dimitrios Lafatas.*

Summary

Prognostics is an emerging field of research that enables the real-time health assessment of an engineering system and the prediction of its future state based on up-to-date information. This field integrates various scientific disciplines including physics/mechanics, computational statistics and probabilistic modeling, machine learning and sensing technologies. The main goal is the prediction of the remaining useful life (RUL) of the engineering system while it is in-service. Lately, there is an effort to study and predict the future status of engineering systems that exhibit a complex degradation process. The availability of condition monitoring (CM) data, the constantly increasing computational power, the development of machine learning algorithms and the advancements on the physics/mechanics for several engineering systems form a solid foundation to achieve that goal.

Among the engineering systems that exhibit a complex degradation process are composite structures. Composite structures have made a significant mark in numerous industries, driven by advantages in structural efficiency, performance, versatility and cost.

It is well known that the damage accumulation process of composite structures depends on several parameters, i.e. the type of material and the lay-up, the loading frequency and sequence, the manufacturing process. Additionally, the multi-phase nature of composites and the variation of defects result in a stochastic activation of the different failure mechanisms. So, one expects that the long-term behaviour of two comparable composites structures, subjected to comparable environmental and loading conditions, will differ and that makes the fatigue damage analysis, and consequently the prediction of RUL, very complex tasks. This difference is profound especially when unexpected phenomena may occur.

The goal of this research is to develop a new RUL prediction model that is able to learn from unexpected phenomena and adapt its parameters accordingly. The model is composed of three elements; 1) sensing techniques to acquire online CM data, 2) machine learning algorithm for developing a damage modelling strategy and 3) stochastic modelling for uncertainty quantification.

Based on the literature review, it was concluded that a frequentist data-driven model has the potential to fulfil the research goal and an extension of the Non-Homogenous Hidden Semi Markov model (NHHSMM) is a good candidate. The first step was to design the structure of the RUL prediction model and define its elements. The next step was to develop the extension of the NHHSMM, and verify its correctness and robustness, utilizing simulated Monte-Carlo (MC) data. A series of assumptions was necessary in order to frame the applicability of the model towards composite structures and to achieve an efficient prediction process.

Finally, the last step was the demonstration of the efficiency and robustness of the developed methodology. Given the fact that the research presented in this thesis took place at the Structural Integrity & Composites Group of the Aerospace Engineering Faculty, unidirectional carbon fibre preregs, commonly used in aerospace industry, were utilized. Open-hole specimens were subjected to constant amplitude fatigue loading up to failure while in-situ impact and manufacturing imperfections were used so as to demonstrate unexpected phenomena. Acoustic emission and digital image correlation techniques were employed in order to collect CM data which were used for the training and testing processes. In addition, a new data fusion methodology, on a feature-level, was presented utilizing the available CM data. Eight specimens were used for the training process and they were subjected only to fatigue loading. Four specimens were used for testing the proposed adaptive model. Three of them were subjected to fatigue and in-situ impact, and created a left, a right outlier and an inlier performer respectively to the training specimens. The last one was subjected just to fatigue loading but created one more left outlier case since it had a manufacturing imperfection. Furthermore, five prognostic performance metrics, found in literature, were employed and two new were introduced, in order to compare the performance of the RUL predictions and it was found that the Adaptive Non-Homogenous Hidden Semi Markov model (ANHHSMM) provides better prognostics, indicating that this model has the potential to predict more accurately the RUL of outlier and inlier cases.

In conclusion, this thesis has addressed important challenges and limitations of the current prognostic models and it provides a solid base for further extensions towards a global version of a real-time adaptive data-driven model.

Samenvatting

Prognostiek is een opkomend onderzoeksveld dat het real-time bepalen van de gezondheid van een technisch systeem mogelijk maakt, alsmede het voorspellen van zijn toekomstige staat, gebaseerd op actuele informatie. Dit veld integreert verschillende wetenschappelijke disciplines, waaronder fysica/mechanica, computerstatistiek en probabilistisch modelleren, machine learning, en sensortechnieken. Het hoofddoel is het voorspellen van het resterende nuttig leven (RNL) van het technisch systeem terwijl het in gebruik is. Recent is er een inspanning in het bestuderen en voorspellen van de toekomstige staat van technische systemen die een complex degradatieproces vertonen. De beschikbaarheid van conditie monitoring (CM) data, de constant toenemende computerkracht, de ontwikkeling van machine learning algoritmes en de voortgang in de fysica/mechanica van een aantal technische systemen vormen een solide basis om dit doel te bereiken.

Onder de technische systemen die een complex degradatieproces vertonen bevinden zich composietconstructies. Composietconstructies hebben een grote stempel gedrukt op vele industrieën, gedreven door voordelen wat betreft constructieve efficiëntie, prestaties, veelzijdigheid en kosten.

Het is algemeen bekend dat het schade-accumulatieproces van composietstructuren van verschillende parameters afhangt, nl: het type materiaal en de oplegging, de belastingsfrequentie en volgorde, en het fabricageproces. Bovendien leidt de multi-fase natuur van composieten en de variatie in defecten tot een stochastische activering van de verschillende faalmechanismen. Men verwacht dus dat het lange termijn gedrag van twee vergelijkbare composietconstructies die worden blootgesteld aan vergelijkbare omgevingsinvloeden en belastingen, zal verschillen. Dit maakt de analyse van de vermoeiingsschade en derhalve de voorspelling van het RNL erg complexe taken. Het verschil in gedrag is in het bijzonder groot als onverwachte fenomenen zich kunnen voordoen.

Het doel van dit onderzoek is het ontwikkelen van een nieuw RNL voorspellingsmodel dat kan leren van onverwachte fenomenen en zijn parameters dienovereenkomstig kan aanpassen. Het model bestaat uit drie elementen: 1) sensortechnieken om online CM data te verzamelen, 2) machine learning algoritme voor het ontwikkelen van een schademodeleringsstrategie en 3) stochastisch modelleren voor getalsmatige bepaling van onzekerheid.

Gebaseerd op het literatuuronderzoek, werd geconcludeerd dat een frequentistisch data-gedreven model de potentie heeft om het onderzoeksdoel te vervullen en een uitbreiding van het Niet-Homogene Verborgene Semi Markov model (NHVSMM) een goede kandidaat is. De eerste stap was het ontwerpen van de structuur van het RNL voorspellingsmodel en het definiëren van zijn elementen. De volgende stap was het ontwikkelen van de uitbreiding van het NHVSMM en verifiëren van zijn juistheid en robuustheid, gebruikmakend van gesimuleerde Monte-Carlo (MC) data. Een serie aannames was nodig om de toepasbaarheid van het model richting composietstructuren te kaderen en om een efficiënt voorspellingsproces te verkrijgen.

Ten slotte was de laatste stap het demonstreren van de efficiëntie en robuustheid van de ontwikkelde methodologie. Gegeven het feit dat het onderzoek dat in dit proefschrift wordt gepresenteerd plaatsvond bij de Structural Integrity & Composites leerstoel van de Faculteit Luchtvaart & Ruimtevaarttechniek, werd gebruik gemaakt van unidirectionele koolstofvezel prepregs, die algemeen gebruikt worden in de luchtvaartindustrie. Open-gat proefstukken werden onderworpen aan vermoeiingsbelasting met constante amplitude tot aan falen, terwijl in-situ inslag en fabricage-imperfecties werden gebruikt om onverwachte fenomenen te demonstreren. Akoestische emissie en digitale beeldcorrelatie technieken werden ingezet om CM data te verzamelen, die werden gebruikt voor trainings- en testprocessen. Bovendien werd een nieuwe datafusie methodologie op een kenmerkniveau gepresenteerd, gebruikmakende van de beschikbare CM data. Acht proefstukken werden gebruikt voor het trainingsproces en zij werden alleen onderworpen aan vermoeiingsbelasting. Vier proefstukken werden gebruikt voor het testen van het voorgestelde alternatieve model. Drie ervan werden onderworpen aan vermoeiing en in-situ inslag, en creëerden zo een linker- en rechter-uitschieter en een ingesloten prestatie in vergelijking tot de trainingsproefstukken. Het laatste proefstuk werd alleen onderworpen aan vermoeiingsbelasting maar vormde nog een linker-uitschieter aangezien het een fabricage-imperfectie bevatte. Verder werden vijf prognostische prestatie-eenheden uit de literatuur ingezet en werden er twee nieuwe geïntroduceerd, om de prestaties van de RNL voorspellingen te vergelijken. Er werd gevonden dat het aangepaste NHVSMM betere prognostiek levert, wat aangeeft dat dit model de potentie heeft om nauwkeuriger de RNL te voorspellen van zowel ingesloten casussen, als van uitschieters.

Concluderend; dit proefschrift heeft belangrijke uitdagingen en beperkingen van de huidige prognostische modellen aangepakt en levert een solide basis voor verdere uitbreidingen naar het doel van een allesomvattende versie van een real-time adaptief datagedreven model.

Ithaka

*As you set out for Ithaka
hope your road is a long one,
full of adventure, full of discovery.
Laistrygonians, Cyclops,
angry Poseidon—don't be afraid of them:
you'll never find things like that on your way
as long as you keep your thoughts raised high,
as long as a rare excitement
stirs your spirit and your body.
Laistrygonians, Cyclops,
wild Poseidon—you won't encounter them
unless you bring them along inside your soul,
unless your soul sets them up in front of you.*

*Keep Ithaka always in your mind.
Arriving there is what you're destined for.
But don't hurry the journey at all.
Better if it lasts for years,
so you're old by the time you reach the island,
wealthy with all you've gained on the way,
not expecting Ithaka to make you rich.*

*Ithaka gave you the marvelous journey.
Without her you wouldn't have set out.
She has nothing left to give you now.*

*And if you find her poor, Ithaka won't have fooled you.
Wise as you will have become, so full of experience,
you'll have understood by then what these Ithakas mean.*

*BY C.P. CAVAFY
Translated by Edmund Keeley*

Contents

Summary.....	vii
Samenvatting.....	ix
Contents	xiii
Nomenclature	xv
List of figures.....	xix
List of tables.....	xxiii
1 Introduction.....	1
1.1. Prognostics: The science of prediction	2
1.2. Research Goal and Scope	3
1.3. Thesis Outline.....	4
References	4
2 Literature review.....	5
2.1. Introduction	6
2.2. Fatigue damage accumulation of composite structures	6
2.3. RUL taxonomies.....	7
2.4. RUL prediction models for composite structures	12
2.5. Adaptive methodologies	16
2.6. Conclusions	18
References	19
3 Methodology	23
3.1. Introduction	24
3.2. Training process	24
3.3. Testing process	29
References	32
4 Adapted RUL prediction model.....	35
4.1. Introduction	36
4.2. Non-Homogeneous Hidden Semi Markov model.....	36
4.3. Diagnostics	39
4.4. Adaptation process	40
4.5. Prognostics	42
References	44
5 Verification process.....	45
5.1. Introduction	46

5.2.	Monte-Carlo inputs	46
5.3.	Simulated MC data Generation	47
5.4.	Parameter estimation process	51
5.5.	Adaptation process	52
5.6.	Prognostics verification	54
5.7.	Conclusions	56
	References	56
6	Experimental campaign.....	57
6.1.	Introduction	58
6.2.	Experimental set-up and material	58
6.3.	Feature extraction process	63
	References	74
7	Validation Process.....	77
7.1.	Introduction	78
7.2.	Parameter estimation process	78
7.3.	Adaptation process	82
7.4.	Validation of the adaptive model	86
7.5.	Prognostic performance metrics	89
	References	93
8	Conclusions and Recommendations	95
8.1.	Introduction	96
8.2.	Conclusions	96
8.3.	Recommendations	98
	Acknowledgments	101
	Curriculum Vitae.....	103
	List of publications	105

Nomenclature

Symbols

a_{ij}	Constant coefficients of data-fusion function
$b_j(k)$	The emission probability of observing the k th value of the condition monitoring data when the device is in hidden state j
D	Total number of condition monitoring samples till failure
E	Impact's energy
f	Frequency of fatigue loading
f_t	Data-fusion output at time point t
K	Number of available training engineering systems
\mathbf{M}	Complete model ($\mathbf{M}=\{\zeta, \boldsymbol{\theta}\}$)
\mathbf{M}^*	Estimated complete model ($\mathbf{M}=\{\zeta, \boldsymbol{\theta}^*\}$)
\mathbf{M}^{**}	Adapted complete model ($\mathbf{M}=\{\zeta, \boldsymbol{\theta}^{**}\}$)
N	Number of hidden states
Q_t	system's hidden state at time point t
R	Ratio of fatigue loading
T_i	Time point of the i th transition
t_i	Time of the i th sample
V	Number of discrete monitoring values
X_i	Hidden state of the system after the i th transition
$y^{(k)}$	Degradation condition monitoring sequence of the k th engineering system
$y(t_i)$	Discrete condition monitoring value at the t_i time point
Z	Discrete condition monitoring space
z_k	the state of the engineering system at time point k
$\alpha(i,j)$	Weibull scale parameters
\mathbf{B}	The set of characteristic parameters associated with the observation process
\mathbf{B}^*	The estimated set of characteristic parameters associated with the observation process
\mathbf{B}^{**}	The adapted set of characteristic parameters associated with the observation process
$\beta(i,j)$	Weibull shape parameters
$\boldsymbol{\Gamma}$	The set of characteristic parameters associated with the degradation process
$\boldsymbol{\Gamma}^*$	The estimated set of characteristic parameters associated with the degradation process
$\boldsymbol{\Gamma}^{**}$	The adapted set of characteristic parameters associated with the degradation process
ζ	Initialization topology ($\zeta=\{N, \Omega, \lambda, V\}$)
$\boldsymbol{\theta}$	Unknown parameters that characterize the degradation process ($\boldsymbol{\theta}=\{\boldsymbol{\Gamma}, \mathbf{B}\}$)
$\boldsymbol{\theta}^*$	Estimated parameters ($\boldsymbol{\theta}^*=\{\boldsymbol{\Gamma}^*, \mathbf{B}^*\}$)
$\boldsymbol{\theta}^{**}$	Adapted parameters ($\boldsymbol{\theta}^{**}=\{\boldsymbol{\Gamma}^{**}, \mathbf{B}^{**}\}$)
λ	Statistical form of transition rate functions
σ_{\max}	Maximum fatigue loading
σ_{\min}	Minimum fatigue loading
Ω	Connectivity between hidden states

Subscripts

arg	Argument
max	Maximum
min	Minimum
std	Standard deviation

Abbreviations

AE	Acoustic Emission
AI	Artificial Intelligence
ANHHSM	Adaptive Non-Homogenous Hidden Semi Markov model
ARMA	Autoregressive Moving Average model
BIC	Bayesian Information Criterion
BNN	Bayesian Neural Network
BVID	Barely Visible Impact Damage
CBM	Condition Based Maintenance
CDF	Cumulative Distribution Function
CDS	Characteristic Damage State
C _{EM}	Convergence
CFRP	Carbon Fiber Reinforced Polymer
CIDC	Confidence Intervals Distance Convergence
CM	Condition Monitoring
CRA	Cumulative Relative Accuracy
DDM	Data-Driven Model
DIC	Digital Image Correlation
DM	Dynamic Modelling
EM	Expectation Maximization
GBT	Gradient Boosted Tree
HMM	Hidden Markov Model
HM	Hybrid Model
HSMM	Hidden Semi Markov Model
LCI	Lower Confidence Interval
MAPE	Mean Absolute Percentage Error
MBM	Model-Based Model
MC	Monte Carlo
MK	Mann-Kendall
MLE	Maximum Likelihood Estimator
MLS	Most Likely State
MMK	Modified Mann-Kendall
MSE	Mean Squared Error
NHSM	Non-Homogeneous Hidden Semi Markov Model
OQNLP	OptQuest/NLP
PCA	Principal Component Analysis
PDF	Probability Density Function

PSO	Particle Swarm Optimization
RA	Rise time/Amplitude
RBFNN	Radial Basis Function Neural Network
RUL	Remaining Useful Life
SHM	Structural Health Monitoring
SM	Static Modelling
UCI	Upper Confidence Interval

List of figures

Figure 2.1	Damage accumulation process during a composite structure's lifetime.	7
Figure 2.2	Schwabacher and Goebel 's taxonomy of prognostic models.	8
Figure 2.3	Sirkorska et al.'s taxonomy of prognostics algorithms.	8
Figure 2.4	Maio and Zio's taxonomy of prognostics algorithms.	9
Figure 2.5	Byington et al's taxonomy of prognostics algorithms.	9
Figure 2.6	Suggested taxonomy of RUL prediction models.	10
Figure 2.7	Sources of uncertainty in engineering systems.	12
Figure 3.1	RUL adaptive methodology.	25
Figure 3.2	Validation of Confidence Intervals Distance Convergence metric a) Hypothetical sets of confidence intervals b) Mass centers under the confidence intervals distance curves.	31
Figure 4.1	Soft (I), hard (II) and multistep (III) types of transition.	38
Figure 4.2	Sojourn times per hidden state based on the NHHSMM Γ^* parameters.	41
Figure 4.3	Sojourn times per hidden state based on the MLS diagnostic measure when the studied engineering system just transited from the hidden state i to $i+1$.	41
Figure 4.4	Dynamic adaptation process flowchart.	43
Figure 5.1	MC observation sequence.	49
Figure 5.2	Right outlier's observation (blue) and degradation (red) processes.	50
Figure 5.3	Left outlier's observation (blue) and degradation (red) processes.	50
Figure 5.4	Inlier's observation (blue) and degradation (red) processes.	50
Figure 5.5	MLS diagnostic estimations of left outlier's case.	52
Figure 5.6	Sojourn time Weibull distributions utilizing the Γ^* and Γ^{**} parameters of left outlier's case.	53
Figure 5.7	Sojourn time Weibull distributions utilizing the Γ^* and Γ^{**} parameters of right outlier's case.	53
Figure 5.8	Sojourn time Weibull distributions utilizing the Γ^* and Γ^{**} parameters of inlier's case.	54
Figure 5.9	RUL predictions of the left outlier.	54
Figure 5.10	RUL predictions of the right outlier.	55
Figure 5.11	RUL predictions of the inlier.	55
Figure 6.1	The experimental set-up.	58
Figure 6.2	Picture of the impact canon.	59
Figure 6.3	DIC data acquisition strategy.	60

Figure 6.4	Tensile strengths of the three quasi-static specimens and their failure patterns.	61
Figure 6.5	Training and testing open-hole specimens.	62
Figure 6.6	Feature extraction process' inputs and outputs.	63
Figure 6.7	Cumulative AE energy observation histories.	64
Figure 6.8	Normalized cumulative AE energy observation histories.	65
Figure 6.9	MMK monotonicity index versus the number of states and clustering centers when V=10 and CM feature is the normalized cumulative energy acoustic emission feature.	66
Figure 6.10	Clustered AE degradation histories of training and testing open-hole specimens.	66
Figure 6.11	Axial strain distribution of specimen01 and its critical area.	67
Figure 6.12	Axial strain degradation histories of twelve open-hole specimens.	67
Figure 6.13	Axial strain degradation histories jumps due to impact loading.	68
Figure 6.14	MMK monotonicity index versus the number of states and clustering centers when V=10 and CM feature is the axial strain feature.	68
Figure 6.15	Clustered axial strain degradation histories of training and testing open-hole specimens.	69
Figure 6.16	Normalized cumulative axial strain observation histories.	69
Figure 6.17	Clustered cumulative normalized axial strain degradation histories of training and testing open-hole specimens.	70
Figure 6.18	MMK monotonicity index versus the number of states and clustering centers when V=10 and CM feature is the normalized cumulative axial strain feature.	70
Figure 6.19	Trendability index versus the fusion polynomial degree.	71
Figure 6.20	Fused degradation histories of twelve open-hole specimens.	73
Figure 6.21	MMK monotonicity index versus the number of states and clustering centers when V=10 and CM feature is the fused data.	73
Figure 6.22	Clustered fused degradation histories of training and testing open-hole specimens.	74
Figure 7.1	Content of Chapter 7.	79
Figure 7.2	BIC for the estimation of the number of hidden states N.	80
Figure 7.3	AE MLS diagnostic estimations of Specimen09-12.	83
Figure 7.4	DIC1 MLS diagnostic estimations of Specimen09-12.	83
Figure 7.5	DIC2 MLS diagnostic estimations of Specimen09-12.	84
Figure 7.6	AE sojourn time Weibull distributions utilizing the Γ^* and Γ^{**} parameters.	84
Figure 7.7	DIC1 sojourn time Weibull distributions utilizing the Γ^* and Γ^{**} parameters.	85
Figure 7.8	DIC2 sojourn time Weibull distributions utilizing the Γ^* and Γ^{**} parameters.	86
Figure 7.9	AE RUL predictions.	87
Figure 7.10	DIC1 RUL predictions.	87

Figure 7.11	DIC2 RUL predictions.	88
Figure 7.12	Precision prognostic performance metric of each specimen, feature and model.	89
Figure 7.13	MSE prognostic performance metric of each specimen, feature and model.	90
Figure 7.14	Zoomed MSE prognostic performance metric of each specimen, feature and model.	90
Figure 7.15	MAPE prognostic performance metric of each specimen, feature and model.	91
Figure 7.16	CRA prognostic performance metric of each specimen, feature and model.	91
Figure 7.17	Monotonicity prognostic performance metric of each specimen, feature and model.	92
Figure 7.18	C_{EM} prognostic performance metric of each specimen, feature and model.	92
Figure 7.19	CIDC prognostic performance metric of each specimen, feature and model.	93

List of tables

Table 5.1	Lifetimes of training MC systems.	49
Table 5.2	Comparison between MC and NHHMM Weibull (Γ) parameters.	51
Table 5.3	Comparison between MC and NHHMM emission matrix (\mathbf{B}) parameters.	51
Table 6.1	Fatigue lifetime and impact times of training and testing specimens.	62
Table 6.2	Optimization results for M=7.	72
Table 6.3	Comparison between DIC2, AE and fusion trendability index.	74
Table 7.1	NHHMM Weibull (Γ^*) parameters.	81
Table 7.2	NHHMM emission matrix (\mathbf{B}^*) parameters.	82
Table 7.3	Comparison between transition time points from hidden state 1 to hidden state 2 with impact time points.	82
Table 7.4	Optimum values of the suggested prognostic performance metrics.	89

1

Introduction

1.1. Prognostics: The science of prediction

Prognosis (Greek: Πρόγνωση) is originally a Greek word, which means to know in advance, to foresee. In the period of the 7th century to the 4th century BC, people all over the known-world would visit the temple of Apollo in Delphi Greece, to consult the Oracle (Greek: Πυθία) for personal matters. The Oracle in a state of awareness and inspiration would provide an enigmatic prophecy letting people take the final decision by themselves. This decision-making process was performed using the information provided by the Oracle. Over the centuries the mystic process of the prophecy became the science of prediction and nowadays it is an emerging research field, known as prognostics.

Prognostics enables the real-time health assessment of an engineering system and the prediction of its future state based on up-to-date information. This field integrates various scientific disciplines including physics/mechanics, computational statistics and probabilistic modeling, machine learning and sensing technologies. It is considered to be the key element for the realization of the condition based maintenance (CBM) (in some industries, i.e. wind energy CBM is referred as predictive maintenance), a practice that guides the engineers to repair or replace only the actual damaged parts of the system, aiming to reduce its maintenance costs and increase its availability. The idea behind the CBM is, by using autonomous software and hardware, to monitor the asset, detect and identify failures, assess its current health state and predict its future health state in order to make reliable decisions about its operation.

Prognostics, in the context of CBM, has been already explored in many engineering domains including aerospace, automotive, wind energy and naval. Each domain has its own specifics and needs and there is no common guideline how to practice CBM. For example, in aerospace industry, safety is the critical factor that determines the boundaries of CBM whereas in wind energy, the performance of a wind park (energy production/downtime) plays the key-role on the decision-making process.

Lately, there is an effort to study and predict the future status of engineering systems that exhibit complex degradation process. The availability of condition monitoring (CM) data, the constantly increasing computational power, the development of machine learning algorithms and the advancements on the physics/mechanics for several engineering systems form a solid foundation to achieve that goal.

Certainly, composite structures belong to this group of engineering systems with complex degradation process. Composite structures have made a significant mark in numerous industries, driven by advantages in structural efficiency, performance, versatility and cost. For example, in aerospace industry, they are used as primary structures (airwings, fuselage, etc.) in commercial aircraft such as Airbus A350 and Boeing 787, for which more than 50% of their structural weight made of composites. Despite the fact that aerospace industry promotes the use of composites, a comprehensive understanding of their long-term mechanical behaviour is missing and the existing design tools and prediction models are conservative and not robust. In order to manage the risk that comes with this deficiency in understanding, large safety factors are applied in design. The overdesign due to these large safety factors reduces the potential efficiency of composite structures, particularly in terms of their weight.

Thus, there is an urgent need to strengthen our understanding of the damage progression process and to develop a reliable assessment of the current (diagnostics) and future health state (prognostics) of a composite structure.

The core business of structural prognostics is the prediction of the remaining useful life (RUL) of the structure while it is in-service. A RUL prediction model should be able to tackle a variety of uncertainties, given the stochastic nature of the damage accumulation process. Due to this stochastic nature, one expects that the long-term behaviour of two comparable structures subjected to comparable environmental and loading conditions will differ. This difference is profound especially when unexpected phenomena may occur. Manufacturing defects, foreign object impacts, extreme oscillations in the environment are among the events that can alter the damage accumulation process and thus the RUL significantly.

1.2. Research Goal and Scope

The goal of this research is to develop a new RUL prediction model that is able to learn from unexpected phenomena and adapt its parameters accordingly. The model will be composed of three elements: 1) sensing techniques to acquire online CM data, 2) machine learning algorithms for developing a damage modelling strategy and 3) stochastic modelling for uncertainty quantification. This new model targets engineering systems, which either underperformed or outperform, due to unexpected phenomena that might occur during their lifetime. The aim is to provide more accurate RUL predictions than the state-of-the-art RUL prediction models.

This thesis focuses on the fatigue life prognosis of aerospace composite structures, which face unexpected phenomena during their service. In order to accomplish the proposed prognostic model, emphasis is given in the following three research topics:

- feature extraction
- data fusion
- prognostic performance metrics.

It is expected that the results of this thesis will advance the field of prognostics and create a generic model that is able to take into account unexpected phenomena of uncertainty assuring reliability and robustness on its predictions. As already mentioned, the main application of this thesis is on aerospace composite structures where the actual degradation state is complex, not directly observable and several unexpected phenomena can occur during the structure's lifetime.

I believe that developing this RUL prediction model is top priority and I, as member of the engineering community working in the field of prognostics, will contribute to a faster realization of CBM in aerospace industry.

1.3. Thesis Outline

This thesis is composed of 8 chapters and here below an outline is provided:

- Chapter 2 reviews the available literature on the field of prognostics and examines whether the available adaptive models are applicable to the case of interest.
- In Chapter 3, a general methodology which includes the new adaptive RUL prediction model, is presented where emphasis is given into the process of training and testing.
- Chapter 4 provides the fundamentals of how to design a generic and flexible probabilistic model. This model is the successor of the Non-Homogeneous Hidden Semi Markov model (NHHSMM) developed by Moghaddass and Zuo [1]. The assumptions made in order to develop the adaptive edition of NHHSMM are discussed. This chapter is the fundamental chapter of this thesis and its equations are directly used in the rest of the thesis.
- In Chapter 5, simulation-based numerical data, utilizing the Monte Carlo (MC) simulation method, are used to verify the prognostics capabilities of the new adaptive RUL prediction model i.e. the Adaptive Non-Homogeneous Hidden Semi Markov model (ANHHSMM). The objective is to verify that the ANHHSMM is able to predict more accurately the RUL than the NHHSMM.
- Chapters 6 and 7 demonstrate the adaptive methodology by testing open-hole carbon reinforced polymer specimens. The training data set consists of CM data collected from specimens, which were subjected only to fatigue loading, while the testing data set consists of CM data collected from four specimens. Three of the testing specimens were subjected to fatigue and in-situ impact loading and the last one was subjected only to fatigue loading but this specimen has an artificial drilling defect on it. The objective of that chapter is to verify that the ANHHSMM is able to predict more accurately the RUL than the NHHSMM, when the testing composite specimens is an outlier, left or right, and to predict the RUL at least with the same level of accuracy when the composite specimen doesn't exhibit extreme behaviour. Furthermore, RUL predictions utilizing different kind of CM features are compared via established and newly proposed prognostic performance metrics.
- In Chapter 8 the results of the thesis are summarized, conclusions are drawn and new directions for future research are presented.

References

- [1] R. Moghaddass and M. J. Zuo, "An integrated framework for online diagnostic and prognostic health monitoring using a multistate deterioration process," *Reliab. Eng. Syst. Saf.*, vol. 124, pp. 92–104, 2014.

2

Literature review

2.1. Introduction

This chapter is devoted to reviewing four topics the literature related to prognostics:

- damage accumulation for composite structures
- prognostics taxonomies
- prognostics of composite structures
- adaptive prognostics

and it is organized as follows; Section 2.2 discusses the fatigue damage accumulation process of composite structures and motivates why this phenomenon has to be described in a stochastic way. Section 2.3 presents the available work on prognostic taxonomies and Section 2.4 the available prognostic studies in composite structures. Section 2.5 reviews adaptive prognostic approaches studies for any kind of engineering system. Finally, in Section 2.5, the literature gaps are identified and the thesis' contribution is formulated so as to fulfil these gaps.

2.2. Fatigue damage accumulation of composite structures

Fatigue of composite structures has been in the center of the research activities the last four decades, where the research community has tried to model the process of damage accumulation and develop predictive tools. Extensive experimental campaigns for different material types and lay-up configurations and a considerable number of models emerged from those activities and revealed that the fatigue damage process is a multistate degradation procedure where several damage mechanisms occur, interact, act synergistically, and lead the structure to final failure.

It is from the very early ages in composites research that researchers attempted to understand the way damage evolves and accumulates in a composite structure. The idea of the multistate process goes back to the 1980s, where Reifsnider et al. in [1] explained in a qualitative manner how damage and failure mechanisms may commence, interact and lead to the final failure. Reifsnider et al. described the damage accumulation as a three-stage process. Therefore, it is a multi-state degradation process which initiates with transverse matrix cracking in the most highly stressed/strained layers. Matrix cracks form, saturate at the Characteristic Damage State (CDS), propagate and coalesce to form early debondings and in very tough matrices lead to early fiber failures locally. Debondings and matrix cracks propagate to form delaminations in the interfaces between the layers whilst fiber bundles begin to fail more frequently accelerating the induced damage in the final stage of the material's service life up to the final macroscopic failure. It should be pointed out that this is a generic description and not a precise one, it is more a qualitative than a quantitative description. The precise damage accumulation sequence depends on the exact layup, the material properties of the composite's constituents, the defects induced during manufacturing, the loading profile, environmental conditions etc. Figure 2.1 summarizes the process of damage accumulation in composite structures under any type of service loading.

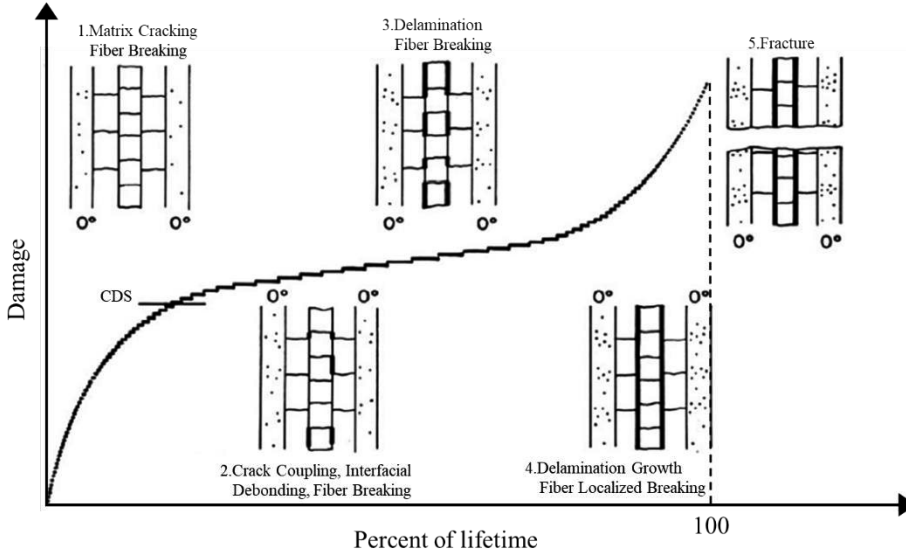


Figure 2.1. Damage accumulation process during a composite structure's lifetime [1].

Ever since, the researchers have focused on developing prediction models implementing phenomenological and progressive damage approaches [2-8]. However, only the progressive damage approaches consider to some extent the damage mechanisms. Despite the efforts and the progress made in the field, it was clear, rather early, that a universal model, which can cover all types of composite structures, lay-up configurations and loading scenarios is very difficult to be established. Additionally, the inhomogeneous nature of the composite material and the stochastic activation of different damage mechanisms should also be taken into account making the damage process a very complex phenomenon to study. When it comes to analyse their effect on the damage process and consequently on the RUL, all these parameters should be considered as uncertainties. Therefore, researchers have to develop approaches for quantifying the uncertainty associated with the RUL. RUL should be defined as a random variable and not as a deterministic value.

2.3. RUL taxonomies

Existing RUL models for quantifying uncertainty can be classified utilizing four different taxonomies found in the literature [9-12]. The taxonomies share common categories but their authors provide different and some cases conflicting definitions. For clarity, each category will be addressed separately when the taxonomy is presented.

Schwabacher and Goebel categorized RUL prediction models into two categories: model-based (MBMs) and data-driven models (DDMs) [9]. Figure 2.2 illustrates the break-down of these two models. According to the authors, MBMs encode human knowledge via a user defined representation of the engineering system. Such a model can be either physics-based or classical. A classical MBM is based on techniques from Artificial Intelligence (AI). DDMs fit a model to the system's behaviour based on the extracted historical data. DDMs can use either conventional algorithms, such as linear regression or Kalman filters, or

algorithms from the machine learning and data mining AI communities, such as neural networks, decision trees, and support vector machines. It is unclear in which category the AI methods belong because, based on the authors' definition, AI methods can be part both of model-based and data-driven prognostic models. In addition, this taxonomy of RUL prediction models excludes models that combine both model-based and data-driven models.

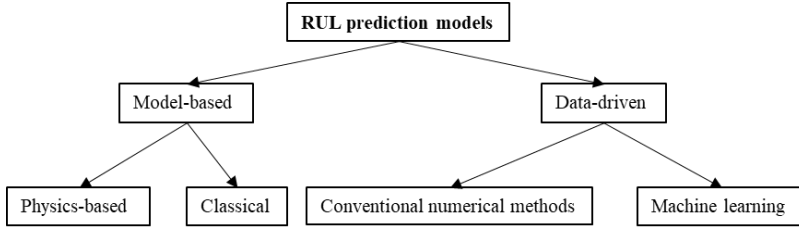


Figure 2.2. Schwabacher and Goebel's taxonomy of prognostic models.

Sikorska et al. proposed that RUL prediction models can be grouped into four categories: knowledge based models, life expectancy models, artificial neural networks and physical models, see Figure 2.3 [11]. Knowledge-based models assess the similarity between an observed situation and a databank of previously defined failures, and they deduce the life expectancy from previous events. Life expectancy models determine the life expectancy of individual machine components with respect to the expected risk of deterioration under known operating conditions. Artificial Neural Networks compute an estimated output for the RUL of a system via a mathematical representation of the studied system that has been derived from observation data rather than a physical understanding of the failure processes. Physical models compute an estimated output for the RUL of a system from a mathematical representation of the physical behaviour of the degradation processes. Based on these definitions it is really difficult to classify nowadays prognostic models since a significant proportion of them presented in the literature are actually a combination of two or more RUL prediction models.

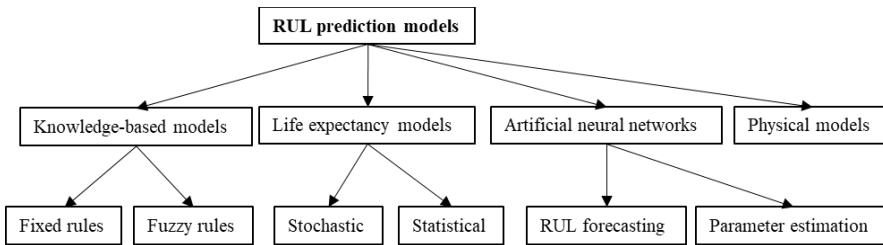


Figure 2.3. Sirkorska et al.'s taxonomy of prognostics algorithms.

Maio and Zio [10] proposed two categories: model-based and data-driven models, similar to Schwabacher and Goebel. MBMs attempt to set up physical models of the system for the prediction of the RUL. On the basis of these models, several approaches have been proposed in order to analyse reliability-based and condition-based maintenance approaches. DDMs utilize monitored operational data related to system's health. DDMs, based on the authors approach, can be divided to statistical techniques such as regression and Autoregressive Moving Average (ARMA) models and AI techniques e.g. neural networks, fuzzy systems and support vector machines. Figure 2.4 illustrates Maio and Zio's taxonomy. Similar to

Schwabacher and Goebel, this taxonomy is not able to categorize a model, which is a combination of MBMs and DDMs.

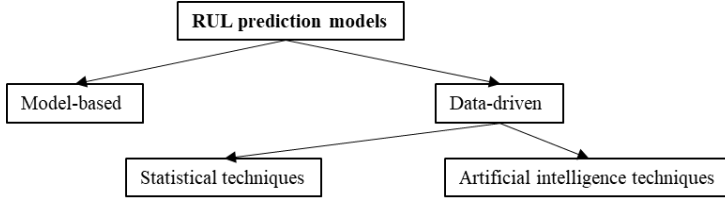
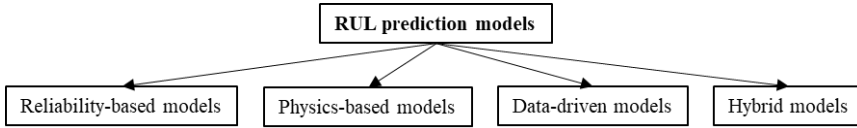


Figure 2.4. Maio and Zio's taxonomy of prognostics algorithms.

Finally, Byington et al [12] classified prognostic models into four categories: reliability based models, physics-based models, data-driven models and hybrid models. Figure 2.5 presents the four aforementioned categories. Byington et al mention that complexity, computational cost and accuracy of prognostic models are inversely proportional to its applicability since increasing RUL predictions' accuracy with low computational cost and complexity is an interesting but also big challenge.



2.5. Byington et al's taxonomy of prognostics algorithms.

The reliability based model is used mainly for uncritical, unmonitored engineering components/systems for which a physical model is not known. This model depends only on historical data derived from similar systems and their average rates of failure. Some characteristic reliability based models are the Weibull analysis, log-normal and Poisson laws. Physics-based models demand a physical model, which is defined as a mathematical representation of failure models and degradation phenomenon. In order to establish this model, a thorough understanding of the system's physics is required. In addition to knowledge of system's physics, knowledge about operation conditions e.g. environmental and loading conditions are required too. On the other hand, data-driven models don't require any kind of physical models because the main idea of these models is to use CM data so as to create a model that correlates these data to system degradation and then use this model for RUL predictions. Lastly, hybrid approaches are combining both data-driven and physics-based models together to get the best characteristics from each.

Byington's taxonomy is the most general one out of the four but none of them includes every trend and type of analysis found in the current literature. Thus, based on this thesis perspective, a new taxonomy is proposed hereafter, see Figure 2.6. This taxonomy consists of two main pillars: static modelling and dynamic modelling. The terms static and dynamic modelling are distinguished based on the availability of online CM data. Knowledge for damage accumulation regarding a specific engineering system can be gained from extracted online CM data. The online data exist only on the dynamic modelling pillar. Accordingly, in static modelling 'offline' data can be used. Offline data is defined as the data which is not extracted during the lifetime of the studied engineering system. These two pillars can be further categorized to DDMs, MBMs and hybrid models (HMs) and distinguish based on

the nature of the available data, online or offline. DDMs is the application of specific algorithms to extract patterns from system's degradation data. Characteristic examples of DDMs [13] are Kalman filters, particle filters, regression, statistical methods, artificial neural networks [14], Markov processes [15,16], support vector machines, Gaussian processes etc. MBMs use physics-based models of the studied system for the estimation of the RUL. It should be mentioned that the term physical models does not contain phenomenological or empirical models. These models can be categorized as DDMs. If the model that characterizes the studied system is a combination of a DDM and MBM then this model is defined as hybrid.

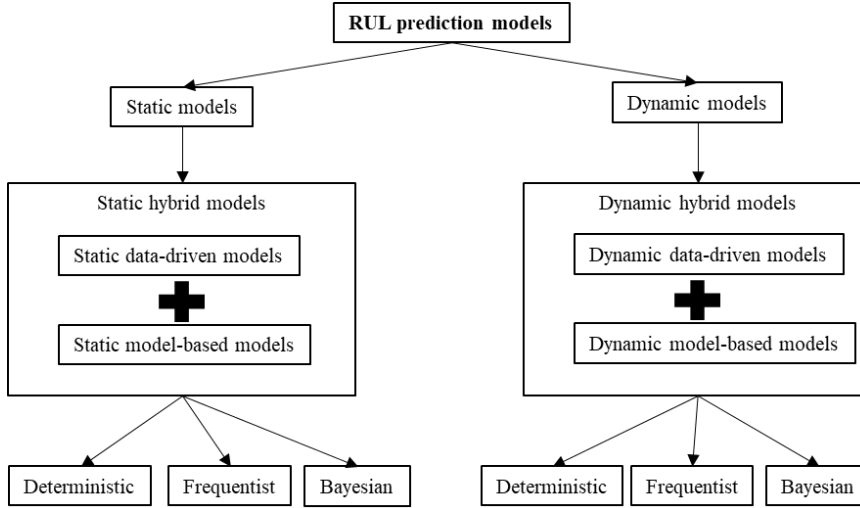


Figure 2.6. Suggested taxonomy of RUL prediction models.

Further, DDMs, MBMs and HMs can be Deterministic, Frequentist and Bayesian. Each transition, i.e. Deterministic to Frequentist and Frequentist to Bayesian, is possible allowing the models to enhance their capabilities regarding the uncertainty. A deterministic model will always produce the same output from a given starting condition or initial state. Therefore, a deterministic model can simulate efficiently only systems in which no uncertainties are involved in the development of future system's states. Frequentist model is based on the existence of inherent variability and is suitable only in the context of random experiments. Traditional statistical principles are primarily based on the concepts of frequentist probability. Bayesian model expresses the degree of the analyst's belief regarding a particular statement and can be assigned even in the absence of inherent variability. The principles of Bayesian statistics are based on the concept of subjective probability.

Since prognostics deal with the assessment of the future, it is important to understand that it is almost impossible to make precise predictions due to the various sources of uncertainty that the future contains. Some researchers have classified the different sources of uncertainty into different categories in order facilitate uncertainty quantification and management. While it has been customary to classify the different sources of uncertainty into physical variability and lack of knowledge, such a classification may not be suitable for CM purposes as mentioned in [17]. Sankararaman et al [17] proposed a completely different approach for

classification, particularly applicable to condition-based monitoring and is outlined hereafter:

- **Present uncertainty:** In order to be able to predict the RUL of an engineering system, CM data are needed, collected by using CM sensors. However, these sensors are engineering systems too and as a result they degrade simultaneously with the studied engineering system. Therefore, the quality of the extracted data is not constant during the degradation process of the studied engineering system since the sensor's noise level varies.
- **Future uncertainty:** The most important source of uncertainty in the context of prognostics is due to the fact that the future is unknown. For example, the operating and environmental conditions are not known precisely.
- **Modelling uncertainty:** As already mentioned it is necessary to use a RUL prediction model so as to estimate the future state behaviour of the studied engineering system. However, practically it is unrealistic to believe that it is possible to develop models which are able to accurately predict reality.
- **Prediction uncertainty:** Even if all the above sources of uncertainty can be quantified accurately, it is necessary to quantify their combined effect on the RUL prediction, and thereby, quantify the overall uncertainty in the RUL prediction. It may not be possible to do this accurately in practice and it may result to additional uncertainty.

However, this classification approach is not able to take into account sources of uncertainties which occurred in the past such as sources which are linked with the installation and manufacturing process of the engineering system or even with the material of the engineering system. Therefore, this thesis proposes to include to the above categories one more source of uncertainty; the past uncertainty. Figure 2.7 represents graphically all the aforementioned possible sources of uncertainty so as to clarify the necessity to compute the uncertainty associated with RUL.

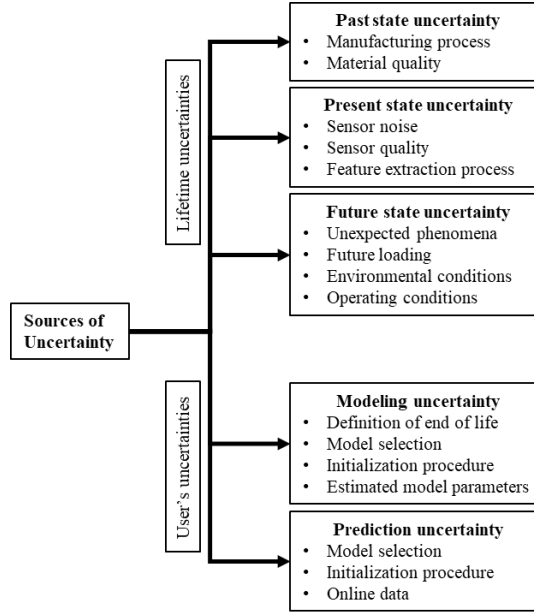


Figure 2.7. Sources of uncertainty in engineering systems.

2.4. RUL prediction models for composite structures

Most of the published work in the area of structural prognostics focuses on metallic components. In the area of composite structures, prognostics is a new dynamically rising field that has emerged the last decade. Although research has already been reported on damage diagnostics [18], that deals with damage detection, localization and quantification. However, limited published work is available regarding prognostics of composite structures. An argument is the complex degradation process of composite structures that makes difficult to find an appropriate RUL prediction model. Recently, some RUL prediction models have been applied to the prognosis of composite structures. Hereafter these prediction models are discussed following the proposed taxonomy.

2.4.1. Static modelling

Static modelling (SM) requires numerical and analytical models, extended experimental campaigns and critical understanding of the basic principles of the composite structure. SM doesn't use online data thus it is not possible to model past, present and future sources of uncertainty. As mentioned in Chapter 1 the ultimate goal of this research is to involve a new RUL prediction model that is capable of real-time learning and adapting its estimated parameters based on online CM data in order to be able to model as much sources of uncertainty as possible. SM fails to satisfy the requirements of real-time learning and adapting and consequently, it will not be considered further.

2.4.2. Dynamic modelling

Dynamic modelling (DM) requires the availability of online CM data. A network of sensors is permanently installed to the structure and it records periodically or continuously data during the in-service life of the structure. The data is associated then to the integrity of the structure and this process is known as structural health monitoring (SHM). It should be noted that the sensors measure the response of the structure to the loading and not directly the damage. Sensitive information is hidden within the data and feature extraction should be performed in order to relate the recordings to different damage states. As long as a correlation is achieved, then, by using appropriate models, prediction of the RUL can be performed. The main advantage of this method is that past, present and future state uncertainties can be taken into account as data collected from the structure of interest is directly used.

2.4.2.1. Online model-based models

MBMs require the existence of a physical model that describes the degradation process of composite structures. To establish a MBM, a thorough understanding of the damage accumulation phenomenon of a composite structure is required. However, physics-based models, showing satisfactory prediction capabilities, are still rather hard to find. Also, even if a physics-based model is obtained, it will be obtained for a specific case e.g. loading conditions, lay-up etc. and its reusability will be very limited to other similar cases. In summary, the research community has mainly descriptive knowledge regarding the damage accumulation in composite structures but a thorough understanding, which would lead to a universal physical model is missing.

There are several scientists who support that empirical/phenomenological models, such as Paris equation, are physics-based models as they describe a physical phenomenon. However, the defending line of this thesis is that they do not represent any physical law, as their parameters need tuning for every case. For example the parameters of Paris power-law relationship[13,19], depend on the type of failure, loading case, geometry and stacking sequence, limiting the applicability of these models to composite coupons rather than in complex composite structures. Therefore, it is generally believed that empirical or phenomenological models such as Paris equation, shear-lag, variational, crack opening displacement models cannot describe efficiently more complex geometries, stacking sequences and loads. In addition, these models are effective only when one damage mechanism is present in the structure and that is by far not the case in composite structures.

In literature [20-25], most research work has been focused on evolving phenomenological/empirical models so as to predict the RUL of composite structures. these models cannot be characterized as physical since they use only empirical or phenomenological equations and their tuned fatigue parameters cannot describe the physical meaning of composite structures' damage evolution. Therefore, RUL prediction models that utilizing phenomenological/empirical equations are categorized not as MBMs but as DDMs. As a conclusion, there isn't any MBM available in literature that deals with composite structures.

2.4.2.2. *Online data-driven models*

2.4.2.2.1. Deterministic analysis

As mentioned in Chapter 1, the procedure of damage accumulation in composite structures especially during fatigue loading, is a complex phenomenon of stochastic nature which depends on a number of parameters and includes many sources of uncertainties. Consequently, it is not possible to predict precise the RUL of composite structures due to the various sources of uncertainty that the past, present and future contain. Therefore, deterministic RUL prediction models are out of this thesis given that these models describe the RUL variable as a determinist value.

2.4.2.2.2. Frequentist analysis

In case of frequentist DDMs all unknown parameters in a model are treated as deterministic variables except the diagnostic and prognostic measures which are handled as random variables. The documented work in frequentist RUL DDMs are presented hereafter.

In Liu et al. [26] a data-driven Gaussian prognostic model was presented. Gaussian process based on acoustic emission (AE) data and Lamb wave signals used to predict the RUL of composite beams subjected to constant amplitude fatigue loading. Composite beams were prepared with unidirectional carbon fibre/epoxy composite material. For the feature extraction process, wavelet transform and principal component analysis (PCA) were applied in order to determine effective damage indices. A damage index is defined using the minimum and maximum value of the sensing feature. Therefore, using a damage index it is not possible to obtain real-time RUL predictions since it is mandatory to know the minimum and maximum value, values which are known usually after the structure has failed.

The same research team in [27] proposed a condition based structural health monitoring and prognosis model to predict the RUL of notched CFRPs composite specimens with $[0/90]_s$ stacking sequence under uniaxial and biaxial fatigue loading utilizing real time sensor signals from strain gages. In addition, a flash thermography system was used in order to estimate the initial healthy and final damaged state of the composite specimen. The proposed RUL prediction model consisted of an online-diagnostics process i.e. direct cross-correlation analysis and the offline prognostics process i.e. Gaussian process. Also in this case study Liu et al. used a damage index approach and as a result this model cannot provide real-time RUL predictions too.

In order to illustrate the frequentist analysis, part of the work during this PhD thesis has been published [28-30]. These studies proposed a novel purely data-driven model for prognosis of the RUL in open hole carbon/epoxy specimens with $[0/45/-45/90]_{2s}$ stacking sequence under constant amplitude fatigue loading. This approach was based on stochastic multi-state degradation modelling utilizing the NHHSM and AE [28] or strain measurements [29]. Regarding the first case, windowed cumulative RA (rise time/amplitude) data were used as damage sensitive feature. In the second case a stereovision system was used to perform 3D full field Digital Image Correlation (DIC) measurements in order to monitor the strain distribution on the coupons' surface during fatigue tests. In both cases the CM data used to estimate the parameters of the NHHSM and successfully used it to obtain RUL predictions in unseen data with uncertainty quantification.

Finally in [30] two data-driven prognostic models, the NHHSMM and Bayesian Neural Networks (BNNs), utilizing AE measurements, were compared via several prognostic performance metrics. Open hole carbon/epoxy specimens tested under fatigue loading. Based on the selected prognostic performance metrics the NHHSMM provides better RUL predictions than BNNs. The aforementioned case studies represent some frequentist data-driven prognostic models that are encountered in the literature on application to composite structures.

2.4.2.2.3. Bayesian analysis

On the contrary, all Bayesian DDMs' unknown parameters are treated as random variables and inference is based upon the (posterior) probability distribution of these parameters. As discussed in Subsection 2.4.2.1, RUL prediction models employing phenomenological or empirical equations are categorized as DDMs. Consider that the published work in Bayesian RUL DDMs of composite structures, is presented hereafter.

Peng et al. [20,31] proposed a real-time fatigue life prognosis model for carbon-epoxy open-hole specimens with layup $[90_3/0_3]_s$ under constant amplitude fatigue loading. This prognosis model combined piezoelectric sensor measurements i.e. Lamb waves, a mechanical stiffness degradation model utilizing a Bayesian inference modified Paris law and a stiffness model, which was a second order multiple variable regression model. The proposed stiffness model correlated the normalized stiffness with Lamb waves' features such as normalized amplitude, correlation coefficient and cross correlation. In order to validate the normalized stiffness estimation the force displacement curve via the hydraulic machine was used. In addition, the modified Paris law described the relationship between the stiffness degradation rate, the stress range and current stiffness.

Chiachio et al. [21,24] utilized a Bayesian filtering model that incorporated information from empirical damage models and CM data so as to enable predictions of the RUL of composite materials. Chiachio et al. realized remaining fatigue life estimations in composite materials under constant amplitude fatigue loading utilizing monitoring data and some damage mechanics empirical models, i.e. shear-lag, variational and crack opening displacement, in order to correlate the macro-scale stiffness reduction and the micro-scale damage. Furthermore, a Bayesian reference of the modified Paris equation was used to model the evolution of matrix-cracks density. A set of 12 piezoelectric sensors were used to monitor the effects of matrix micro-cracks density and delamination and a set of triaxial strain gauges to measure the normalized effective stiffness. Also, periodic X-rays were taken to visualize and evaluate the micro-crack density. This information was used to develop a mapping between the Lamb wave signals and micro-crack density. Utilizing the estimated micro-crack density and all of the aforementioned damage mechanics models the current stiffness was assessed. Taking into consideration this assessment and the Bayesian modified Paris equation the RUL was predicted. In this study notched dog-bone geometry carbon-epoxy specimens with stacking sequence $[0_2/90_4]_s$ were used. A key finding from this study is that the shear-lag model is the best option regarding this specific case study.

Corbetta et al. [25] proposed a particle filter-based Bayesian model for damage prognosis of composite laminates exhibiting concurrent matrix cracks and delamination. This study enhanced the methodology proposed in previous papers by extending the Bayesian framework to multiple damage mechanisms, and validates the approach using damage

progression data from notched cross-ply CFRP coupons subject to tension-tension fatigue. A multiple damage-mode model, which was embedded in modified Paris equation, for the estimation of the strain energy release rate and the remaining stiffness of damaged laminates constitutes the core of the particle filtering algorithm. Also, the damage state can be evolved into the future enabling simulation of damage progression and prediction of RUL of the composite material.

2.4.2.3. Online hybrid models

Currently, hybrid models are not available due to the lack of physical based models that can thoroughly describe the fatigue damage process of composite structures. However, hybrid models will be soon the state of the art since these models combine both model-based and data-driven approaches aiming to get the best from each i.e. MBMs can compensate the lack of data and DDMs can compensate the lack of knowledge about composites' damage evolution.

2.5. Adaptive methodologies

Composite structures usually operate in non-uniform environments and altering operational conditions e.g. loads, whereby CM data are changing. The composite structure's life is heavily influenced by the way it is operated, maintained, the environmental and operation conditions, which are not always the designed ones, since unexpected phenomena can be occurred during the structure's lifetime. For the latter, let's consider an example from the aviation industry. Foreign objects impacts, such as birdstrikes, hail, tool drops etc., may occur anytime during the lifetime of the aircraft. These events fall into category of unexpected phenomena that may create damage, which has not been anticipated into the design phase. The implication of such an unexpected phenomenon to the integrity of the structural component could be severe and a common practice, as long as the operators record the event, is to interrupt the aircraft operation and initiate inspection and repair actions resulting to unplanned costs. In this case, the role of a RUL prediction model would be to assess the effect of the unexpected phenomenon and to provide an updated prediction.

However, the current state-of-the-art RUL prediction models may not be suitable for the following reasons. A MBM will not be able to take into account these unexpected phenomena since it is not realistic to involve any physical law that is able to describe all the possible unexpected phenomena. On the other hand, 'classic' DDMs have a strong limitation, because they are able to predict degradation processes efficiently, only when the testing data are extracted under the same conditions as the training data. For the case of the foreign object impact, the RUL predictions of the structural composite component of the aircraft will be accurate only if the training data contains data related to the impact. In other words, a DDM may not provide accurate RUL predictions of the testing composite structure if the training composite structures have not experienced that unexpected phenomenon before. However, in order to create a training database, which covers all the possible testing scenarios is impractical. Consequently, there is a need to develop RUL models with real-time adapting capabilities in order to be able to predict more accurate the RUL of composite structures that either underperform or outperform due to unexpected phenomena that might occur during the service life. Nevertheless, there is no literature available about adaptive

prognostics in composite structures. Due to that, the literature study is extended to adaptive prognostics of engineering systems in general.

A few adaptive prognostic models have been proposed in the literature the last 15 years. Orchard et al. [32] utilized two different approaches for outer feedback correction loops in particle filters algorithms. These loops incorporate information for the short term prediction error in order to improve the performance of the overall prognostic framework. However, important initialization parameters such as the number of prediction steps (k), the variance vector of the kernel noise $[p \ q]^T$ have to be predefined. Both approaches were tested using data from an artificial fault test in a critical component of rotorcraft transmission system. Results show that outer feedback correction loops improve the precision and accuracy of the predicted RUL.

Sbarufatti et al. [33] proposed a model for batteries' prognostics, which is a combination of particle filters and radial basis function neural networks (RBFNNs). This model could be considered adaptive as the RBFNNs are trained online. To be more specific the neural networks parameters are identified online by the particle filters as soon as new observations of the battery terminal voltage become available. The RBFNNs algorithm has shown to be able to provide satisfactory prognostic predictions over normal and aging scenarios. However, before RBFNNs use, the dataset has to be significantly corrupted by adding artificial noise. In general, the choice of the noise variances is not an easy task since too small values may hamper a proper exploration of the state-space, and at the same time too large values don't guarantee an efficient state estimation.

Furthermore, in Khan et al [34] an adaptive degradation prognostic model, utilizing particle filter with a neural network degradation model, was proposed in order to predict the RUL of turbofan jet engines. The RUL predictions were generated using two different algorithms for benchmarking the results, the nominal RBHNNs with particle filters and the similarity based prognostics. The RUL predictions for both algorithms are characterized by volatility but more importantly the similarity based approach does not support the prediction of RUL confidence intervals which is an essential output for the reliability of the algorithm. Furthermore, the proposed prognostic model requires the initialization of the random walk step size (σ_a). The σ_a selection is not a straight forward choice, since a large value of it will give fast convergence but high fluctuations whereas a small value will produce a smoother but a slower convergence of the parameter estimation process, and at the same time is an important selection regarding the final prognostics. As a result, the selection of σ_a is driven from the case-study.

Darogheh et al. proposed a hybrid prognosis model, which integrates particle filters and neural networks for gas turbine engines [35]. It is worth mentioning that the integration of particle filters and neural networks is a common combination in the literature, since both of these algorithms are available in many commercial and open source programming language and their implementation is relative easy in respect to other algorithms. The authors developed a hybrid prediction model based on extending particle filters to the future time horizon by utilizing an observation forecasting scheme. This scheme is provided by using the neural network approach as a nonlinear time series forecasting scheme. Neural networks are trained adaptively based on the newly received data in the case that the deviations between the forecasted observation from this network and the real observation increase from

one test data to another test data set. Nonetheless, the main disadvantage of this hybrid prognosis model is the absence of confidence intervals.

Si et al. [36] utilized a Wiener-process-based model with a recursive filter algorithm for RUL predictions. A state space model updates the drift coefficients, which are defined as random variables, and an expectation maximization (EM) algorithm re-estimates all the unknown parameters as soon as new data is available. The proposed model is applied to estimate the RUL of gyros in an inertial navigation system. The proposed model of Si et al. excels in most of the cases that are presented in [37] and [38]. However, Wiener models assume that the degradation process of the studied system and the operation time are linearly connected, which is not always the case.

A very recent work of Cadini et al. [39] proposed to exploit the flexibility of neural networks so as to adaptively learn from a monitored metallic structure and derive models for diagnostics and prognostics in real time. In order to achieve that neural networks are embedded within a particle filtering scheme and the training process of the network is performed in real time as CM data become available during the structure's operation. As a result, the proposed RUL model is capable of sequentially updating itself utilizing the available CM data. This model was demonstrated on simulated and real fatigue crack growth tests of metallic aeronautical panels. The main drawbacks of the Cadini et al.'s RUL model are the required convergence time to the actual RUL, which tends to be larger than similar RUL models, the volatile RUL predictions and the divergent behavior of confidence intervals towards the end of life. However, the proposed model may play a role in structural prognostics in the future where physics-based or more accurate empirical/phenomenological models become available.

2.6. Conclusions

Based on the conducted literature review, there is clearly a need to develop models with real-time adapting capabilities in order to be able to predict more accurately the RUL of composite structures that either underperform or outperform due to unexpected phenomena that might occur during the service life. These composite structures are often referred as outliers and the prediction of their RUL is a challenging task. These adaptive models have to be data-driven in case of composite structures because the incomplete knowledge about the physics behind the evolution and interaction of composites' damage mechanisms and the unrealistic involvement of any physical law, that is able to describe all the possible unexpected phenomena, make a MBM not a visible option.

The DDM could be frequentist or a Bayesian based. This study is focusing on a frequentist approach mainly for the following two reasons; in prognostics one crucial parameter is the computational time of an estimation, to be more specific how many time units the algorithm needs to predict system's reliability and as it is known Bayesian inference may be computationally intensive due to integration over many parameters. On the other hand frequentist inference tends to be less computationally intense [40]. Furthermore, Bayesian inference is subjective to the selection of prior distributions. There is no single method for choosing a prior, so different people will produce different priors and may therefore arrive at different posteriors and conclusions.

Therefore, this study is focusing on the development of a new data-driven frequentist prognostic model, which will be capable of sequentially updating itself using the available online CM data gathered during the composite structure's operation, avoiding the typical limitations associated to non-adaptive RUL models, which are, in general, not capable of capturing the effect of unexpected phenomena in RUL predictions.

References

- [1] K. L. Reifsnider and A. Talug, "Analysis of fatigue damage in composite laminates," *Int. J. Fatigue*, vol. 2, no. 1, pp. 3–11, Jan. 1980.
- [2] T. P. Philippidis and A. P. Vassilopoulos, "Life prediction methodology for GFRP laminates under spectrum loading," *Compos. Part A Appl. Sci. Manuf.*, vol. 35, no. 6, pp. 657–666, Jun. 2004.
- [3] M. Quaresimin, L. Susmel, and R. Talreja, "Fatigue behaviour and life assessment of composite laminates under multiaxial loadings," *Int. J. Fatigue*, vol. 32, no. 1, pp. 2–16, Jan. 2010.
- [4] R. Sarfaraz, A. P. Vassilopoulos, and T. Keller, "A hybrid S–N formulation for fatigue life modeling of composite materials and structures," *Compos. Part A Appl. Sci. Manuf.*, vol. 43, no. 3, pp. 445–453, Mar. 2012.
- [5] W. Van Paepegem and J. Degrieck, "Coupled residual stiffness and strength model for fatigue of fibre-reinforced composite materials," *Compos. Sci. Technol.*, vol. 62, no. 5, pp. 687–696, 2002.
- [6] C. Kassapoglou, "Fatigue of composite materials under spectrum loading," *Compos. Part A Appl. Sci. Manuf.*, vol. 41, no. 5, pp. 663–669, May 2010.
- [7] M. M. Shokrieh and F. Taheri-Behrooz, "A unified fatigue life model based on energy method," *Compos. Struct.*, vol. 75, no. 1–4, pp. 444–450, Sep. 2006.
- [8] S. Haojie, Y. Weixing, and W. Yitao, "Synergistic Damage Mechanic Model for Stiffness Properties of Early Fatigue Damage in Composite Laminates," *Procedia Eng.*, vol. 74, pp. 199–209, Jan. 2014.
- [9] M. Schwabacher and K. Goebel, "A Survey of Artificial Intelligence for Prognostics," *AAAI Fall Symp.*, pp. 107–114, 2007.
- [10] F.D. Maio and E. Zio, "Failure Prognostics By a Data-Driven Similarity-Based Approach," *Int. J. Reliab. Qual. Saf. Eng.*, vol. 20, no. 01, p. 1350001, 2013.
- [11] J. Z. Sikorska, M. Hodkiewicz, and L. Ma, "Prognostic modelling options for remaining useful life estimation by industry," *Mech. Syst. Signal Process.*, vol. 25, no. 5, pp. 1803–1836, 2011.
- [12] C. S. Byington, M. J. Roemer, G. J. Kacprzymki, and T. Galie, "Prognostic enhancements to diagnostic systems for improved condition-based maintenance," in *IEEE Aerospace Conference Proceedings*, 2002, vol. 6, pp. 2815–2824.

- [13] J. M. Karandikar, N. H. Kim, and T. L. Schmitz, "Prediction of remaining useful life for fatigue-damaged structures using Bayesian inference," *Eng. Fract. Mech.*, vol. 96, pp. 588–605, 2012.
- [14] A. P. Vassilopoulos and E. F. Georgopoulos, "Novel computational methods for fatigue life modeling of composite materials," *Fatigue Life Predict. Compos. Compos. Struct.*, pp. 139–173, 2010.
- [15] R. Moghaddass and M. J. Zuo, "An integrated framework for online diagnostic and prognostic health monitoring using a multistate deterioration process," *Reliab. Eng. Syst. Saf.*, vol. 124, pp. 92–104, 2014.
- [16] R. Moghaddass and M. J. Zuo, "Multistate degradation and supervised estimation methods for a condition-monitored device," *IIE Trans., Institute Ind. Eng.*, vol. 46, no. 2, pp. 131–148, 2014.
- [17] S. Sankararaman and K. Goebel, "Why is the Remaining Useful Life Prediction Uncertain?," *Annu. Conf. of the Progn. and Heal. Manag. Soc.* 2013, pp. 1–13.
- [18] N. Eleftheroglou, T.H. Loutas and S. Malefaki, "Stochastic modeling of fatigue damage in composite materials via Non Homogeneous Hidden Semi Markov Processes.," in *Statistical, Stochastic and Data Analysis Methods and Applications*, no. February 2016, 2015, pp. 19–33.
- [19] T. Peng et al., "Probabilistic fatigue damage prognosis of lap joint using Bayesian updating," *J. Intell. Mater. Syst. Struct.*, vol. 26, no. 8, pp. 965–979, 2015.
- [20] T. Peng and Y. Liu, "Probabilistic fatigue life prediction of composite laminates using Bayesian updating," *17th AIAA Non-Deterministic Appr. Conf.*, pp. 1–15, 2015.
- [21] J. Chiachio, M. Chiachio, A. Saxena, S. Sankararaman, G. Rus, and K. Goebel, "Bayesian model selection and parameter estimation for fatigue damage progression models in composites," *Int. J. Fatigue*, vol. 70, pp. 361–373, 2015.
- [22] J. Chiachio, M. Chiachio, A. Saxena, G. Rus, and K. Goebel, "An Energy-Based Prognostic Framework to Predict Fatigue Damage Evolution in Composites," *Annu. Conf. Progn. Heal. Manag. Soc.*, pp. 1–9, 2013.
- [23] M. Chiachio, J. Chiachio, A. Saxena, and K. Goebel, "An energy-based prognostic framework to predict evolution of damage in composite materials," *Struct. Heal. Monit. Aersp. Struct.*, no. May, pp. 447–477, 2016.
- [24] J. Chiachio, M. Chiachio, S. Sankararaman, A. Saxena, and K. Goebel, "Condition-based prediction of time-dependent reliability in composites," *Reliability Engineering and System Safety*, vol. 142, pp. 134–147, 2015.
- [25] M. Corbette, A. Saxena, M. Giglio, and K. Goebel, "Evaluation of Multiple Damage-Mode Models for Prognostics of Carbon Fiber-reinforced Polymers," *Inter.l Workshop on Struct. Heal.Monit.*, 2015.
- [26] Y. Liu, S. Mohanty, and A. Chattopadhyay, "A Gaussian process based prognostics framework for composite structures," *Model. Signal Process. Control Smart Struct.* 2009, vol. 7286, p. 72860J, 2009.

- [27] Y. Liu, S. Mohanty, and A. Chattopadhyay, "Condition based structural health monitoring and prognosis of composite structures under uniaxial and biaxial loading," *J. Nondestruct. Eval.*, vol. 29, no. 3, pp. 181–188, 2010.
- [28] N. Eleftheroglou, D. Zarouchas, T. Loutas, R. Alderliesten, and R. Benedictus, "Structural health monitoring data fusion for in-situ life prognosis of composite structures," *Reliab. Eng. Syst. Saf.*, vol. 178, 2018.
- [29] N. Eleftheroglou, D. S. Zarouchas, T. H. Loutas, R. C. Alderliesten, and R. Benedictus, *Online remaining fatigue life prognosis for composite materials based on strain data and stochastic modeling*, vol. 713. 2016.
- [30] T. Loutas, N. Eleftheroglou, and D. Zarouchas, "A data-driven probabilistic framework towards the in-situ prognostics of fatigue life of composites based on acoustic emission data," *Compos. Struct.*, vol. 161, 2017.
- [31] T. Peng, Y. Liu, A. Saxena, and K. Goebel, "In-situ fatigue life prognosis for composite laminates based on stiffness degradation," *Compos. Struct.*, vol. 132, pp. 155–165, 2015.
- [32] M. E. Orchard, F. A. Tobar, and G. J. Vachtsevanos, "Outer Feedback Correction Loops in Particle Filtering-based Prognostic Algorithms: Statistical Performance Comparison," *Stud. Informatics Control*, vol. 18, no. 4, pp. 295–304, 2009.
- [33] C. Sbarufatti, M. Corbetta, M. Giglio, and F. Cadini, "Adaptive prognosis of lithium-ion batteries based on the combination of particle filters and radial basis function neural networks," *J. Power Sources*, vol. 344, no. November, pp. 128–140, 2017.
- [34] F. Khan, O. Eker, A. Khan, and W. Orfali, "Adaptive Degradation Prognostic Reasoning by Particle Filter with a Neural Network Degradation Model for Turbofan Jet Engine," *Data*, vol. 3, no. 4, p. 49, 2018.
- [35] N. Daroogheh, A. Baniamerian, N. Meskin, and K. Khorasani, "A hybrid prognosis and health monitoring strategy by integrating particle filters and neural networks for gas turbine engines," *2015 IEEE Conf. Progn. Heal. Manag. Enhancing Safety, Effic. Availability, Eff. Syst. Through PHAf Technol. Appl. PHM 2015*, pp. 1–8, 2015.
- [36] X. S. Si, Z. X. Zhang, and C.-H. Hu, "Data-Driven Remaining Useful Life Prognosis Techniques," Springer; 1st ed. 2017 edition .
- [37] N. Z. Gebraeel, M. A. Lawley, R. Li, and J. K. Ryan, "Residual-life distributions from component degradation signals: A Bayesian approach," *IIE Trans. (Institute Ind. Eng.)*, vol. 37, no. 6, pp. 543–557, 2005.
- [38] W. Wang, M. Carr, W. Xu, and K. Kobbacy, "A model for residual life prediction based on Brownian motion with an adaptive drift," *Microelectron. Reliab.*, vol. 51, no. 2, pp. 285–293, 2011.
- [39] F. Cadini, C. Sbarufatti, M. Corbetta, F. Cancelliere, and M. Giglio, "Particle filtering-based adaptive training of neural networks for real-time structural damage diagnosis and prognosis," *Struct. Control Heal. Monit.*, vol. 26, no. 12, pp. 1–19, 2019.
- [40] O. J. Bloom Jeremy, "Comparison of frequentist and Bayesian inference,." 18.05 class 20, *Comparison of frequentist and Bayesian inference.*, 2014.

3

Methodology

3.1. Introduction

As already mentioned in Chapter 2, there is a need for developing data-driven frequentist models, which will be able to adapt their estimated parameters using online CM data. These models will be part of a more general methodology. Figure 3.1 summarizes the proposed adaptive methodology and it consists of two processes; the training and testing. The training process contains the training CM data, the feature extraction process and the selected stochastic model. The feature extraction process is designed only based on the training CM data and during the testing process exactly the same feature extraction process is followed. In addition, the initialization step of the selected stochastic model is utilized and stochastic model's parameters θ are estimated (θ^*) during the training process. The testing process uses the training process' output θ^* , the testing CM data, the pre-designed feature extraction process and diagnostics in order to predict the RUL of the testing engineering system. The diagnostics part is the adaptation's backbone element since this measure is the 'trigger' of the adaptation model and the main indicator of any possible unexpected event. After the adaptation, prognostics for the testing engineering system can be calculated. The aim of this new adaptive model is to provide more accurate RUL prediction for systems, which may face uncertainties during their operation life that were not encountered during the training process. In order to evaluate the performance of the new adaptive model, prognostic performance metrics are introduced in the testing process. In Section 3.1 and 3.2 the main elements of the training and testing processes are described and explained, respectively.

3.2. Training process

This section reviews the main elements of the training process, namely, the feature extraction process and the selected stochastic model.

3.2.1. Feature extraction process

A set of metrics in order to illustrate a feature extraction process has been proposed in the literature and consists of monotonicity, prognosability and trendability [1]. Monotonicity characterizes a parameter's general increasing or decreasing trend, prognosability measures the spread of a parameter's failure value and finally, trendability indicates whether degradation histories of a specific parameter have the same underlying trend.

In order to produce features with strong prognostic capability, the aforementioned metrics can be used either as identification of an appropriate prognostic feature (to compare possible features) or as a feature design property. Monotonicity is an important prognostic feature since in this thesis it is assumed that systems do not undergo repair actions or self-healing and as a result the CM degradation histories are expected to have monotonic trend. It should be noted that this assumption is not valid for some components such as batteries, which may experience some degree of self-repair during short periods of nonuse [2]. However, for mechanical components or systems with a combination of electronic and mechanical components, this assumption holds. Based on the literature [3-5], a feature that is sensitive to the degradation process is desirable to have a monotonic trend. To quantify the monotonicity the Mann-Kendall (MK) criterion can be used [6], Equation (3.1).

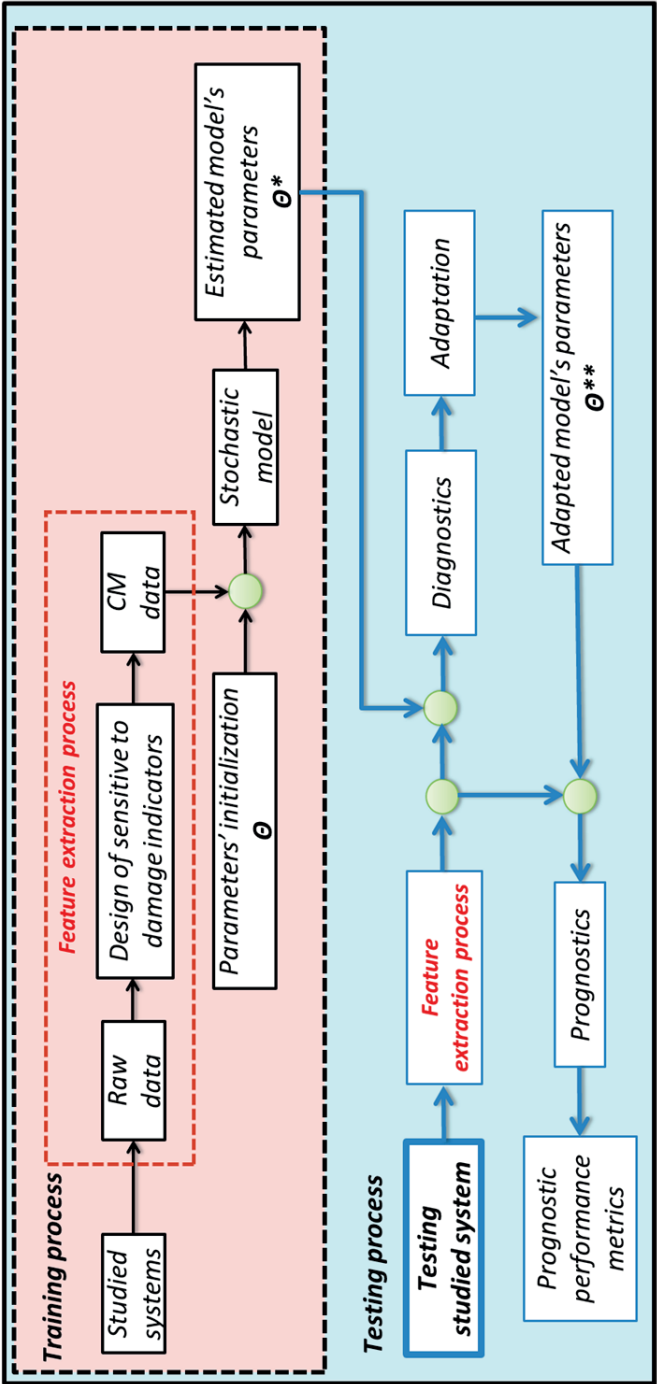


Figure 3.1. RUL adaptive methodology

$$MK = \sum_{i=1}^D \sum_{j=1, j>i}^D (t_j - t_i) \cdot \text{sgn}(y(t_j) - y(t_i)) \quad (3.1)$$

where $y(t_i)$ the feature value at time of measurement t_i , D the number of measurements

$$\text{and } \text{sgn}(x) = \begin{cases} -1 & \text{if } x < 0 \\ 0 & \text{if } x = 0 \\ 1 & \text{if } x > 0 \end{cases}.$$

In this thesis the Modified Mann-Kendall (MMK) criterion is introduced so as to quantify the feature monotonicity, Equation (3.2), for the following reasons:

- MK values have not any informative meaning in terms of how monotonic a feature is. For example, in [7] study the MK values' range from $[10^5, 4 \times 10^5]$. However, MMK value expresses a percentage of monotonicity in the range of $[-1, 1]$. If $\text{MMK}=1$, the degradation history is strictly increasing, while if $\text{MMK}=-1$, the degradation history is strictly decreasing. In any other case the degradation history is not strictly monotonic.
- Each degradation history has the same monotonicity weight no matter its length. On the other hand, the classical MK criterion is biased since a longer degradation history gives a higher MK value.

$$\text{Monotonicity} = \frac{MK}{\sum_{i=1}^D \sum_{j=1, j>i}^D (t_j - t_i)} \cdot 100\% \quad (3.2)$$

Prognosability and trendability are defined via the work of Coble and Hines [1]. Prognosability is calculated as the variance of the failure values for each degradation history divided by the mean range of the history. This is exponentially weighted to give the desired zero to one scale:

$$\text{Prognosability} = e^{\frac{\text{std}(y(t_D))}{\text{mean}|y(t_D)-y(t_1)|}} \quad (3.3)$$

where $y(t_i)$ the feature value at time of measurement t_i and D the number of measurements. The trendability of a CM feature is more complex to define than the other two metrics. A candidate feature is trendable if each degradation history of the population can be modeled with the same functional form. This can be measured to some degree by comparing the fraction of positive first and second derivatives in each history. Again, when using real world

data, these parameters should be smoothed to give a more accurate estimate of the derivatives. The formalization of trendability is given by Coble and Hines [1]:

$$\text{Trendability} = 1 - \text{std}(z_i) \quad (3.4)$$

where

$$z_i = \frac{\text{no.of } \frac{dy}{dt} > 0}{D-1} + \frac{\text{no.of } \frac{d^2y}{dt^2} > 0}{D-2}, \quad y(t_i) \text{ the feature value at time of measurement } t_i \text{ and } D \text{ the number of measurements of the } i^{\text{th}} \text{ degradation history.}$$

These three intuitive metrics can be formalized to give a quantitative measure of prognostic feature suitability but also, as already mentioned, they can be used as a feature design property in terms of combining different CM features so as to involve a new one with higher monotonicity, prognosability and trendability.

The process of extracting information from different CM techniques and integrate them into a consistent, accurate and reliable feature (hyper-feature) is known as data fusion and it has been already successfully applied to damage diagnostics [8,9]. In principle, data fusion can be implemented in three levels; raw multi-sensor data fusion, feature-level fusion and decision-level fusion. Raw data fusion should be treated with caution as sensor recordings may have different acquisition, pre-filtering and amplification settings. In addition, raw data fusion needs to have as input commensurate data in terms of values' range. As a result, feature-level and decision-level fusion are more common [10]. In this thesis a feature-level data fusion methodology is proposed.

The fusion scheme receives as inputs at least two features, e.g. feature X and feature Y, where the following equation explains the rationale behind the fusion process.

$$f(X, Y) = \sum_{j=0}^M \sum_{i=0}^{i+j \leq M} a_{ij} \cdot X^j \cdot Y^i \quad (3.5)$$

where f is the fused output feature, a_{ij} are constant coefficients that control the weight of the exponential X and Y features' product and M the maximum polynomial degree power that these features can use. The aforementioned three metrics, i.e. monotonicity, prognosability and trendability, are adopted to enable the data fusion process and are expressed in Equation (3.6) by defining a fitness function as a weighted sum of the three metrics. Fitness function is used as an objective function to be maximized and thus determine which polynomial degree M and constant coefficients a_{ij} give the best prognostic fused feature.

$$\text{Fitness} = a * \text{Monotonicity} + b * \text{Prognosability} + c * \text{Trendability} \quad (3.6)$$

and the constants a, b, and c control how important each metric is in the optimization and they are user-defined parameters.

The constant polynomial coefficients a_{ij} , for each polynomial degree M, are based on the optimization problem described in Equation (3.7) with the fitness as the objective function.

For the aforementioned optimization problem, different optimization techniques can be used i.e. Nelder-Mead, Neural Networks, Particle Swarm Optimization (PSO), Genetic Algorithms and OptQuest/NLP (OQNLP). The unconstrained optimization problem is formulated as:

$$\alpha_{ij}^* = \arg \max_{a_{ij}} \left(\text{Fitness}(a_{ij}, M) \right) \quad (3.7)$$

In conclusion, the outputs of the proposed data fusion methodology are the optimum polynomial degree M and the optimum constant coefficients a_{ij} based on the Fitness function, Equation (3.7).

3.2.2. Stochastic model

As already discussed in Chapter 2, this study is focusing on the involvement of a new data-driven frequentist prognostic model, the ANHHSMM, which is an extension of the NHHSMM.

NHHSMM is the most extensive version of Hidden Markov models (HMMs). Although HMMs were initially introduced and studied in the late 1960s and early 1970s [11] they became popular recently. Peng and Dong highlighted that HMMs have a rich mathematical structure and can form a solid theoretical foundation for use in engineering applications [12]. An added benefit of employing HMMs is the ease of model interpretation in comparison with pure ‘black-box’ modeling methods such as artificial neural networks that are often employed in advanced prognostic models [13]. However, HMMs’ main disadvantage is that they assume an exponentially distributed state duration (sojourn time), which is not always the case. Hidden Semi Markov models (HSMM), relaxes this assumption allowing the unconstrained modeling of sojourn times. HSMMs have been utilized successfully for prognostic RUL predictions in condition monitoring of machines [12] and [14]. In HMMs and HSMMs, there is the limitation that the state transitions are not dependent on the age of the engineering system or on the sojourn time in the current state.

The work of Moghaddass and Zuo extended the HSMMs to NHHSMMs in order to overcome this limitation [15]. According to NHHSMM, state transitions are a dynamic procedure, which depends on the current hidden state, the time spent in this state (sojourn time), the total age of the engineering asset or any combination of these parameters. A similar work from Peng and Dong also extended the HSMMs to NHHSMMs using an iteration algorithm [12]. This algorithm uses the transition matrix obtained from the HSMM in order to create a new one, which includes aging factors. Three different types of aging factors, i.e. constant, multiple and exponential form, are presented by Peng and Dong. The work of Moghaddass and Zuo doesn’t include any kind of limitations regarding the dependency between the state transitions and the aging parameter. Therefore, it can be characterized as the most extensive one until now in the literature of Markov models.

The NHHSMM excels in many aspects, as it is a DDM and it doesn’t have any sojourn time limitation, in comparison with other available prognostic models. Two studies of Loutas et al. compare the NHHSMM with gradient boosted trees (GBTs) and Bayesian feed-forward neural networks (BNN), [16] and [17] respectively. In the first paper, the authors predicted the RUL of in-service reciprocating compressors using temperature as health indicator data measured in Head End and Crank End discharge valves. In the second paper, the authors predict the RUL of composite structures subjected to fatigue loading utilizing AE

measurements as health indicator data. According to the benchmark between the NHHSM and GBTs and BNN, the NHHSM performs better using several metrics and it gives more coherent predictions for both studies. Thus an adaptive extension of the NHHSM seems to be very promising. The adaptive version of the NHHSM will be presented in full details in the next chapter.

3.3. Testing process

This section reviews the main elements of the testing process, namely, diagnostics, prognostics and prognostic performance metrics.

3.3.1. Diagnostics and prognostics

In real world engineering systems, diagnostics and prognostics are calculated through several dynamic reliability measures reflecting certain aspects of the degradation process. These dynamic reliability measures are estimated using the CM data extracted from the testing engineering system utilizing exactly the same feature extraction process as the training CM data used. In this thesis dynamic means that the measure is calculated over time given the most updated sequence of the CM data.

As a result, dynamic diagnostic measures employ all the available CM data up to the current time point to provide information regarding the current actual degradation level. Using CM data for diagnostic purposes has been reported frequently in the literature [18,19]. The most commonly used measure is the current degradation level of the system (hidden or damage state), which can be estimated using methods such as the Viterbi algorithm [11]. The Viterbi algorithm is a dynamic programming algorithm and it is able to identify the most likely sequence of damage states via a sequence of CM data. Moghaddass and Zuo [20] were the first ones who involved diagnostic measures with the ability to reflect the dynamic behaviour of the degradation process for a multistate degradation process.

While dynamic prognostic measures can help maintenance makers to determine the time to initiate maintenance setup so as to prevent the engineering system's failure, prognostics provide information regarding the RUL of the studied system. Over the past years, there has been a significant increase on prognostic methodologies [21,22]. Moghaddass and Zuo [20] developed prognostic measures that can be calculated based on real-time CM data according to NHHSM. In Chapter 4, the mathematical derivations for important diagnostic and prognostic measures are mentioned for a degradation process under NHHSM.

3.3.2. Prognostic performance metrics

Prognostics aim to avoid failures in critical systems through the RUL estimations. However, as it is mentioned in Chapter 2 it is challenged by past, present and future uncertainties involved with operating loads, model inaccuracies, data noise and environmental conditions among others. This imposes a strict validation requirement through a rigorous performance evaluation before they can be certified for critical applications. As a result, prognostic performance metrics has gained significant attention in the past few years. Metrics can create a standardized language with which technology developers and users can communicate their findings and compare results.

In this thesis seven prognostic performance metrics are employed in order to evaluate the predictive performance of the ANHHSM. The first five are metrics widely used in literature [23,24]: Precision, Mean Squared Error (MSE), Mean Absolute Percentage Error (MAPE), Cumulative Relative Accuracy (CRA), Convergence (C_{Em}) while the last two were developed within the framework of this thesis. The prognostic performance metrics are defined as:

1. Precision

$$\text{Precision} = \sqrt{\frac{\sum_{i=1}^D (E_m(t_i) - \overline{E_m}(t_i))^2}{D-1}}, \text{ where } \overline{E_m} \text{ is the mean value of error } E_m \text{ and}$$

$E_m(t_i) = RUL_{\text{actual}}(t_i) - \text{meanRUL}(t_i)$ and $t_i \in [1, D]$ is the discrete time moment when the i^{th} SHM observation is recorded.

2. Mean Squared Error (MSE)

$$\text{MSE} = \sqrt{\frac{\sum_{i=1}^D (E_m(t_i))^2}{D}}.$$

3. Mean Absolute Percentage Error (MAPE)

$$\text{MAPE} = \frac{1}{D} \sum_{i=1}^D \left| \frac{100 \cdot E_m(t_i)}{RUL_{\text{actual}}(t_i)} \right|.$$

4. Cumulative Relative Accuracy (CRA)

$$\text{CRA} = \frac{\sum_{i=1}^D \text{RA}(t_i)}{D} \text{ where } \text{RA}(t_i) = 1 - \left| \frac{E_m(t_i)}{RUL_{\text{actual}}(t_i)} \right|.$$

5. Convergence (C_{Em})

$$C_{Em} = \sqrt{(x_c - t_1)^2 + y_c^2}$$

where

$$x_c = \frac{\sum_{i=1}^{D-1} (t_{i+1}^2 - t_i^2) \cdot |E_m(i)|}{2 \cdot \sum_{i=1}^{D-1} (t_{i+1} - t_i) \cdot |E_m(i)|} \quad \text{and} \quad y_c = \frac{\sum_{i=1}^{D-1} (t_{i+1} - t_i) \cdot E_m(i)^2}{2 \cdot \sum_{i=1}^{D-1} (t_{i+1} - t_i) \cdot |E_m(i)|}.$$

6. Monotonicity

The prognostic's function monotonicity can be measured based on the proposed MMK monotonicity criterion, see Equation (3.2), where $y(t_i)$ is replaced with $\text{meanRUL}(t_i)$. In case of the studied function, which is the RUL prediction function, the preferable value of MMK=-1 since it is expecting that the engineering system's RUL is decreasing monotonically during its lifetime.

7. Confidence Intervals Distance Convergence (CIDC)

Goebel et al. [25] stated that as the amount of data increases during the fatigue life, the confidence intervals distance should converge towards the actual life. In order to quantify this statement, a new metric is introduced; the CIDC. This metric is an extension of the metric of convergence in [23] but in this case the centroid is under the confidence intervals distance curve. In general, lower Euclidian distance means faster convergence. Let (x_c, y_c) be the center of mass of the area under the

confidence intervals distance curve, then the CIDC can be represented by the Euclidean distance between the (x_c, y_c) and the origin $(t_1, 0)$, where:

$$CIDC = \sqrt{(x_c - t_1)^2 + y_c^2}$$

where

$$x_c = \frac{\sum_{i=1}^{D-1} (t_{i+1}^2 - t_i^2) \cdot (UCI(i) - LCI(i))}{2 \cdot \sum_{i=1}^{D-1} (t_{i+1} - t_i) \cdot (UCI(i) - LCI(i))}, \quad y_c = \frac{\sum_{i=1}^{D-1} (t_{i+1} - t_i) \cdot (UCI(i) - LCI(i))^2}{2 \cdot \sum_{i=1}^{D-1} (t_{i+1} - t_i) \cdot (UCI(i) - LCI(i))}$$

and

UCI, LCI the upper and lower selected confidence intervals.

Figure 3.2 demonstrates how the CIDC metric works in two hypothetical sets of confidence intervals 1 and 2. The confidence intervals in case 2 converge faster than confidence intervals 1, see Figure 3.2(a). In Figure 3.2(b) the Euclidean distance of the mass center 2 and the origin ($CIDC_2 = 9.7419$) is lower than the Euclidean distance of the mass center 1 and the origin ($CIDC_1 = 10.5048$) thus, the CIDC metric is validated.

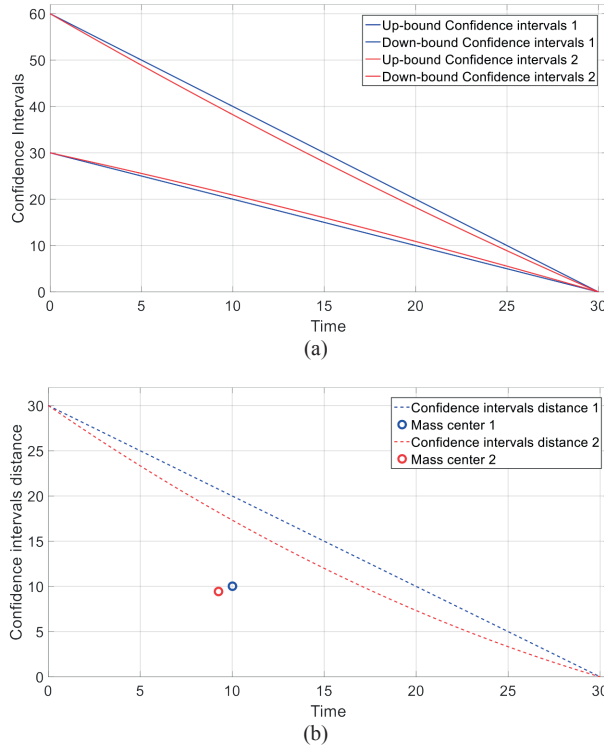


Figure 3.2. Validation of Confidence Intervals Distance Convergence metric a) Hypothetical sets of confidence intervals b) Mass centers under the confidence intervals distance curves

References

- [1] J. Coble and J. W. Hines, "Identifying optimal prognostic parameters from data: a genetic algorithms approach," *Proc. Annu. Conf. Progn. Heal. Manag. Soc.*, pp. 1–11, 2009.
- [2] S. Kadry, *Diagnostics and Prognostics of Engineering Systems: Methods and Techniques: Methods and Techniques*. IGI Global, 2012.
- [3] F. Qian and G. Niu, "Remaining useful life prediction using ranking mutual information based monotonic health indicator," *Proc. 2015 Progn. Syst. Heal. Manag. Conf. PHM 2015*, pp. 1–5, 2016.
- [4] L. Liao, "Discovering prognostic features using genetic programming in remaining useful life prediction," *IEEE Trans. Ind. Electron.*, vol. 61, no. 5, pp. 2464–2472, 2014.
- [5] Y. Lei, N. Li, L. Guo, N. Li, T. Yan, and J. Lin, "Machinery health prognostics: A systematic review from data acquisition to RUL prediction," *Mech. Syst. Signal Process.*, vol. 104, pp. 799–834, 2018.
- [6] S. Yue and P. Pilon, "A comparison of the power of the t test , Mann- Kendall and bootstrap tests for trend detection / Une comparaison de la puissance des tests t de Student , de Mann-Kendall et du bootstrap pour la détection de tendance," vol. 6667, pp. 20–38, 2011.
- [7] N. Eleftheroglou, D. Zarouchas, T. Loutas, R. Alderliesten, and R. Benedictus, "Structural health monitoring data fusion for in-situ life prognosis of composite structures," *Reliab. Eng. Syst. Saf.*, vol. 178, 2018.
- [8] S. F. Jiang, C. M. Zhang, and S. Zhang, "Two-stage structural damage detection using fuzzy neural networks and data fusion techniques," *Expert Syst. Appl.*, vol. 38, no. 1, pp. 511–519, 2011.
- [9] X. E. Gros, "Pixel Level NDT Data Fusion," *Appl. NDT Data Fusion*, vol. 32, pp. 25–57, 2011.
- [10] D. L. Hall, S. Member, and J. Llinas, "An Introduction to Multisensor Data Fusion," vol. 85, no. 1, 1997.
- [11] L. R. Rabiner, "A tutorial on hidden Markov models and selected applications in speech recognition," *Proc. IEEE*, vol. 77, no. 2, pp. 257–286, 1989.
- [12] Y. Peng and M. Dong, "A prognosis method using age-dependent hidden semi-Markov model for equipment health prediction," *Mech. Syst. Signal Process.*, vol. 25, no. 1, pp. 237–252, 2011.
- [13] P. Baruah and R. B. Chinnam, "HMMs for diagnostics and prognostics in machining processes," *Int. J. Prod. Res.*, vol. 43, no. 6, pp. 1275–1293, 2005.
- [14] M. Dong and D. He, "A segmental hidden semi-Markov model (HSMM)-based diagnostics and prognostics framework and methodology," *Mech. Syst. Signal Process.*, vol. 21, no. 5, pp. 2248–2266, 2007.
- [15] R. Moghaddass and M. J. Zuo, "Multistate degradation and supervised estimation methods for a condition-monitored device.," *IIE Transactions*, 46:2, 131-148, DOI: 10.1080/0740817X.2013.770188
- [16] T. Loutas, N. Eleftheroglou, G. Georgoulas, P. Loukopoulos, D. Mba, and I. Bennett, "Valve Failure Prognostics In Reciprocating Compressors Utilizing Temperature Measurements, PCA-based Data Fusion And Probabilistic Algorithms," *IEEE Trans. Ind. Electron.*, vol. PP, no. c, pp. 1–1, 2019.

- [17] T. Loutas, N. Eleftheroglou, and D. Zarouchas, "A data-driven probabilistic framework towards the in-situ prognostics of fatigue life of composites based on acoustic emission data," *Compos. Struct.*, vol. 161, 2017.
- [18] C. Scheffer, H. Engelbrecht and P.S. Heyns, "A comparative evaluation of neural networks and hidden Markov models for monitoring turning tool wear,". *Neural Comput & Applic* 14, 325–336, <https://doi.org/10.1007/s00521-005-0469-9>, 2005.
- [19] M. Shu, B. Hsu, and K. C. Kapur, "Dynamic performance measures for tools with multi-state wear processes and their applications for tool design and selection," *Inter.l Jour. of Production Research* 48(16):4725-4744, 2010.
- [20] R. Moghaddass and M. J. Zuo, "An integrated framework for online diagnostic and prognostic health monitoring using a multistate deterioration process," *Reliab. Eng. Syst. Saf.*, vol. 124, pp. 92–104, 2014.
- [21] J. Z. Sikorska, M. Hodkiewicz, and L. Ma, "Prognostic modelling options for remaining useful life estimation by industry," *Mech. Syst. Signal Process.*, vol. 25, no. 5, pp. 1803–1836, 2011.
- [22] X. S. Si, W. Wang, C. H. Hu, and D. H. Zhou, "Remaining useful life estimation - A review on the statistical data driven approaches," *Eur. J. Oper. Res.*, vol. 213, no. 1, pp. 1–14, 2011.
- [23] A. Saxena, J. Celaya, B. Saha, S. Saha, and K. Goebel, "Metrics for Offline Evaluation of Prognostic Performance," *Int. J. Progn. Heal. Manag.*, vol. 1, no. 1, pp. 1–20, 2010.
- [24] T. Peng et al., "Probabilistic fatigue damage prognosis of lap joint using Bayesian updating," *J. Intell. Mater. Syst. Struct.*, vol. 26, no. 8, pp. 965–979, 2015.
- [25] K. Goebel, B. Saha, A. Saxena, and M. Field, "A Comparison of Three Data-Driven Techniques for prognostics," *NASA doc.*, pp. 1–13, 2008.

4

Adaptive RUL prediction model

4.1. Introduction

This chapter introduces the basic structure of the ANHHSMM, a successor of the NHHSM developed by Moghaddass and Zuo [1], and explains how this stochastic process can be used for multistate degradation modeling when states are hidden (not directly observable) and unexpected events may occur. Furthermore, the main assumptions and elements of the NHHSM are described in Section 4.2. Section 4.3 presents the diagnostic measure, which evaluates the current health status of the studied engineering system and Section 4.4 presents the adaptation process and three additional assumptions, which were used to design the ANHHSMM. Finally, in Section 4.5, prognostic measures, which predict the RUL of the engineering system, are introduced.

4.2. Non-Homogeneous Hidden Semi Markov model

This section presents and discusses the main assumptions that Moghaddass and Zuo [1] made so as to involve the NHHSM. Moghaddass and Zuo's assumptions are presented just for the consistency of the thesis. In addition, the basic structure and key elements of the NHHSM are presented in that section too.

4.2.1. Assumptions

Moghaddass and Zuo's assumptions set the scope with regards to practical applications. The main NHHSM's assumptions are itemized as follows [1]:

- I. The engineering system has N known possible discrete levels of degradation states ranging from the perfect functioning state (state 1) to the complete failure state (state N). Each health state may reflect a certain level of damage, operational performance, efficiency, and/or physical properties.
- II. Except the failure state, which is assumed to be self-announcing, the state of the engineering system is only indirectly observable through CM data.
- III. At any level of health states, the engineering system can degrade according to three types of transitions, which are; (I) transition to the neighbour state (soft degradation), (II) transition to the failure state (hard failure), and (III) transition to any intermediate state (multi-step degradation).
- IV. Transition rate function is used as the main describer of the degradation process. Each degradation transition can follow an arbitrary distribution. Degradation transitions between two states may depend on the states involved in the transition, the time spent at the current state, the total age of the engineering system, or any combination of these factors.
- V. CM data cannot directly reflect the actual damage state of the studied engineering system. Also, in this thesis a single CM indicator is used for health monitoring. This single indicator can be the output of a feature fusion process, which transforms a set of indicators to a single one. This indicator is calculated at certain discrete points referred to as observation points.

- VI. The time between two observation points is small enough, so that at most one transition may occur in the interval between two observation points.
- VII. The CM indicator can take one of the V possible outcomes denoted by z_1, z_2, \dots, z_V .
- VIII. The CM indicator is stochastically related to the actual levels of degradation. This relationship is represented by a nonparametric discrete probability distribution referred to as the observation probability distribution (\mathbf{B}) with discrete values (z_1, z_2, \dots, z_V) . In a general form, the probability that z_k is observed when the device is in state j ($Q_t = j$) is defined as $b_j(k) = \Pr(Y_t = z_k | Q_t = j)$, $\forall t, 1 \leq k \leq D$.
- IX. The engineering system is not repairable or self-healed.

It should be pointed out that the above-described assumptions are related to the NHHSMM. Three additional assumptions for the adaptation process will be discussed in Section 4.4.

4.2.2. Model Selection Process

The primary step in order to use the NHHSMM for diagnostic and prognostic purposes is to define a reasonable and efficient, in terms of computational time, structure for the associated multistate model, in other words to find the best set of characteristic parameters for the selected model. That process is called model selection process and it involves two steps; the initialization step and the parameter estimation step.

The main elements regarding the initialization step that determine a multistate topology are the following $\xi = \{N, \Omega, \lambda, I, V\}$ parameters:

- Number of hidden states (N). N refers to the number of discrete levels of degradation. This value can be defined with respect to the actual degradation states that the system might experience during its lifetime. Many studies have assumed that this parameter is known [2]. However, hidden states are not quantitatively but just qualitatively correlated with the degradation process. As a result, there are also many studies that the number of hidden states is treated as a decision making variable [3]. The parameter N is the most important one since it affects all the other elements of the multistate structure. In addition, as already mentioned in the previous Subsection 4.2.1 the main assumption in this thesis is that the system under study starts to operate on its perfect functioning state, hidden state 1, until its total failure i.e. state N . The final state N is not hidden but self-announcing and always corresponds to the failure state. As a result, the last observation of the available training data should be unique dictating a common failure threshold in the training data.
- Transition between the hidden states (Ω). This parameter defines the connectivity between the N selected hidden states. As noted in the previous Subsection 4.2.1 the studied engineering system is assumed to be not repairable or self-healed and subsequently the possible transition types can be only left-to-right transitions. A

possible left-to-right transition can be: (I) soft (gradual transition to neighbour hidden state), (II) hard (sudden transition from any hidden state to failure state N) and (III) multistep (transition to an intermediate state between the current hidden state and the failure state). Figure 4.1 illustrates the three possible types of left-to-right transition.

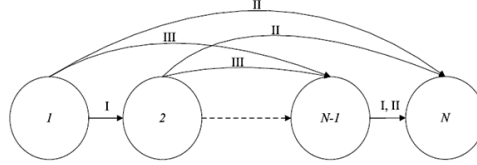


Figure 4.1. Soft (I), hard (II) and multistep (III) types of transition.

- Transition rate function (λ). This parameter is the main describer of the degradation process since each transition is going to follow this λ rate function. The transition process depends on the involved hidden states, the sojourn time of the current hidden state, the total operation time (aging) and any other combination between the aforementioned parameters. In this current study the selected transition type is the Non-Homogeneous semi Markovian degradation type. Commonly used distributions for the λ function are the Weibull, Gaussian, Exponential and Gamma failure rates [4]. In this study the Weibull failure rate is used since it is the most generic one and the most commonly used distribution to represent degradation [5].
- Condition monitoring feature (I). A CM feature is assumed to be a single indicator having hidden or indirect connection with the actual degradation level of the studied engineering system. This connection, between the damage/hidden states and the selected CM feature, is a stochastic relationship and is modeled via a nonparametric discrete probability distribution and represented by an observation probability matrix. In real word applications, finding such a single indicator having a stochastic relationship with the actual damage state is really challenging and difficult task.
- Discrete CM indicator space ($\mathbf{Z}=\{z_1, z_2, \dots, z_V\}$). As mentioned in the previous bullet point the final CM feature is represented in a nonparametric discrete form and consequently it has to be converted to several discreet levels. The selection of the value V is crucial for the observation process since the emission probability matrix has N (number of hidden states) rows and V (number of discrete monitoring values) columns. Therefore, the value V reflects how the selected CM feature is represented. Different methods e.g. vector quantization and clustering can be used in order to determine the value V [6].

Once ζ parameters are determined, the structures of the multistate degradation and observation process are known and the parameter estimation step can be introduced.

With regards to the parameter estimation step, parameters $\boldsymbol{\theta}=\{\boldsymbol{\Gamma}, \mathbf{B}\}$ have to be estimated since these ones characterize the degradation process ($\boldsymbol{\Gamma}$) and observation process (\mathbf{B}). $\boldsymbol{\Gamma}$ parameters characterize the distributions of transition rates between hidden states. For example, if a Weibull distribution is used to represent a Non-Homogeneous Semi-Markov

transition between two states two parameters, the shape and scale, need to be estimated for this transition.

The second group of parameters to be estimated (**B**) represents the stochastic relationship between the hidden state of the studied engineering system and the observation process. As already mentioned this relationship is represented in a nonparametric and discrete form by the observation probability matrix. The entries of this matrix are some of the unknown parameters of the N. This matrix has N (number of hidden states) rows and V (number of discrete monitoring values) columns. The entry in the element (i,j) of the emission probability matrix represents the probability that z_j CM value is observed when the system is in hidden state i.

Let's assume that there are K independent degradation histories, extracted from K similar engineering systems. This set of K degradation histories called training data set. Each degradation history of the selected CM feature was extracted while the engineering system was operating.

Moghadass and Zuo [1] proposed a method for defining the Maximum Likelihood Estimator (MLE) θ^* of the model parameter θ . The MLE utilization leads to maximize the likelihood function $L(\theta, y^{(1:K)})$ Equation (4.1), where $y^{(k)}$ is the k-th degradation history.

$$L(\theta, y^{(1:K)}) = \prod_{k=1}^K Pr(y^{(k)}|\theta) \xrightarrow{L'=\log(L)} L'(\theta, y^{(1:K)}) = \sum_{k=1}^K \log(Pr(y^{(k)}|\theta))$$

$$\theta^* = \arg \max_{\theta} \left(\sum_{k=1}^K \log(Pr(y^{(k)}|\theta)) \right) \quad (4.1)$$

The MLE approach begins with a random initialization of $\theta=\{\Gamma, \mathbf{B}\}$ parameters and it aims to the iterative maximization of the $\sum_{k=1}^K \log(Pr(y^{(k)}|\theta))$ value. This procedure concludes to the estimation of parameters θ^* , that describe the most probable model for a given training data set and initialization parameters ζ . With $\mathbf{M}^*=\{\zeta, \theta^*\}$ the estimated complete model is denoted for further diagnostic and prognostic use.

4.3. Diagnostics

As the degradation process has a monotonic behaviour then a feature sensitive to the degradation process with monotonic behaviour should be found. However, finding such a monotonic behaviour is an interesting and challenging topic for real time applications [7]. In order to provide useful information for the current degradation state of an engineering system, diagnostic measures have to be developed. In this subsection, the Most Likely State (MLS) is presented, which employs CM data that reflects the current degradation state of the system under study.

MLS is capable to monitor the overall health status of an engineering system since it is sensitive to the degradation process and characterized by monotonicity [8]. There are two

main reasons why monotonicity is of importance [7]. Firstly, an oscillating measure cannot reflect the damage development trends perfectly. Secondly, as in this thesis the studied engineering system is assumed to be non-repairable or self-healed, the damage has to increase during the system's lifetime as a result a proper diagnostic measure has to follow this monotonic trend. Therefore, a measure with monotonic trend can better represent the degradation process. It should be pointed out here that the common assumption throughout this subsection is that the structure of the multistate model (\mathbf{M}^*) is already known.

At any time point t the MLS can be calculated as follows:

$$\text{MLS}(t|y_{1:t}, \mathbf{M}^*) = \underset{i}{\operatorname{argmax}} \Pr(Q_t = i | y_{1:t}, \mathbf{M}^*) \quad (4.2)$$

and this measure maximizes the probability $\Pr(Q_t = i | y_{1:t}, \mathbf{M}^*)$ of being at the hidden state i at the time point t given the available testing CM data up to time t , where Q_t is the hidden state of the system at the t observation time point and $\mathbf{M}^* = \{\zeta, \theta^*\}$ the estimated complete model.

4.4. Adaptation process

In addition to the NHHSM's assumptions, presented in Subsection 4.2.1, three additional assumptions should be considered for the development of the ANHHSM:

- X. The emission matrix does not depend on time because it correlates CM data and hidden states. Furthermore, the CM data range remains the same since the last observation, as already mentioned (Assumption I), should be unique dictating a common failure threshold in the training and testing data set. As a result, it is assumed that the emission matrix remains the same during the adaptation process ($\mathbf{B}^* = \mathbf{B}^*$).
- XI. The scale and shape parameters of the Weibull failure rate distribution describe the degradation process Γ . The shape parameter can be interpreted as a value that indicates when the failure rate remains constant, decreases or increases over time. On the other hand, the scale parameter shifts the distribution along the abscissa scale. Assuming that the studied system has the same volume of damage at the end of its lifetime, the scale Weibull parameter adapts only, enabling the sojourn time of each hidden state to shift in time. In order to quantify this shift the aforementioned dynamic diagnostic measure MLS is used. During the testing process, the MLS is estimated enabling the observation of the transition time from the current hidden state i to any new hidden state j . Therefore, the sojourn time of the i hidden state can be defined ($\text{Mean}_{\Gamma i, j}^{**}$). However, the probability density function (PDF) of sojourn time, at hidden state i , is estimated based on the NHHSM's Γ^* parameters ($\text{Mean}_{\Gamma i, j}^*$) and a comparison between these two sojourn times ($\text{Mean}_{\Gamma i, j}^{**}$, $\text{Mean}_{\Gamma i, j}^*$) can be achieved. Since the target of the ANHHSM is to estimate more accurately the RUL of the testing engineering system the scale Γ^* parameters are dynamically adapted so as to have mean sojourn times the

values which the MLS has defined. This adaptation is determined via introducing the Equation (4.3) [9].

$$\text{Scale}_{\Gamma_i, j^{**}} = \frac{\text{Mean}_{\Gamma_i, j^{**}}}{\text{Gamma}(1 + 1/\text{Shape}_{\Gamma_i, j^*})} \quad (4.3)$$

- XII. The ratios between the training and testing sojourn times of hidden state i and $i+1$ should be constant. To demonstrate this last assumption, which dynamically updates the sojourn times of the future hidden states based on the current and past hidden states' sojourn time adaptation, the following flowcharts and pseudo code are presented.

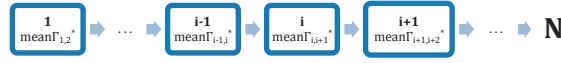


Figure 4.2. Sojourn times per hidden state based on the NHHSM Γ^* parameters.

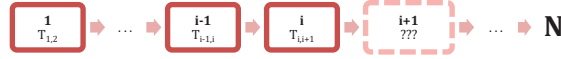
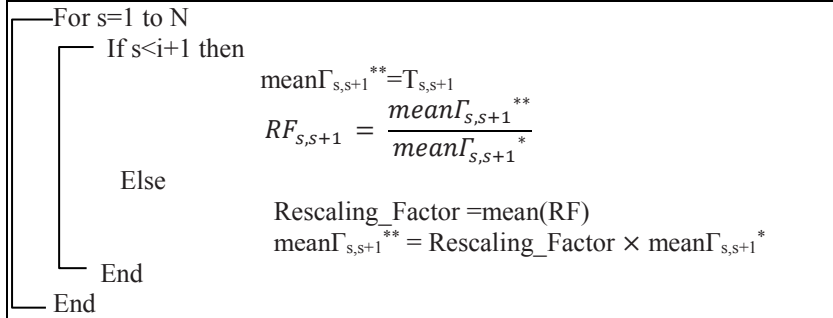


Figure 4.3. Sojourn times per hidden state based on the MLS diagnostic measure when the studied engineering system just transited from the hidden state i to $i+1$.

The following pseudo code adapts dynamically the sojourn time of each hidden state when the engineering system just transited from the hidden state i to $i+1$.



Based on the aforementioned three assumptions the dynamic adaptation process, which is the key element of the ANHHSM, receives as inputs the extracted testing CM data and the estimated model's parameters θ^* . The flowchart of the adaptation process is presented in Figure 4.4.

4.5. Prognostics

Although important diagnostic measures, such as MLS, can provide useful information on the current damage state of the studied engineering system, prognostic measures are more attractive to maintenance decision makers as they provide information on the future health status of an engineering system, which can be used for maintenance decision making. This subsection is devoted to important prognostic measures, which are calculated from the available testing CM data, the complete adapted model $\mathbf{M}^{**}=\{\boldsymbol{\zeta}, \boldsymbol{\theta}^{**}\}$ and provide information regarding the RUL of the testing engineering system.

Prognostics tries to estimate the probability of being in hidden states $1, \dots, N-1$ at a specific time points in future using the conditional reliability function. The conditional reliability function, $R(t|y_{1:t_p}, D > t_p, \mathbf{M}^{**}) = \Pr(D > t|y_{1:t_p}, D > t_p, \mathbf{M}^{**})$, that is, the probability that the studied engineering system continues its operation after a time t given; time t is less than life-time D ($D > t$), time point t is further than the current time t_p , the engineering system has not failed yet ($D > t_p$), the testing data $y_{1:t_p}$ and the complete adapted model \mathbf{M}^{**} . The cumulative distribution function (CDF) of RUL is defined at any time point via the conditional reliability according to the following equation:

$$\Pr(RUL_{t_p} \leq t|y_{1:t_p}, \mathbf{M}^{**}) = 1 - R(t + t_p | y_{1:t_p}, \mathbf{M}^{**}) \quad (4.4)$$

In this study the mean and confidence intervals of RUL are proposed as prognostic measures. These measures were calculated via the CDF of RUL [5]. Equation (4.5) defines the mean RUL expression.

$$\overline{RUL}(t|y_{1:t_p}, L > t_p, M) = \int_0^\infty R(t + \tau | y_{1:t_p}, L > t_p, M) d\tau \quad (4.5)$$

In prognostics, an estimate of the uncertainty associated with the mean RUL predictions is of utmost importance, in order to give a confidence of the predicted mean value. The calculation of confidence intervals is based on the calculation of the $a\%$ and $(1-a)\%$ lower and upper percentiles respectively. It is important to note that simulation-based numerical data, via the MC simulation method, are used in Chapter 5 so as to verify the efficiency and correctness of the ANHHSMM.

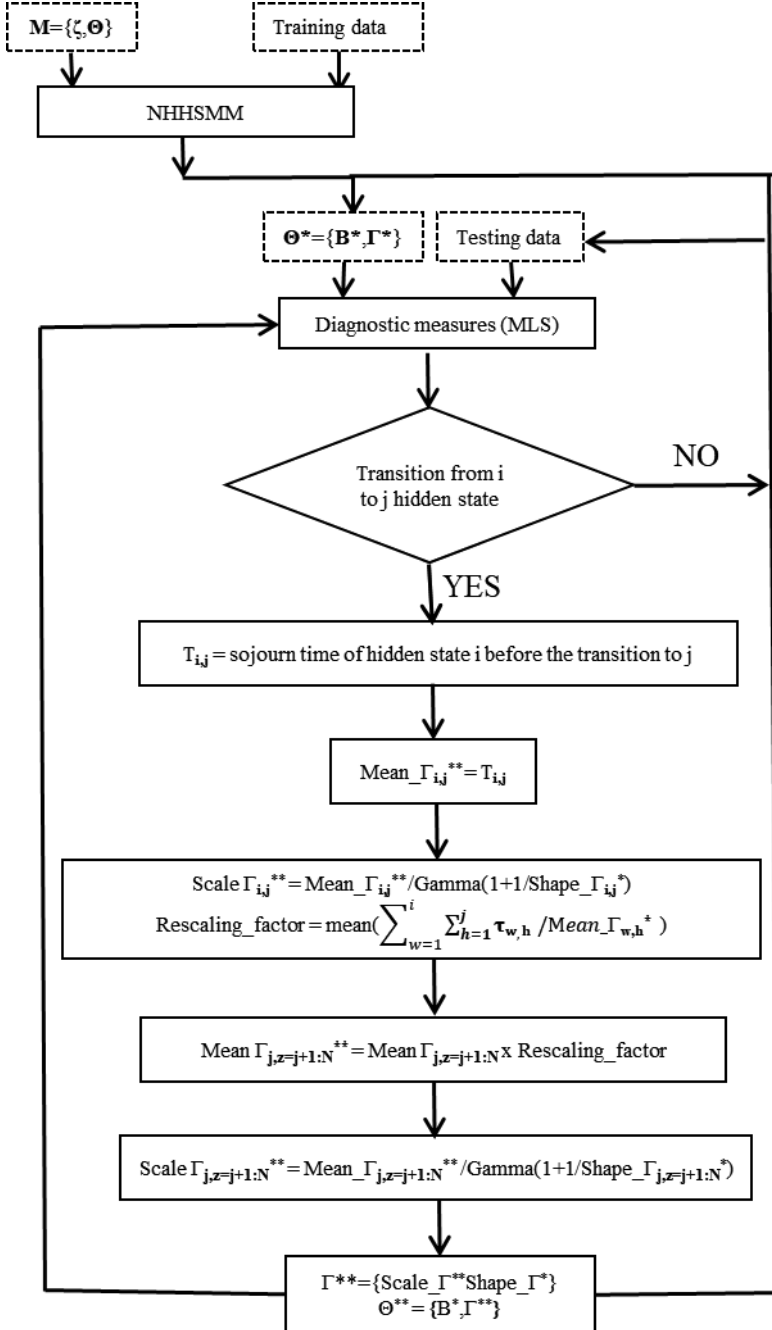


Figure 4.4. Dynamic adaptation process flowchart.

References

- [1] R. Moghaddass and M. J. Zuo, "Multistate degradation and supervised estimation methods for a condition-monitored device," *IIE Trans. (Institute Ind. Eng., vol. 46, no. 2, pp. 131–148, 2014.*
- [2] B. M. Hsu and M. H. Shu, "Reliability assessment and replacement for machine tools under wear deterioration," *Int. J. Adv. Manuf. Technol., vol. 48, no. 1–4, pp. 355–365, 2010.*
- [3] P. Baruah and R. B. Chinnam, "HMMs for diagnostics and prognostics in machining processes," *Int. J. Prod. Res., vol. 43, no. 6, pp. 1275–1293, 2005.*
- [4] Ramin Moghaddass, "Equipment Degradation Diagnostics and Prognostics Under a Multistate Deterioration Process," *Dissertation, 2013.*
- [5] R. Moghaddass and M. J. Zuo, "An integrated framework for online diagnostic and prognostic health monitoring using a multistate deterioration process," *Reliab. Eng. Syst. Saf., vol. 124, pp. 92–104, 2014.*
- [6] H. Jégou, M. Douze, and C. Schmid, "Product quantization for nearest neighbor search," *IEEE Trans. Pattern Anal. Mach. Intell., vol. 1, no. 33, pp. 117–128, 2011.*
- [7] Z. Shen, Z. He, X. Chen, C. Sun, and Z. Liu, "A monotonic degradation assessment index of rolling bearings using fuzzy support vector data description and running time," *Sensors (Switzerland), vol. 12, no. 8, pp. 10109–10135, 2012.*
- [8] N. Eleftheroglou and T. Loutas, "Fatigue damage diagnostics and prognostics of composites utilizing structural health monitoring data and stochastic processes," *Struct. Heal. Monit., vol. 15, no. 4, 2016.*
- [9] B. Deng and D. Jiang, "Determination of the Weibull parameters from the mean value and the coefficient of variation of the measured strength for brittle ceramics," *J. Adv. Ceram., vol. 6, no. 2, pp. 149–156, 2017.*

5

Verification process

5.1. Introduction

In this chapter, simulation-based numerical data, utilizing the MC simulation method, are used to evaluate the prognostics validity of the ANHHSMM. The objective is to verify that the ANHHSMM is able to predict more accurately the RUL than the NHHSM, when the studied engineering system is a left or right outlier and to predict the RUL with the same level of accuracy when the system doesn't exhibit extreme behavior utilizing MC simulated data. The degradation process $\mathbf{\Gamma}$ and observation process \mathbf{B} have to be defined in order to extract the aforementioned MC simulated data. The MC data prognostics of the ANHHSMM will then be compared with the NHHSM's prognostics and the actual RUL, which was originally used to generate the MC data.

5.2. Monte-Carlo inputs

Let's assume that an engineering system, is operating under N discrete levels of degradation. The system will start from hidden state one (health state) and pass through all hidden states before failure (Ω : soft transitions). All states are hidden except the failure state (N), as it is self-announcing as the model dictates. It is assumed that the gradual transition to the neighbour hidden state j depends on the two hidden states involved in the transition and the sojourn time spent at the current state i . For transition rate function (λ) the Weibull failure rate distribution is used as follows:

$$\lambda_{i,j}(s, t) = \frac{\beta_{i,j}}{a_{i,j}} \left(\frac{t}{a_{i,j}} \right)^{\beta_{i,j}-1} \quad \text{if } 1 \leq i \leq N-1, \quad j = i+1 \quad (5.1)$$

in this context, it is important to evaluate the effectiveness of the model by introducing a realistic scenario for the N discrete levels of degradation. The NHHSM data-driven approach has already been applied for a series of applications, e.g. [1] and [2], where it was found that $N=4$ is a representative number to describe the degradation process until failure of those specific systems, thus four levels are adopted for further explanation and demonstration of the model's capabilities. Furthermore, it is challenging for the proposed adaptive model to select four discrete levels because, as mentioned in Chapter 4, the adaptation process occurs when a transition from one hidden state to another takes place. Therefore, the hypothesis is that for a large number of N discrete levels, more transitions are modelled, so more opportunities occur to adapt, giving more chances to the model to update its RUL prediction. Thus, by keeping the N number small the flexibility and effectiveness of the model are limited.

The Weibull scale and shape parameters of the MC simulation are as follows:

$$\mathbf{\alpha} = \begin{pmatrix} - & 64 & - & - \\ - & - & 46 & - \\ - & - & - & 25 \end{pmatrix} \quad \mathbf{\beta} = \begin{pmatrix} - & 12 & - & - \\ - & - & 10 & - \\ - & - & - & 6 \end{pmatrix}$$

Where the elements in the i^{th} row and j^{th} column of the scale $\mathbf{\alpha}$ and shape $\mathbf{\beta}$ matrices are the parameters of the Weibull distribution associated with the transition from hidden state i to hidden state j .

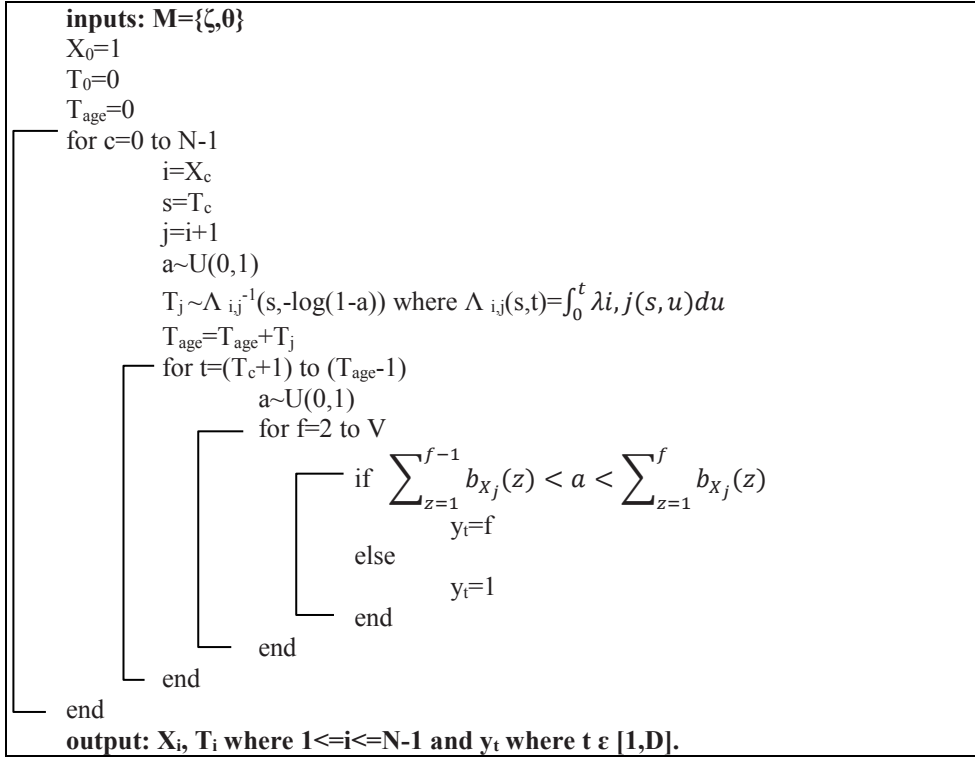
Regarding the observation process **B**, it is assumed that the CM indicator has ten possible discreet values ($V=10$), which are defined by $\mathbf{Z}=\{1,2,3,4,5,6,7,8,9,10\}$. The stochastic relationship between the hidden states and the CM data is represented by the nonparametric discrete distribution emission matrix (**B**). This matrix has four rows since $N=4$ and ten columns since $V=10$, where the element in the i^{th} row and j^{th} column of this matrix represents the probability that the observation will be equal with j when the system is in the hidden state i . It should be noted that the sum of values in each row equals to 1. The emission matrix **B** is defined below:

$$\mathbf{B} = \begin{pmatrix} 0.30 & 0.25 & 0.20 & 0.10 & 0.08 & 0.05 & 0.02 & 0 & 0 & 0 \\ 0.03 & 0.06 & 0.10 & 0.12 & 0.20 & 0.25 & 0.18 & 0.05 & 0.01 & 0 \\ 0 & 0.02 & 0.05 & 0.08 & 0.10 & 0.15 & 0.20 & 0.25 & 0.15 & 0 \\ 0 & 0 & 0 & 0 & 0 & 0 & 0 & 0 & 0 & 1 \end{pmatrix}$$

Considering the above information the initialization parameters $\zeta=\{N,\Omega,\lambda,V\}$, the degradation and observation parameters $\theta=\{\Gamma,\mathbf{B}\}$ are defined. As a result the model is now fully defined $\mathbf{M}=\{\zeta,\theta\}$.

5.3. Simulated MC data Generation

MC method simulates the stochastic behaviour of the studied idealistic system and as a result simulated observation histories are extracted and used as inputs for the parameter estimation process. Based on the parameter estimation process's outputs diagnostics and prognostics can be obtained and compared with the actual values. In this subsection, the MC data generation procedure is described. The simulation process explained here generates multiple sequences of degradation states and their corresponding observation values based on the previously defined model parameters **M**. The simulation process is based on the inverse transform technique. The following pseudo code is used so as to generate one degradation history:



where X_n and T_n are respectively the hidden state and the time at the n^{th} transition, $T_{i,j}^s$ is a random number for the time transition from hidden state i to j , given that hidden state i is reached at time s and V is the maximum discrete CM value. Based on the defined model **M** there are transitions as $X_1=2$, $X_2=3$ and $X_3=4$ with corresponding times T_1 , T_2 and T_3 and **Y** the observation process, where y_i ($1 \leq i \leq L$), which is the corresponding values of the MC observation process with length D associated with (X_n, T_n) .

The output of the above described simulation process is thirteen MC degradation histories ($K=13$), which are generated for the training and testing process. For the training process, ten MC degradation histories, Table 5.1 presents the lifetime of these ten engineering systems, will be used as inputs for the parameter estimation process while the remaining three will be used as testing data. One of the training MC degradation histories is shown in Figure 5.1. The choice of this MC degradation history was random, similar results were obtained for the rest of the other MC engineering systems.

Table 5.1. Lifetimes of training MC systems.

Training MC engineering systems	Lifetime unit
1	131
2	149
3	129
4	139
5	149
6	135
7	150
8	136
9	144
10	124

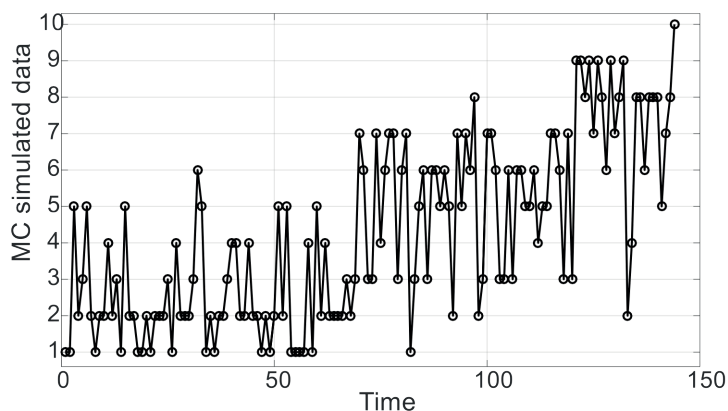


Figure 5.1. MC observation sequence.

Regarding the testing process three MC degradation histories generated and can be used to verify the adaptability of the proposed probabilistic model. The testing data consists of two outliers, one left and one right, and one inlier MC system. The two outliers have significantly shorter (left outlier) and longer (right outlier) lifetimes than any of training systems' lifetimes. The inlier and outliers' MC degradation (red) and observation (blue) processes are presented in Figures 5.2-5.4.

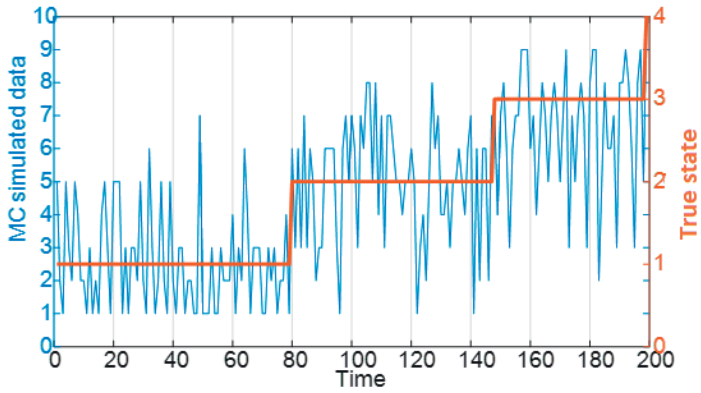


Figure 5.2. Right outlier's observation (blue) and degradation (red) processes.

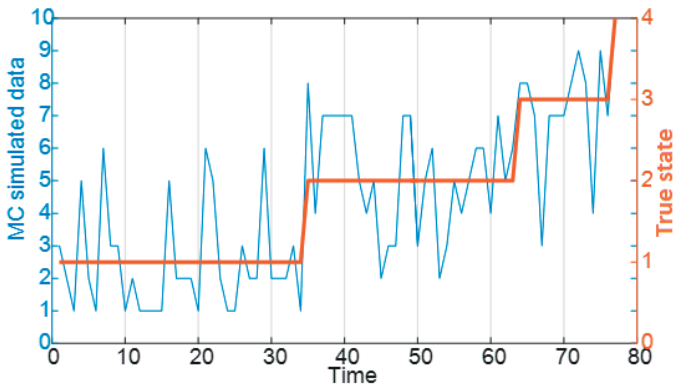


Figure 5.3. Left outlier's observation (blue) and degradation (red) processes.

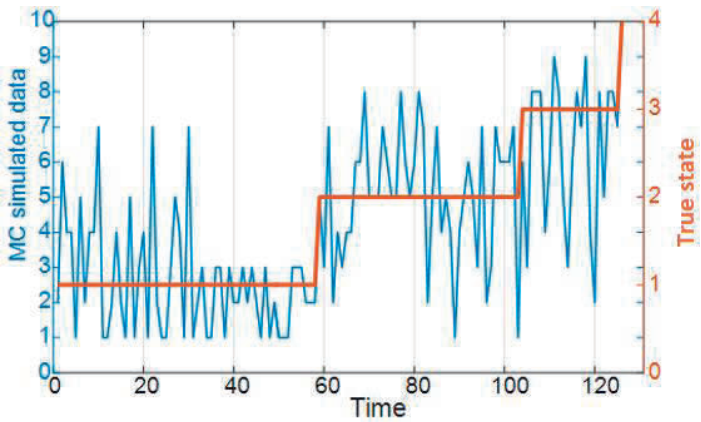


Figure 5.4. Inlier's observation (blue) and degradation (red) processes.

5.4. Parameter estimation process

The proposed parameter estimation process requires the initialization parameters $\zeta = \{N, \Omega, \lambda, V\}$. The initialization parameters ζ are exactly the same with the MC initialization parameters, so in that case $N=4$, Ω : soft transitions, λ : Weibull failure rate and $V=10$, since in the adaptive parameter estimation process the ζ parameters are initialization parameters and the goal is to estimate the observation process (**B**) and degradation process (**Γ**) parameters (**$\theta = \{\Gamma, B\}$**). Therefore, the parameter estimation process requires initial estimates for all the unknown **θ** parameters. For the transition distributions the initial value of 50 is assumed for all the scale parameters (**α**) and the initial value of 4 is assumed for all shape parameters (**β**). The selection of these initial values is based on the training data set's lifetimes. The mean value of our training data set failure time, see Table 5.1, is 138 time units and the mean Weibull value of each hidden state, except the final one, setting the scale parameter equal to 50 and the shape parameter equal to 4 is 45. As a result utilizing these initialization parameter the assumed failure time is $3 \times 45 + 1 = 136$ time units which is pretty close to the mean training data set failure time (138 time units). In case of setting totally different scale and shape initial values, the parameter estimation process' computational time will be affected and became less efficient. For the emission matrix (**B**) the discrete uniform distribution is utilized whereby a finite number of values are equally likely to be observed. The selection of the discrete uniform distribution makes sense since it is not known how the hidden states are connected with the CM data. To be more specific, the initial value of $(1/(M-1))$ is assumed for all entries except those in the last row and the last column, which are related to the observable failure state, $B(4,10)=1$. The threshold of 0.001 is considered as the stopping criterion for the log-likelihood function improvement (Equation 4.1). The final estimated **$\theta^* = \{\Gamma^*, B^*\}$** parameters are presented and compared with MC parameters in Tables 5.2 and 5.3.

Table 5.2. Comparison between MC and NHHSMM Weibull (**Γ**) parameters.

Scale Parameters	MC value	Estimated value	Shape Parameters	MC value	Estimated value
$\alpha(1,2)$	64	68	$\beta(1,2)$	12	16
$\alpha(2,3)$	46	49	$\beta(2,3)$	10	13
$\alpha(3,4)$	25	26	$\beta(3,4)$	6	6

Table 5.3. Comparison between MC and NHHSMM emission matrix (**B**) parameters.

MC values									
$B = \begin{pmatrix} 0.30 & 0.25 & 0.20 & 0.10 & 0.08 & 0.05 & 0.02 & 0 & 0 & 0 \\ 0.03 & 0.06 & 0.10 & 0.12 & 0.20 & 0.25 & 0.18 & 0.05 & 0.01 & 0 \\ 0 & 0.02 & 0.05 & 0.08 & 0.10 & 0.15 & 0.20 & 0.25 & 0.15 & 0 \\ 0 & 0 & 0 & 0 & 0 & 0 & 0 & 0 & 0 & 1 \end{pmatrix}$									
Estimated values									

$$B^* = \begin{pmatrix} 0.27 & 0.26 & 0.21 & 0.10 & 0.08 & 0.06 & 0.02 & 0 & 0 & 0 \\ 0.03 & 0.04 & 0.12 & 0.11 & 0.20 & 0.24 & 0.19 & 0.06 & 0.01 & 0 \\ 0 & 0.02 & 0.04 & 0.07 & 0.10 & 0.17 & 0.20 & 0.24 & 0.16 & 0 \\ 0 & 0 & 0 & 0 & 0 & 0 & 0 & 0 & 0 & 1 \end{pmatrix}$$

5.5. Adaptation process

The suggested adaptation process receives as inputs the testing MC data and the estimated parameters θ^* . The adaptation process will be applied three times, once per observation sequence i.e. left outlier, right outlier and inlier case. Only the left outlier will be presented hereafter in details, since the adaptation process for the other two cases is exactly the same.

Figure 5.5 presents the left outlier's MLS estimations as calculated from Equation (4.2) at each time point. Figure 5.5 reflects that this MC system is an outlier since the sojourn time of the hidden state 1 based on MLS is just 34 time units and based on the NHHSMM is 66 time units, see Figure 5.6. Similar results were obtained for the sojourn time of the hidden state 2 since MLS sojourn time is 26 time units and NHHSMM sojourn time is 47 time units. Utilizing the NHHSMM estimated parameters θ^* , the testing data and the MLS estimations the ANHHSMM can be defined and dynamically adapt the parameters θ^* to θ^{**} , following the process which described in Section 4.3. The outcome (Weibull pdfs) of the ANHHSMM (dashed lines) is presented in Figure 5.6 and it is compared with the NHHSMM's estimated parameters.

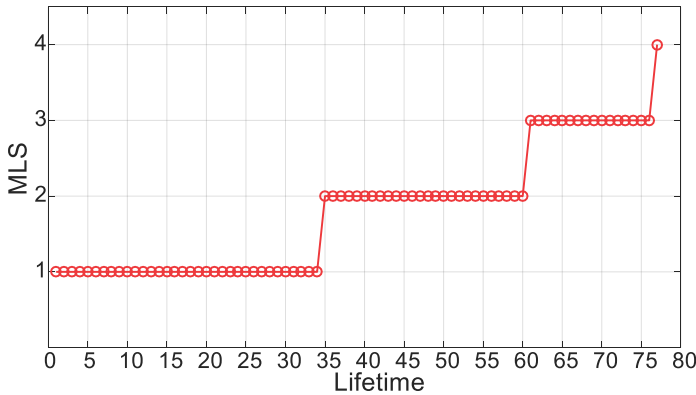


Figure 5.5. MLS diagnostic estimations of left outlier's case.

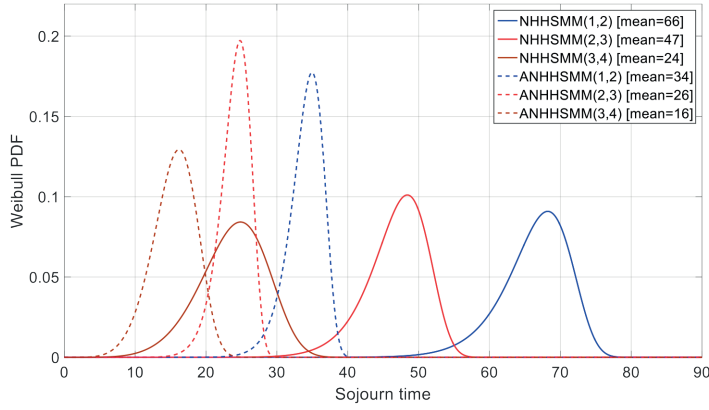


Figure 5.6. Sojourn time Weibull distributions utilizing the Γ^* and Γ^{**} parameters of left outlier's case.

Based on Figure 5.6 the ANHHSM Weibull pdfs are shifted to the left side as it was desired since the testing MC system is the left outlier while the NHHSM Weibull pdfs don't manage to capture the swift properly. In this direction the ANHHSM prognostic estimations are expected to be more accurate, comparing with the NHHSM estimations since the mean sojourn time values are getting shorter.

Figures 5.7 and 5.8 present the adaptation output for the right outlier and the inlier case correspondingly. Based on Figure 5.7 the ANHHSM Weibull pdfs are shifted to the right side as it is desired since the testing MC system is a right outlier, while for the inlier case the Weibull pdfs are not shifted significantly as Figure 5.8 presents.

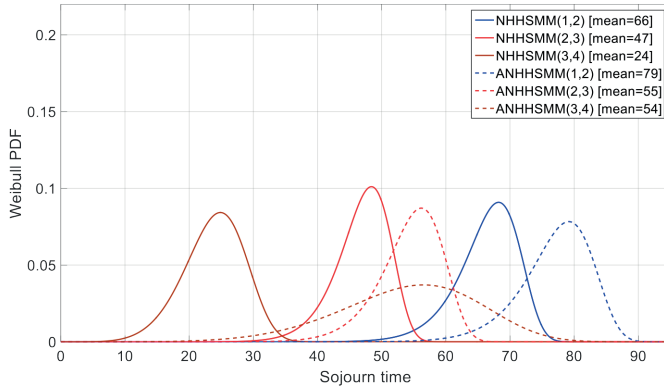


Figure 5.7. Sojourn time Weibull distributions utilizing the Γ^* and Γ^{**} parameters of right outlier's case.

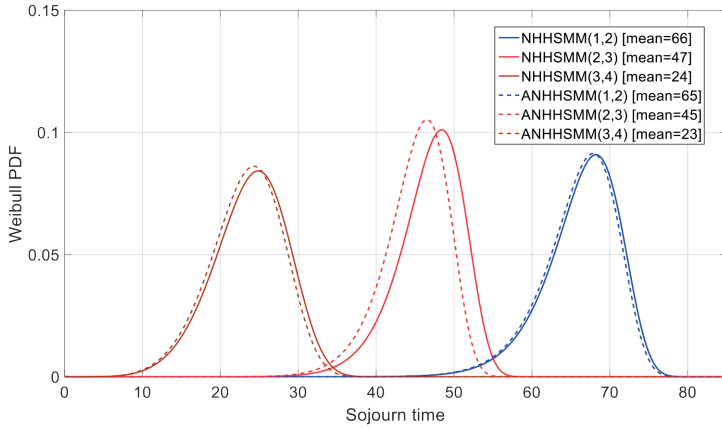


Figure 5.8. Sojourn time Weibull distributions utilizing the Γ^* and Γ^{**} parameters of inlier's.

5.6. Prognostics verification

Following the aforementioned adaptive framework, a four-state ($N=4$) model allowing only soft state transitions was developed where θ^* and θ^{**} parameters were estimated according to the training and testing MC data respectively. The conditional RUL CDF is calculated using Equation (4.4), in real-time at each time point utilizing all the testing MC data up to that time point. The mean RUL and the 2.5% and 97.5% percentiles that define a 95% CI are also highlighted. Figures 5.9–5.11 present the prognostic results of the ANHHMM for the left, right outlier and the inlier case respectively. As already mentioned previously, each testing MC observation sequence was unseen, that is, they did not participate in the training process. For example of the left outlier, the minimum failure time of this training data set is 150 time units while the left outlier's failure time is 77 time units, see Figure 5.3.

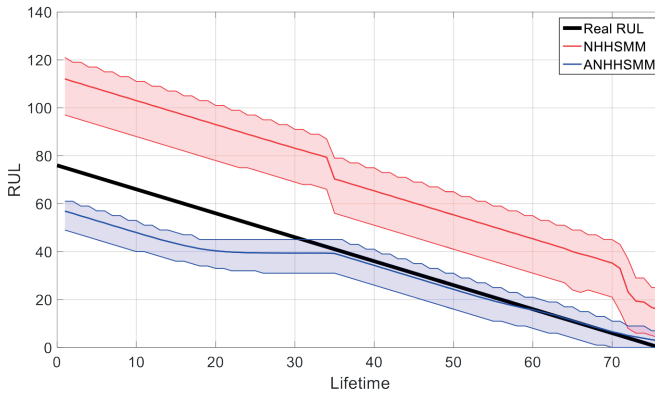


Figure 5.9. RUL predictions of the left outlier.

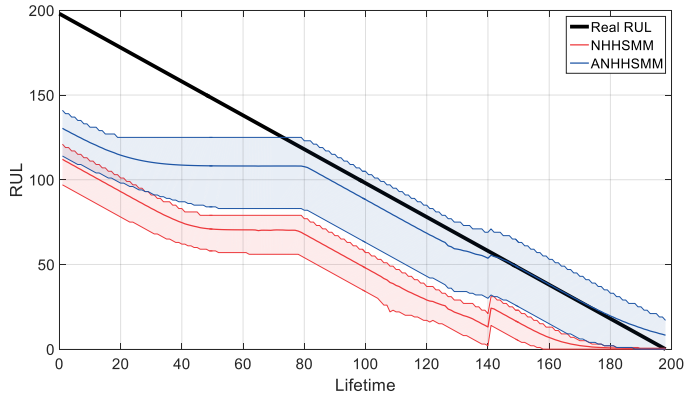


Figure 5.10. RUL predictions of the right outlier.

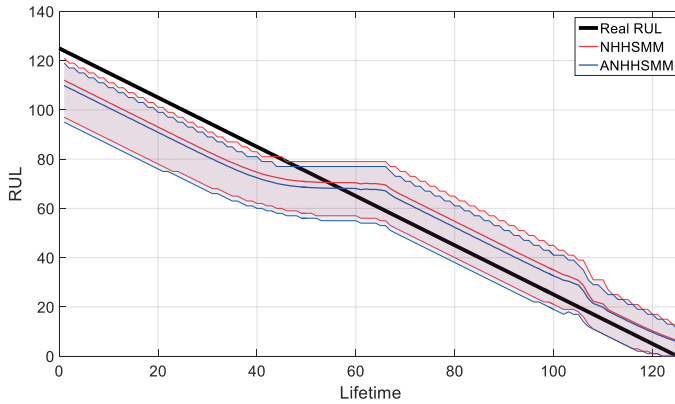


Figure 5.11. RUL predictions of the inlier.

The ANHSM provides clearly better prognostics from the NHHSM for the two outliers, since the mean ANHSM RUL predictions are able to approach more satisfactorily the real RUL predictions and it provides equally acceptable prognostics as the NHHSM for the inlier case. The outstanding performance of the ANHSM for both the right and left outliers, demonstrates that the proposed adaptive framework has succeed its objective; the mean ANHSM RUL predictions are satisfactorily close to the real RUL predictions and the confidence intervals contain the real RUL curve during almost the whole lifetime of the left and right outlier. Furthermore, the ANHSM can identify at a very early stage an outlier and adapt the RUL predictions in an efficient and accurate way since it succeeds the initial RUL predictions to be closer to the real values than the NHHSM's RUL predictions.

5.7. Conclusions

In this chapter, the efficiency and the correctness of the ANHHSMM were verified via simulated MCdata. Ten MC observation histories were used for training and three for the testing process. In conclusion, the results demonstrate that the ANHHSMM provides better prognostics regardless if the engineering is an outlier or inlier. As a result, adapting in real-time the NHHSMM's parameters using the MLS diagnostic measures has the potential to predict the RUL of outlier and inlier cases more efficiently and accurately.

References

- [1] T. Loutas, N. Eleftheroglou, G. Georgoulas, P. Loukopoulos, D. Mba, and I. Bennett, "Valve Failure Prognostics In Reciprocating Compressors Utilizing Temperature Measurements, PCA-based Data Fusion And Probabilistic Algorithms," *IEEE Trans. Ind. Electron.*, vol. PP, no. c, pp. 1–1, 2019.
- [2] N. Eleftheroglou, D. Zarouchas, T. Loutas, R. Alderliesten, and R. Benedictus, "Structural health monitoring data fusion for in-situ life prognosis of composite structures," *Reliab. Eng. Syst. Saf.*, vol. 178, 2018.

6

Experimental campaign

6.1. Introduction

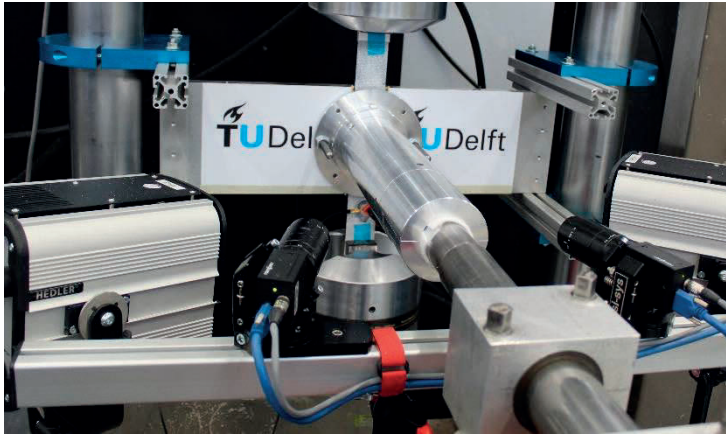
To demonstrate the adaptability and the efficiency of the proposed model, open-hole carbon/epoxy specimens were subjected to in-situ impact and constant amplitude fatigue loading up to failure. The training data set consists of CM data collected from eight specimens, which were subjected only to fatigue loading, while the testing data set consists of CM data collected from four specimens. Three of the testing specimens were subjected to fatigue and in-situ impact loading and the fourth specimen was subjected only to fatigue loading but it had an artificial drilling defect on it. The impact and the artificial drilling defect were introduced only to the testing process aiming to influence the fatigue life and produce outlier cases. Thus, the in-situ impact and the artificial drilling defect can be considered as unexpected phenomena and unseen events regarding the training process. Based on the analysis of the different sources of uncertainty, see Figure 2.5, the in-situ impact can be categorized as a lifetime future state uncertainty and the artificial drilling defect as a lifetime past state uncertainty.

6.2. Experimental set-up and material

Figure 6.1 presents the experimental set-up. The set-up consists of a 100 kN MTS fatigue controller and a bench fatigue machine, an impact canon, an AE system and two cameras for DIC measurements.



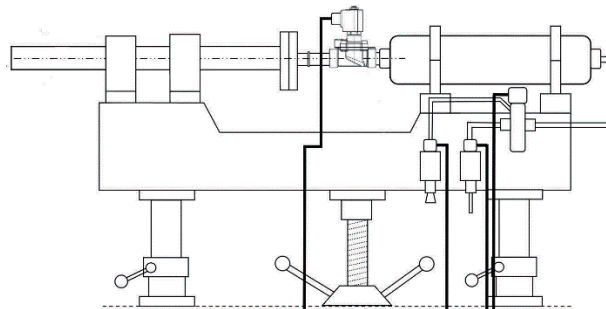
(a)



(b)

Figure 6.1. The experimental set-up.

The impact cannon consists of three parts, the actual (impact) cannon, the nitrogen gas bottle and a safety box. The impact cannon accelerates a projectile in the barrel to a high velocity after which the projectile impacts on the test specimen. The acceleration of the projectile is done with the use of nitrogen up to a desired pressure. The required pressure for the required impact energy is determined utilizing a number of test impacts so as to identify which pressure creates a barely visible impact damage (BVID). BVID is defined as the likely impact damage at the threshold of reliable detection utilizing a visual inspection procedure. The actual cannon consists of a barrel, gas tank, electro-pneumatic valve, valve switch and a pressurization system. The pressurization system contains a pressure sensor, an inlet valve, a safety valve and an operator panel. Figure 6.2 presents a more detailed picture of the impact canon and its components. Because shooting a projectile is inherently dangerous, a safety aluminium cylinder was designed and connected to the canon as Figure 6.1(b) shows. The cylinder was then secured to an aluminium frame, which surrounded the specimen, using two screws. This way, the canon could be used during the fatigue tests without the need to interrupt and remove the specimens.



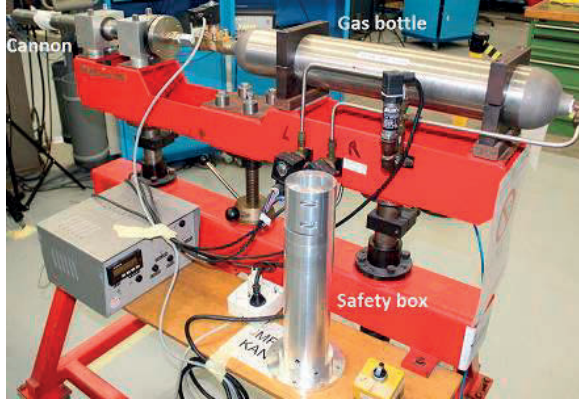


Figure 6.2. Picture of the impact canon [1].

DIC is used for full-field strain measurements, consists of two 8-bit “Point Grey” cameras with “XENOPLAN 1.4/23” lenses. Both cameras have a resolution of 5 MP. DIC was calibrated before the first test and the calibration quality was checked before each new experiment. Vic-Snap 8 software was used to acquire images, which are then processed using the Vic-3D 8 software. In processing these images, the subset size was set to 21×21 pixels with a step size (distance between subsets) of 7 pixels. In order to acquire DIC images the following procedure was designed; every 500 cycles the fatigue test was interrupted, the load was set automatically within one second at σ_{\min} and then the load ramped to σ_{\max} within a second and two images were acquired. After that the fatigue test continued for the next 500 cycles, see Figure 6.3. The process of image acquiring was automated and by triggering the DIC system via the fatigue controller. In case of the in-situ impact, the safety aluminum cylinder covered the specimens monitoring area so DIC images could not be acquired for strain analysis. Therefore, the fatigue controller was paused during the in-situ impact loading.

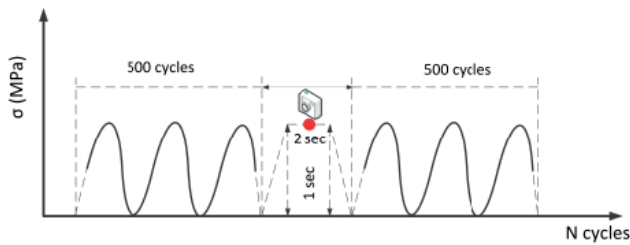


Figure 6.3. DIC data acquisition strategy

An AMSY-6 Vallen Systeme GmbH, 8-channel AE system with the sampling rate of 2 MHz, was employed to record the acoustic emission signals continuously. One broadband single-crystal piezoelectric transducer, i.e. VS900-M, was attached using a clamping device, at the side of specimens between the rigid grip (lower) of the fatigue machine side and of the safety aluminium cylinder. Ultrasound gel was applied between the surfaces of the sensor and the specimen to ensure good acoustical coupling. A standard pencil lead break procedure was used to check connection between the specimen and the sensor prior to the fatigue test and to define the recording threshold, which is equal to 50 dB.

For the in-situ impact tests, two different procedures are possible. For the first one, the canon can be mounted on the frame without interrupting the fatigue test. Although this way the in-situ impact is more realistic, there are technical challenges to address; it is extremely difficult to control at which load level, within the fatigue cycle, the impact occurred and as the safety aluminum cylinder covered the specimens, DIC images could not be acquired for strain analysis immediately after the impact. For the second procedure, the fatigue tests can be interrupted at the desired fatigue cycle and the desired load level. The canon is mounted on the frame, the impact is occurred, then the canon is removed and the fatigue test continues. The procedure of mounting and removing the canon from the test frame lasted for about 3-5 minutes. In this way, it is easier to control at which load the impact would occur and acquire images for the DIC analysis. It is assumed that this short interruption would not affect the fatigue life of the specimens. Based on the aforementioned reasons the second in-situ impact procedure was followed.

The material used for this study is a unidirectional Prepreg tape Hexply® F6376C-HTS(12K)-5-35%. A laminate with $[0/45/90/-45]_{2s}$ lay-up and average thickness of 2.28mm was manufactured using hand lay-up, with a debulking procedure performed after every three plies. The laminate was cured in an autoclave at 180 °C and 9 bar gauge pressure for 120 min time, following the cycle recommended by the manufacturer. Afterwards, the laminate was roughly cut using a Carat liquid-cooled diamond saw, followed by precise cutting using a Proth Industrial liquid-cooled saw. Fifteen specimens, with the following geometrical details; dimensions [400mm x 45mm] and a central hole of 10mm diameter, were tested. Three specimens were tested under quasi-static loading with a displacement rate of 1.5 mm/min in order to define the mean tensile failure load ($S=36$ kN), see Figure 6.4. Twelve specimens were tested under constant fatigue loading with load control at 90% of the mean static tensile failure load with $R=0.1$ and $f=10$ Hz. Out of twelve specimens, three were exposed to in-situ impact and one had an artificial drilling defect. The in-situ impact was occurred at the hole, as this location experiences the highest stresses, aiming to maximize the effect of impact on the damage accumulation process. The selected energy was $E=6$ J (impact velocity 20 m/sec) for all three cases and it can be categorized as high speed low energy impact. Furthermore, during the impact, the specimens were under tension equal to the mean fatigue load (16.2 kN). The time of impact was limited to the period between the start of the fatigue test and until damage could be observed by visual inspection.

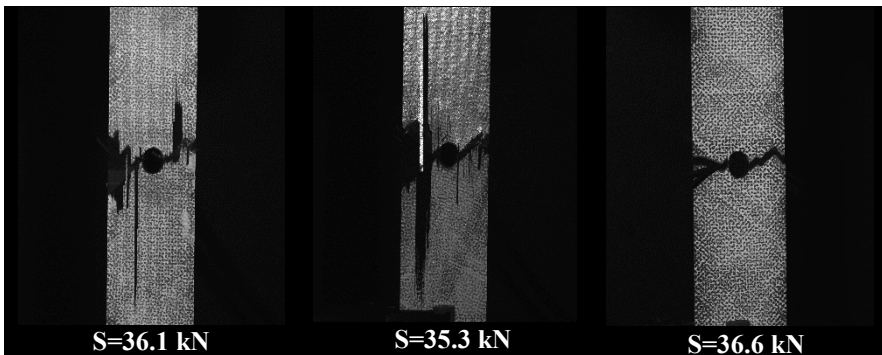


Figure 6.4. Tensile failure loads of the three quasi-static specimens and their failure patterns.

Table 6.1 presents the fatigue lifetime of the training and testing specimens and when the impact occurred. Specimens 09-11 are the testing specimens for which the impact occurred at 5000, 8300 and 2400 sec of their fatigue life respectively. Specimen 12 is the one with the artificial drilling defect (see specimen 12 in Figure 6.5). In terms of clarity in Figure 6.5 all the training and testing specimens are presented. The testing data consists of four specimens; three outliers, one left (specimen10) and one right (specimen11) caused by a future state uncertainty, one left (specimen12) caused by a past state uncertainty, and an inlier (specimen09).

Table 6.1. Fatigue lifetime and impact times of training and testing specimens.

Specimens	Impact time (sec)	Lifetime (sec)
1	-	80996
2	-	57465
3	-	59938
4	-	48978
5	-	67982
6	-	75993
7	-	95357
8	-	106981
Mean value	-	74211.25
9	5000	52418
10	8300	37973
11	2400	130497
12	artificial drilling defect	14976

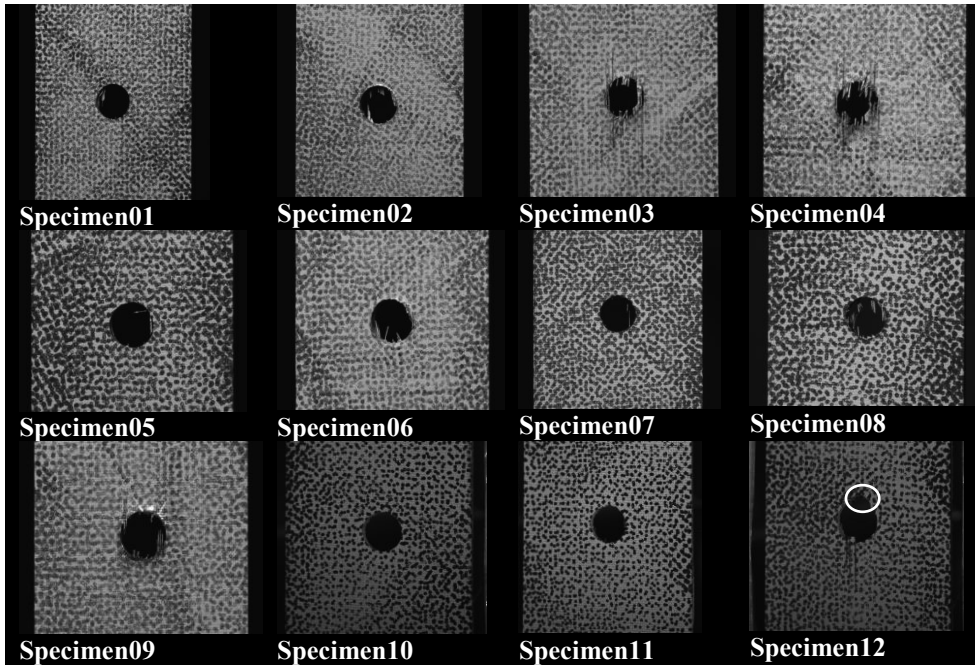


Figure 6.5. Training and testing open-hole specimens.

6.3. Feature extraction process

As mentioned in Chapter 3, it is often desirable to monitor features with a monotonic trend so as to correlate measurements with damage detection [2]. Figure 6.6 summarizes the feature extraction outputs.

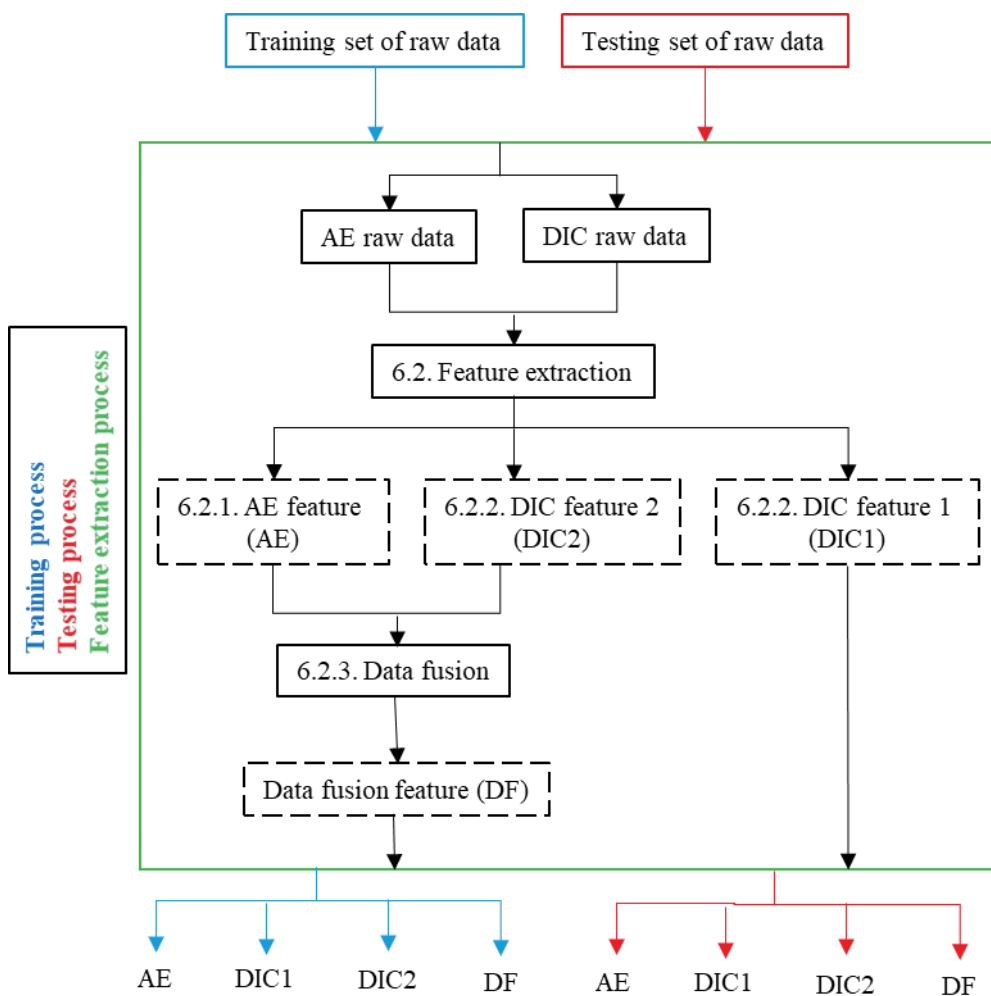


Figure 6.6. Feature extraction process' inputs and outputs.

6.3.1. AE Condition Monitoring data

AE hits are recorded in a non-periodic random manner and the process of monotonic feature extraction is not straightforward. In my previous studies, windowed cumulative AE features such as RA and amplitude, calculated in periodic intervals of constant duration, were used, [2] and [3]. However, in this current study it was not possible to identify any AE feature with monotonic trend without accumulating the feature's values. Therefore, the proposed health indicator is the cumulative energy feature, which by default demonstrates a monotonic

behavior. The AE degradation histories for the twelve specimens are shown in Figure 6.7 while the testing specimens are presented using a dash line. It is important to mention that the feature extraction process is executed utilizing only the training histories since the testing ones are unknown during the whole training process.

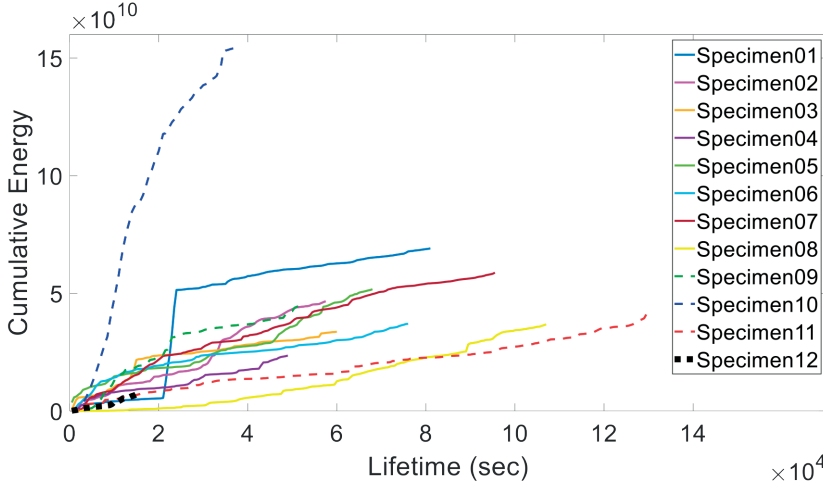


Figure 6.7. Cumulative AE energy observation histories.

Furthermore, as mentioned in Chapter 4, one of the main assumptions of the NHHSM requires the last observation to be unique for all the training data so as to define a common end-of-life threshold [4]. However, as Figure 6.7 presents, it is hard to find such a threshold using the cumulative AE energy observation training histories. For the reason that the threshold should be drawn using as reference the training specimen04, in that case the threshold corresponds almost to 50% of the lifetime in all the other specimens, resulting to an unrepresentative training data set.

The only way to tackle this issue is to normalize each cumulative energy history with the maximum energy value, as Figure 6.8 showcases. However, by normalizing the feature with the maximum value, hinders the real-time applicability of the RUL for the testing specimens, because prior knowledge of the maximum AE energy cannot be obtained.

The normalized cumulative AE energy observation histories of Specimens 1 to 8 will be used as inputs for the parameter estimation process. Regarding the testing process the remaining four observation histories, i.e. Specimen 9 to 12, will be used to verify the adaptability of the proposed probabilistic methodology.

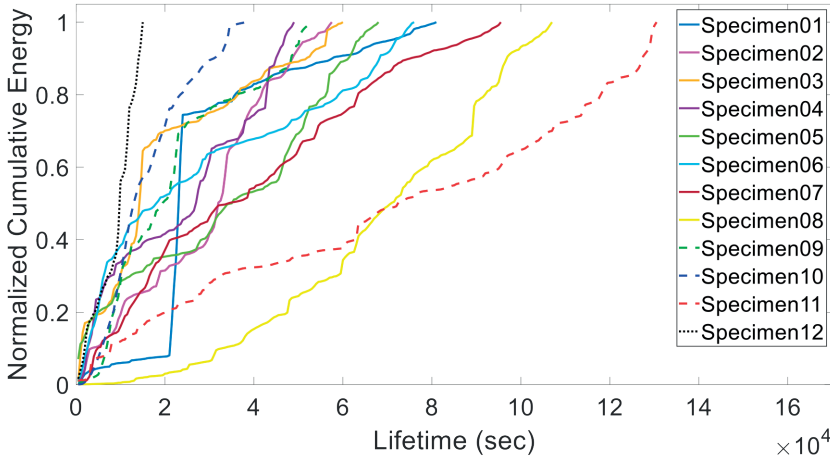


Figure 6.8. Normalized cumulative AE energy observation histories.

In addition, as discussed earlier in Chapter 4, the final CM feature should be represented in a nonparametric discrete form. Therefore, the normalized cumulative energy histories need to be converted to several discrete values. In literature several clustering techniques are used so as to convert the value of a feature in a continuous domain to a discrete domain, among them unsupervised k-means clustering has been successfully applied in the domain of CM [5].

The key element and challenge of using k-means clustering are to find the optimal number of clusters V that represents the number of discrete values for the CM feature. In general, if a very small number of clusters V are selected, the feature cannot be a reasonable representative of the degradation process since it is not possible to vary much with the lifetime of the specimen. Therefore, the V should be reasonably large to better reflect the degradation process. However, considering a very large number of clusters V is computationally expensive. In order to identify the optimal number of clusters monotonicity can be used since, as mentioned, it is a desirable characteristic of any CM feature.

To evaluate the variability of a monotonic trend, the MMK criterion, Equation (3.2), can be utilized. Figure 6.9 presents the change in the monotonicity index by increasing the number of clusters. It can be seen that the monotonicity converges for $V \geq 10$. Therefore, the number of possible CM outcomes is selected as 10 ($V=10$) and the clustering centers for the training and testing specimens are presented in Figure 6.9. Figure 6.10 presents the final CM outputs. Once again only the training histories used so as to estimate the number of clusters V and the center of each cluster. These discretized CM histories are considered as the input for parameter estimation process.

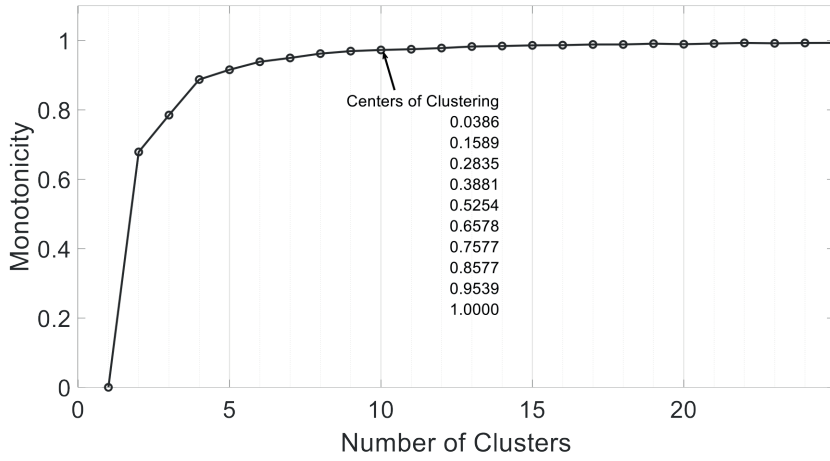


Figure 6.9. MMK monotonicity index versus the number of states and clustering centers when $V=10$ and CM feature is the normalized cumulative energy acoustic emission feature.

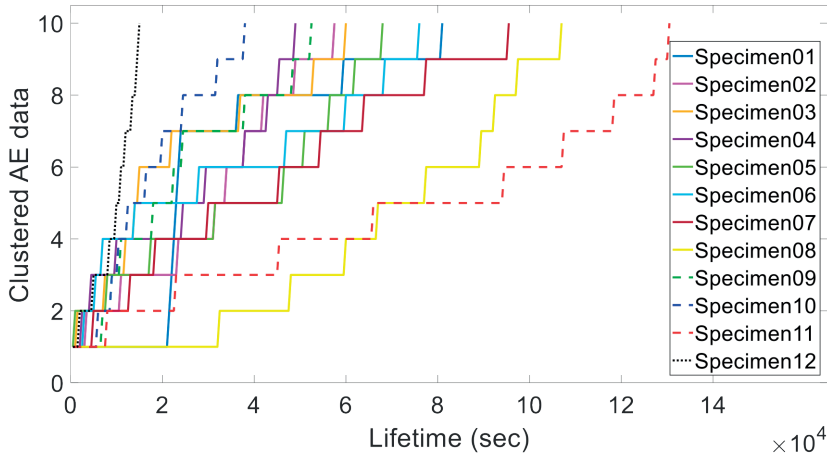


Figure 6.10. Clustered AE degradation histories of training and testing open-hole specimens.

6.3.2. DIC Condition Monitoring data

DIC technique enabled strain measurements in the entire surface of the specimen. Figure 6.11 presents the axial strain distribution, strain in the load direction Y axis, as calculated at the maximum loading during the fatigue test of specimen01 after 500 fatigue cycles. Based on the analytical model of Lekhnitskii [6], which calculates the effect of a notch on the stress/strain distribution, the write rectangle, highlighted at the Figure 6.11, was chosen as the critical point to extract axial strains. Figure 6.12 presents the training and testing axial strain degradation histories, which were extracted for the aforementioned critical point.

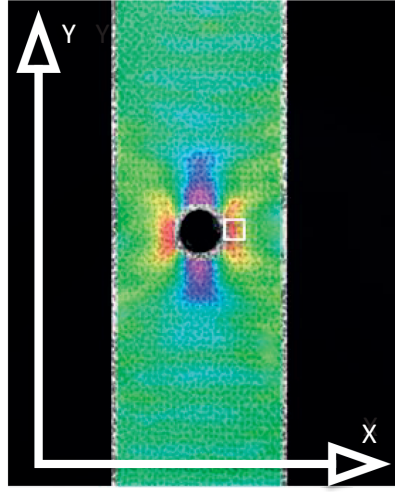


Figure 6.11. Axial strain distribution of specimen01 and its critical area.

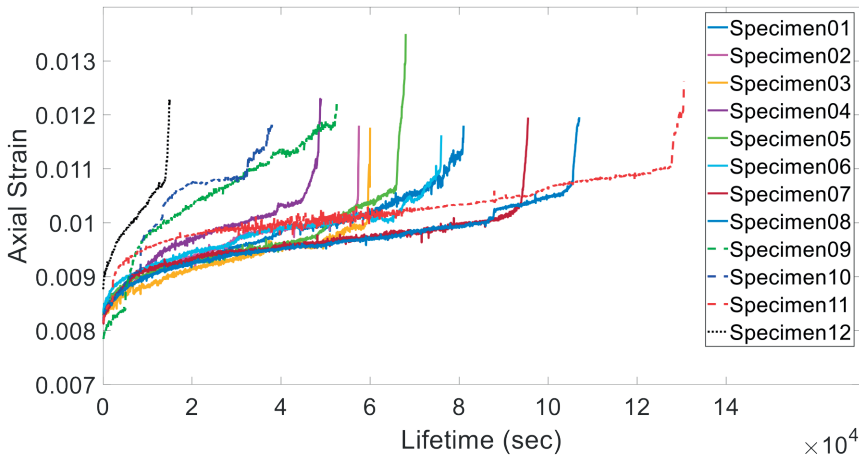


Figure 6.12. Axial strain degradation histories of twelve open-hole specimens.

Based on Figure 6.12 the axial strain feature fulfils the desired monotonic trend and the main assumption of the NHHSMM, which requires the last observation to be unique for all the training data. Therefore, the axial strain feature can be used as it is for the parameter estimation process.

In Figure 6.13, the extracted axial strain data of specimen09 to specimen11 (testing specimens with impact), specimen12 (artificial drilling defect) and specimen05 (training specimen) are presented in order to show that the feature of axial strain is able to capture at least qualitative an unexpected event in real-time. In case of the future state uncertainty, jumps' time points of specimens 09-11 are exactly the same with the impact time points and in case of the past state uncertainty the initial axial strain of specimen12 is larger than the all the other specimens.

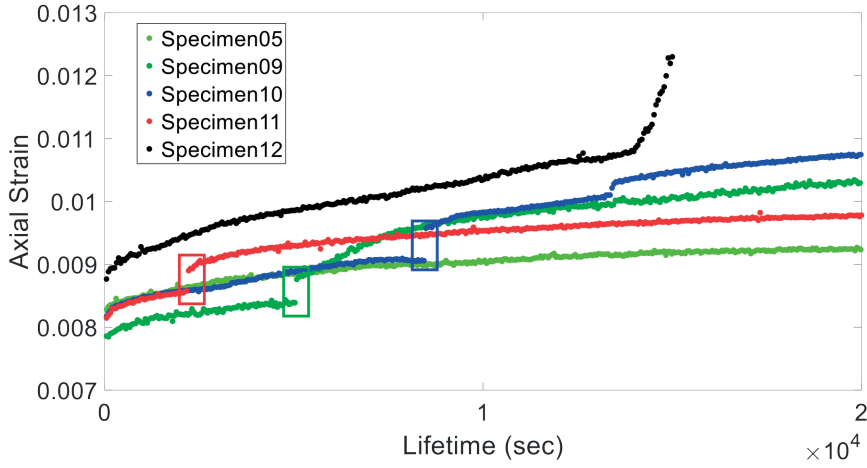


Figure 6.13. Axial strain degradation histories jumps due to impact loading.

The final CM feature should be presented in a discrete form by the clusters V and it can be calculated using the MMK criterion. The MMK converges for the number of clusters V equals to 10 for the axial strain data, as Figure 6.14 presents. Figure 6.15 presents the final clustered axial strain data after the thresholding process.

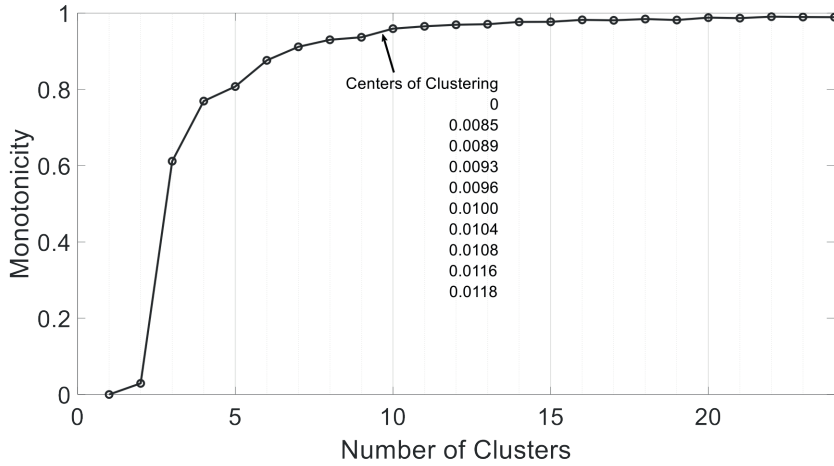


Figure 6.14. MMK monotonicity index versus the number of states and clustering centers when $V=10$ and CM feature is the axial strain feature.

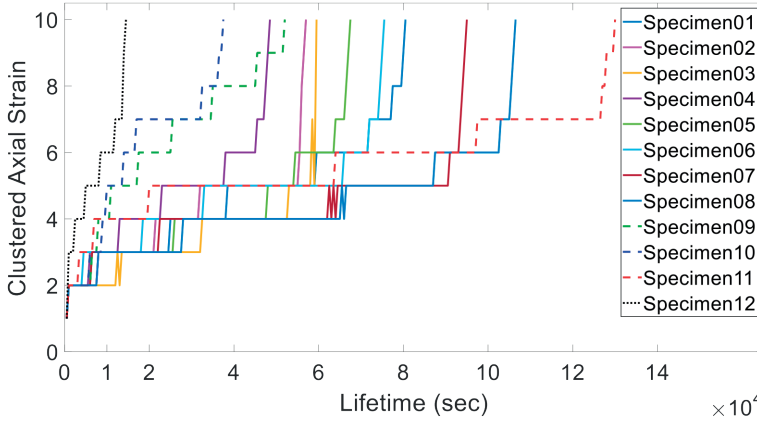


Figure 6.15. Clustered axial strain degradation histories of training and testing open-hole specimens.

However, it is important in terms of clarity and validation to compare AE RUL predictions to DIC RUL predictions independently on the feature extraction process. Therefore, one more DIC feature is designed exactly the same as the final AE feature. Figure 6.16 presents the cumulative normalized axial strain feature, designed based on the axial strain degradation histories as presented in Figure 6.12. As it was expected, the new feature is a linear function of the lifetime. The fatigue life of the laminate used in this study is dominant by the fatigue behaviour of the 0 degrees plies/laminas since the selected lay-up is $[0/45/90/-45]_{2s}$. It is known that the axial strain in the direction of 0 degrees for those plies remain almost constant throughout the fatigue course. Therefore, the cumulative axial strain feature is an integration over a constant variable i.e. the axial strain. As a result, the cumulative axial strain feature is a linear function over time. Hereafter, this new feature is called DIC2 while the clustered axial strain feature is called DIC1. The final discretized DIC2 feature is presented in Figure 6.17 utilizing ten clusters since once again the MMK converges for the number of clusters V equals to 10 as Figure 6.18 presents.

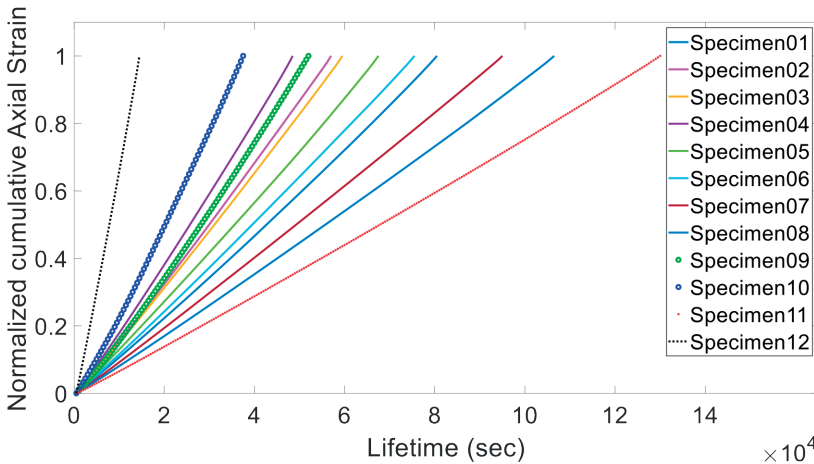


Figure 6.16. Normalized cumulative axial strain observation histories.

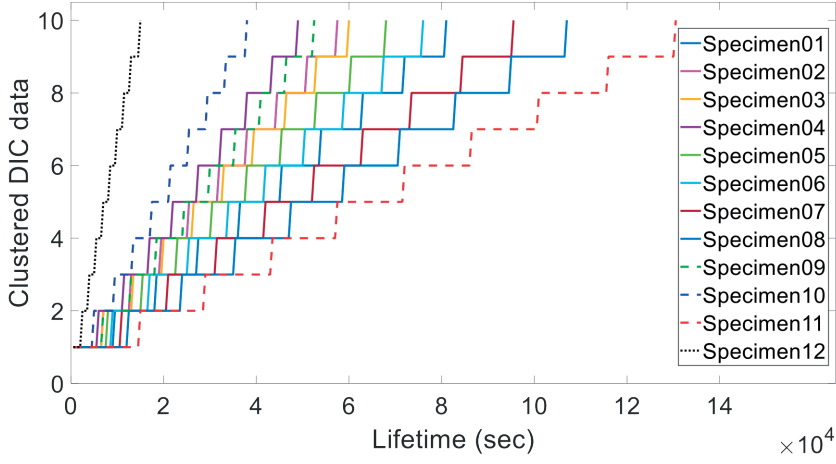


Figure 6.17. Clustered cumulative normalized axial strain degradation histories of training and testing open-hole specimens.

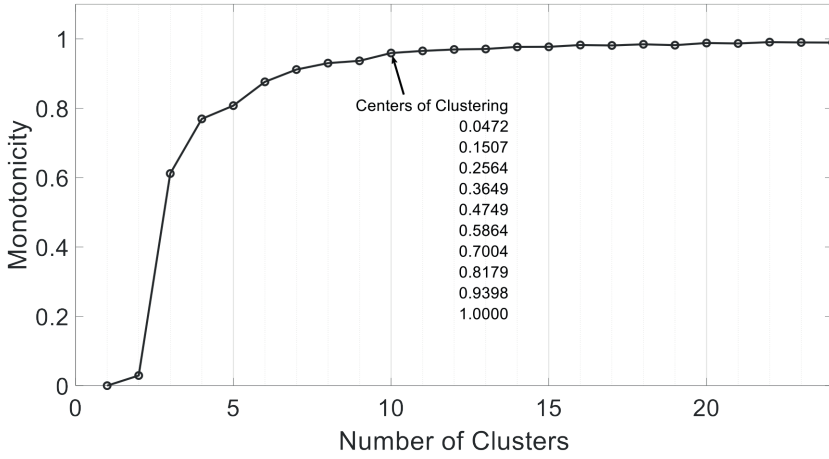


Figure 6.18. MMK monotonicity index versus the number of states and clustering centers when $V=10$ and CM feature is the normalized cumulative axial strain feature.

6.3.3. Fused condition monitoring data

The fusion scheme receives as input the clustered normalized cumulative AE energy (AE) and the clustered normalized cumulative axial strain (DIC2) features, based on the following Equation (6.1).

$$f(DIC2, AE) = \sum_{j=0}^M \sum_{i=0}^{i+j \leq M} a_{ij} \cdot DIC2^j \cdot AE^i \quad (6.1)$$

where f is the fused output feature, a_{ij} are constant coefficients that control the weight of the exponential DIC2 and AE features' product and M the fusion polynomial degree power.

In this thesis, the fusion scheme is based only on trendability since inputs' monotonicity and prognosability indexes have already the maximum values. Therefore, only the trendability index, Equation (3.4), is adopted to enable the data fusion process. Trendability is used as an objective function to determine which polynomial degree M and constant coefficients a_{ij} give the maximum trendability index.

The constant polynomial coefficients a_{ij} , for each polynomial degree M , are based on the optimization problem described in Equation (6.2) with the trendability obtained by the equation (3.4) as the objective function. For the aforementioned optimization problem, different optimization techniques were used i.e. Nelder-Mead, Neural Networks, Particle Swarm Optimization (PSO), Genetic Algorithms and OptQuest/NLP (OQNLP). For this exercise, it was found that OQNLP [7] is the most efficient optimization technique in respect to the computational time for estimating the parameters a_{ij} and M . The unconstrained optimization problem is formulated as:

$$\alpha_{ij}^* = \arg \max_{a_{ij}} \left(\text{Trendability}(a_{ij}, M) \right) \quad (6.2)$$

the results of the optimization study, Equation (6.2), are presented for various polynomial degrees M in Figure 6.19. The MMK monotonicity converges for a polynomial degree $M \geq 7$. Therefore, the polynomial degree is selected as $M = 7$.

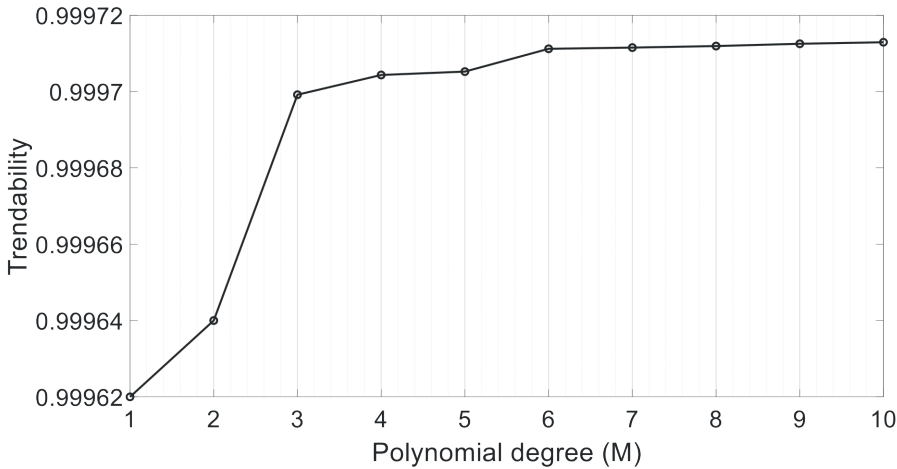


Figure 6.19. Trendability index versus the fusion polynomial degree.

For a polynomial degree with $M=7$, Table 6.2 summarizes the optimization results for the constant coefficients a_{ij} where is concluded that the fused data are designed mainly using the DIC2 feature since the AE coefficients are much smaller than the DIC coefficients.

Table 6.2. Optimization results for $M=7$.

	AE⁰	AE¹	AE²	AE³	AE⁴	AE⁵	AE⁶	AE⁷
DIC2⁰	-3.411e9	2.223e6	1	1	1	1	1	1
DIC2¹	2.161e8	1	1	1	1	1	1	0
DIC2²	-6.292e6	1	1	1	1	1	0	0
DIC2³	1.073e6	1	1	1	1	0	0	0
DIC2⁴	-4.095e3	1	1	1	0	0	0	0
DIC2⁵	1	1	1	0	0	0	0	0
DIC2⁶	1	1	0	0	0	0	0	0
DIC2⁷	1	0	0	0	0	0	0	0

The fused features are depicted in Figure 6.20. MMK convergence study is presented in Figure 6.21 and the final fusion feature in Figure 6.22. Based on the aforementioned optimization results (Table 6.2), the fused feature (Figure 6.22) and the DIC2 feature (Figure 6.17) are exactly the same thus the RUL predictions utilizing the fused data and the DIC2 data are expecting to be the same.

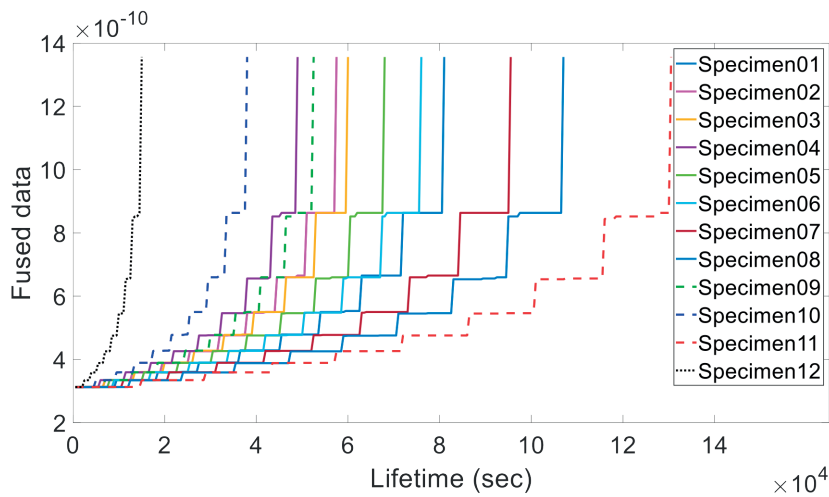


Figure 6.20. Fused degradation histories of twelve open-hole specimens.

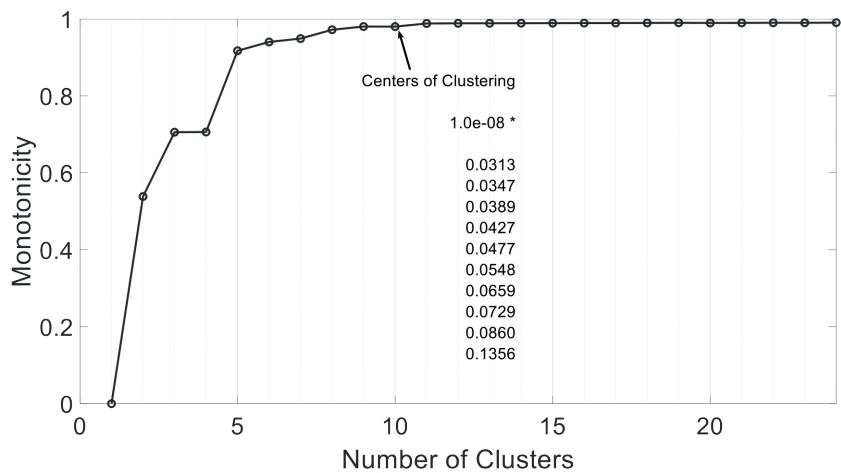


Figure 6.21. MMK monotonicity index versus the number of states and clustering centers when V=10 and CM feature is the fused data.

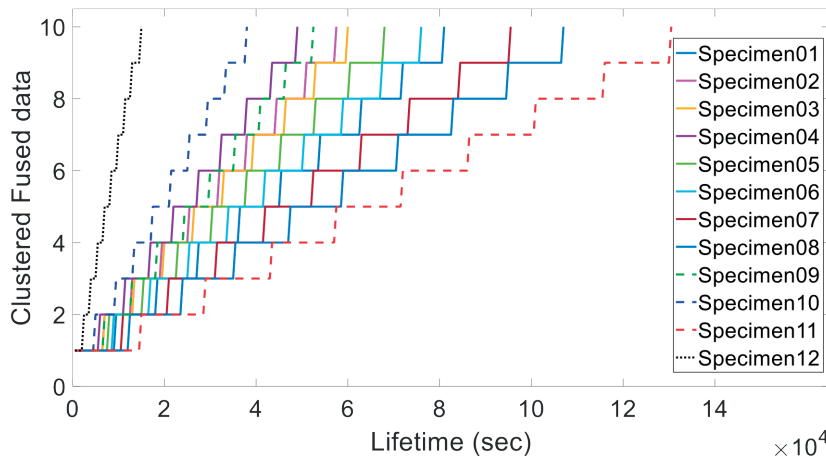


Figure 6.22. Clustered fused degradation histories of training and testing open-hole specimens.

Finally, Table 6.3 presents the trendability index for each CM feature i.e. AE, DIC2 and fused data and it is observed that the fused data has the highest trendability rate.

Table 6.3. Comparison between DIC2, AE and fusion trendability index.

	DIC2	AE	FUSION
Trendability	0.99963	0.78247	0.99971

References

- [1] L. Bollen, P., Kusters and W. Bex, "High Speed Impact Cannon T&TF Instruction," 2013.
- [2] N. Eleftheroglou, D. Zarouchas, T. Loutas, R. Alderliesten, and R. Benedictus, "Structural health monitoring data fusion for in-situ life prognosis of composite structures," *Reliab. Eng. Syst. Saf.*, vol. 178, 2018.
- [3] N. Eleftheroglou and T. Loutas, "Fatigue damage diagnostics and prognostics of composites utilizing structural health monitoring data and stochastic processes," *Struct. Heal. Monit.*, vol. 15, no. 4, 2016.
- [4] R. Moghaddass and M. J. Zuo, "Multistate degradation and supervised estimation methods for a condition-monitored device," *IIE Trans. Institute Ind. Eng.*, vol. 46, no. 2, pp. 131–148, 2014.
- [5] J. Yu. "A hybrid feature selection scheme and self-organizing map model for machine health assessment". *Applied Soft Computing Journal*, 11(5):4041–4054, 2011.

- [6] Lekhnitskii S.G., Tsai S.W., Cheron T. *Anisotropic plates*. Gordon and Breach Science Publishers New York. New York; 1963.
- [7] Ugray Z, Lasdon L, Plummer J, Glover F, Kelley J, Marti R. “Scatter search and local NLP solvers: a multistart framework for global optimization”. *INFORMS J Comp* 2007;19(3):328–40

7

Validation Process

7.1. Introduction

The objective of this chapter is to benchmark ANHHSMM against the state-of-the-art NHHSMM, for testing data, which exhibit outlier behaviour in respect to training data, and to predict the RUL at least with the same level of accuracy when the composite specimen doesn't exhibit extreme behaviour, although it experienced an unexpected event. The benchmark of the RUL predictions is performed using established in literature and newly proposed prognostic performance metrics. Figure 7.1 summarizes the content of Chapter 7.

7.2. Parameter estimation process

As discussed in Chapter 4, the first step of using the ANHHSMM is to determine the $\zeta = \{N, \Omega, \lambda, I, V\}$ initialization parameters for the aforementioned four features i.e. AE, DIC1, DIC2 and Fusion feature. The CM features (I) and their discrete monitoring indicator space Z (V=10) are already defined in Chapter 6. The transition rate's statistical function (λ), from hidden state i to hidden state j , follows a Weibull type degradation. Homogeneous transitions, towards the neighborhood state (soft types of transition) and non-homogeneous hard failures i.e. direct transitions from any state to the failure state (hard types of transition) are allowed only:

$$\lambda_{i,j}(s, t) = \begin{cases} \frac{\beta_{i,j}}{a_{i,j}} \left(\frac{t}{a_{i,j}} \right)^{\beta_{i,j}-1} & \text{if } 1 \leq i \leq N-1, j = i+1 (\text{soft failures}) \\ \frac{\beta_{i,j}}{a_{i,j}} \left(\frac{s+t}{a_{i,j}} \right)^{\beta_{i,j}-1} & \text{if } 1 \leq i \leq N-2, j = N (\text{hard failures}) \end{cases} \quad (7.1)$$

where t is the sojourn time at state i and s the time of entry into state i .

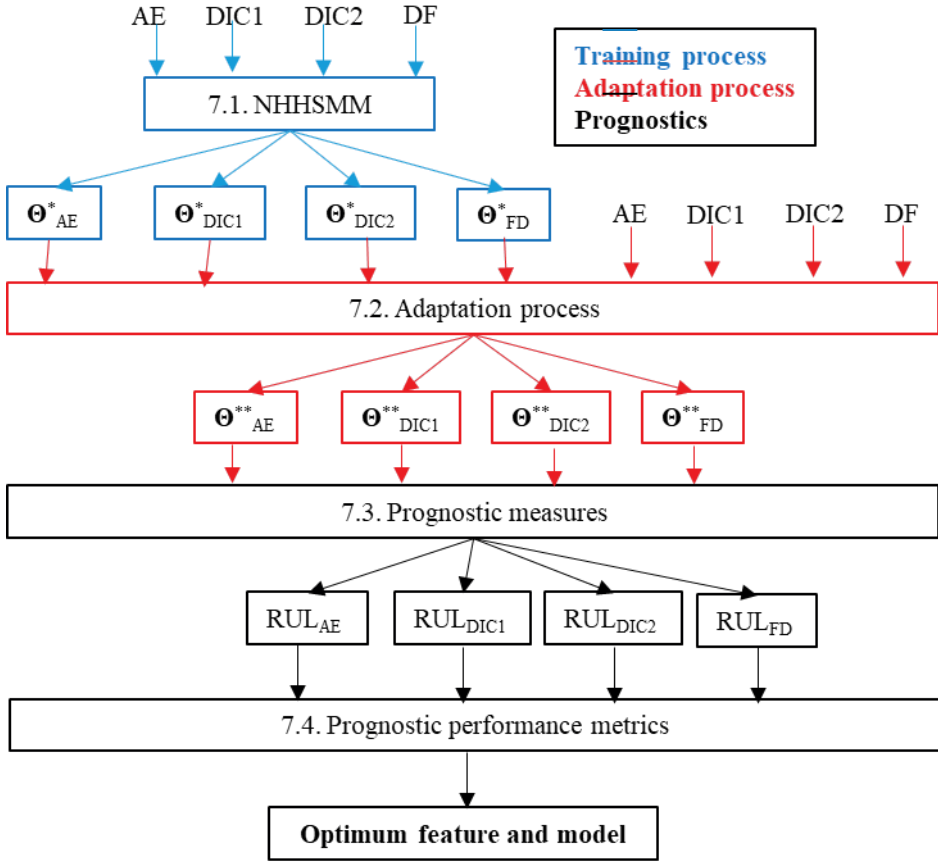


Figure 7.1. Content of Chapter 7.

Having already at hand the final degradation histories from the AE, DIC and fused CM data in Figures 6.10, 6.15, 6.17 and 6.22, the only remaining model parameter is the number of hidden states N . Therefore, the initialization parameter N is considered as the only element that is unknown and not predefined and needs to be estimated. This is a model selection process and a classical way, though non-optimal, is the maximization of the Bayesian Information Criterion (BIC) utilizing the training CM data.

$$BIC(M_i) = \sum_{k=1}^K \log(Pr(y^{(k)}, Q^{(k)} | M_i)) - w \frac{H_i}{2} \log(n) \quad (7.2)$$

where M_i is the candidate model, $y^{(k)}$ the CM data from K training degradation histories, $Q^{(k)}$ the state sequence of the k th training example, H_i is the number of estimated parameters of model M_i and n the number of all observations of K training sequences. Parameter w is the weight of the penalty term and is taken as $w=1$ in the thesis. It is notable that the computation complexity obviously increases exponentially as the number of hidden states N increases.

Figure 7.2 depicts the BIC for all $K=8$ observation sequences of each available feature. BIC gives the highest probability for $N=4$ in all cases.

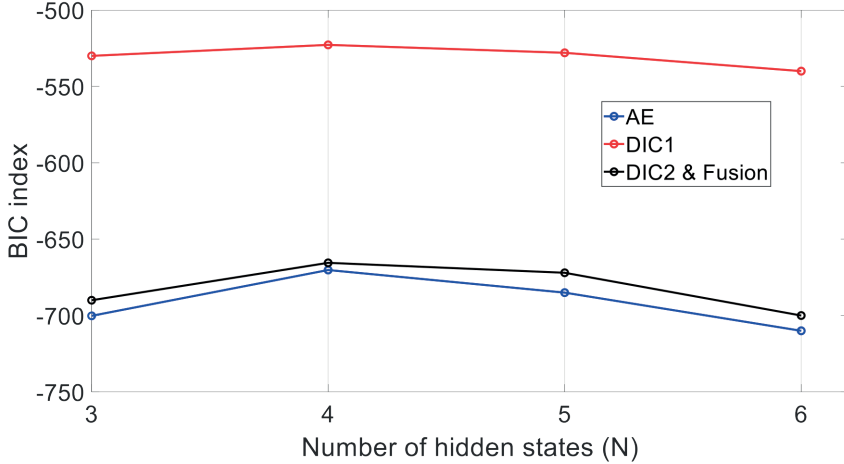


Figure 7.2. BIC for the estimation of the number of hidden states N .

After defining the number of hidden states N the initialization process is totally defined:

- $N=4$
- Ω : soft and hard transitions
- λ : Weibull failure rate
- I : AE, DIC1, DIC2 and fused feature
- $V=10$

For further details about the calculation of the initialization parameters, the reader is referred to the work of [1] and [2]. A four-state model is thus trained for each CM feature, assuming all neighborhood state transitions of the type $1 \rightarrow 2$, $2 \rightarrow 3$, $3 \rightarrow 4$ as well as hard-type failures of the type $1 \rightarrow 4$, $2 \rightarrow 4$. The goal of the parameter estimation process is to estimate the observation process (\mathbf{B}) and degradation process ($\mathbf{\Gamma}$) parameters ($\boldsymbol{\theta} = \{\mathbf{\Gamma}, \mathbf{B}\}$), therefore, the adaptation/parameter estimation process requires initial estimations for all the unknown $\boldsymbol{\theta}$ parameters.

For the transition distributions the initial value of 50 is assumed for all scale parameters ($\boldsymbol{\alpha}$) and the initial value of 1 is assumed for all shape parameters ($\boldsymbol{\beta}$). The selection of these initial values is based on the training data set's lifetimes. In our case the mean value of our training data set failure time, see Table 6.1, is 74211.25 sec and the mean Weibull value of each hidden state, except the final one, setting the scale parameter equal to 27305 and the shape parameter equal to 4 is 24749 sec. As a result utilizing these initialization parameter the assumed failure time is $3 \times 24749 + 1 = 74278$ sec which is pretty close to the mean training data set failure time (74211.25 sec). In case of setting totally different scale and shape initial values the parameter estimation process' output will be the same for the estimated values but the computational time will increase and become less efficient.

For the emission matrix (**B**) the discrete uniform distribution is utilized, whereby a finite number of values are equally likely to be observed. The selection of the discrete uniform distribution it makes sense since we don't know how the hidden states are connected with the CM data. To be more specific, the initial value of $(1/(V-1))$ is assumed for all entries except those in the last row and the last column, which are related to the observable failure state, $B(4,10)=1$. The threshold of 0.0001 is considered as the stopping criterion for the log-likelihood function improvement (Equation (4.1)). The final estimated $\theta^*=\{\Gamma^*,\mathbf{B}^*\}$ parameters are presented in Tables 7.1 and 7.2 for each CM feature.

In our training sets, hard-type failures were not observed and this leads to unrealistic estimated values of the coefficients $\alpha_{1,4}, \beta_{1,4}, \alpha_{2,4}, \beta_{2,4}$ which were consequently excluded from the adaptation, diagnostic and prognostic tasks. This is interesting since the training set actually imposes on the estimated Weibull coefficients the type of transitions that actually take place, excluding transitions non-existent in the training set.

Furthermore, the aforementioned statement regarding the similarity between DIC2 and fusion features is validated through the estimated \mathbf{B}^* and Γ^* parameters since for both features they are exactly the same. Therefore, for the rest of the thesis the fusion feature is excluded since fusion prognostics are going to be exactly the same with DIC2 prognostics.

Table 7.1. NHHSMM Weibull (Γ^*) parameters.

	Scale Parameters	Estimated value	Shape Parameters	Estimated value
AE	$\alpha(1,2)$	33149	$\beta(1,2)$	2.00
	$\alpha(2,3)$	27441	$\beta(2,3)$	2.44
	$\alpha(3,4)$	22727	$\beta(3,4)$	1.85
DIC1	$\alpha(1,2)$	44390	$\beta(1,2)$	4.44
	$\alpha(2,3)$	23637	$\beta(2,3)$	2.36
	$\alpha(3,4)$	22252	$\beta(3,4)$	2.23
DIC2	$\alpha(1,2)$	27054	$\beta(1,2)$	4.51
	$\alpha(2,3)$	26511	$\beta(2,3)$	4.14
	$\alpha(3,4)$	27203	$\beta(3,4)$	4.29
Fusion	$\alpha(1,2)$	27054	$\beta(1,2)$	4.51
	$\alpha(2,3)$	26511	$\beta(2,3)$	4.14
	$\alpha(3,4)$	27203	$\beta(3,4)$	4.29

Table 7.2. NHHSM emission matrix (\mathbf{B}^*) parameters.

AE	$\mathbf{B}^* = \begin{pmatrix} 0.29 & 0.21 & 0.22 & 0.28 & 0 & 0 & 0 & 0 & 0 & 0 \\ 0 & 0 & 0 & 0.01 & 0.32 & 0.33 & 0.34 & 0 & 0 & 0 \\ 0 & 0 & 0 & 0 & 0 & 0 & 0.01 & 0.49 & 0.5 & 0 \\ 0 & 0 & 0 & 0 & 0 & 0 & 0 & 0 & 0 & 1 \end{pmatrix}$
DIC1	$\mathbf{B}^* = \begin{pmatrix} 0.29 & 0.70 & 0.01 & 0 & 0 & 0 & 0 & 0 & 0 & 0 \\ 0 & 0 & 0.59 & 0.40 & 0.01 & 0 & 0 & 0 & 0 & 0 \\ 0 & 0 & 0 & 0.02 & 0.57 & 0.27 & 0.08 & 0.03 & 0.03 & 0 \\ 0 & 0 & 0 & 0 & 0 & 0 & 0 & 0 & 0 & 1 \end{pmatrix}$
DIC2	$\mathbf{B}^* = \begin{pmatrix} 0.34 & 0.33 & 0.33 & 0 & 0 & 0 & 0 & 0 & 0 & 0 \\ 0 & 0 & 0 & 0.33 & 0.34 & 0.33 & 0 & 0 & 0 & 0 \\ 0 & 0 & 0 & 0 & 0 & 0 & 0.33 & 0.33 & 0.34 & 0 \\ 0 & 0 & 0 & 0 & 0 & 0 & 0 & 0 & 0 & 1 \end{pmatrix}$
Fusion	$\mathbf{B}^* = \begin{pmatrix} 0.34 & 0.33 & 0.33 & 0 & 0 & 0 & 0 & 0 & 0 & 0 \\ 0 & 0 & 0 & 0.33 & 0.34 & 0.33 & 0 & 0 & 0 & 0 \\ 0 & 0 & 0 & 0 & 0 & 0 & 0.33 & 0.33 & 0.34 & 0 \\ 0 & 0 & 0 & 0 & 0 & 0 & 0 & 0 & 0 & 1 \end{pmatrix}$

7.3. Adaptation process

The suggested adaptation process receives as inputs the testing AE, DIC1 and DIC2 degradation histories and the estimated parameters θ^*_{AE} , θ^*_{DIC1} , θ^*_{DIC2} . In this case-study the adaptation process will be applied twelve times, once per degradation history; present state left outlier (specimen10), present state right outlier (specimen11), inlier case (specimen09) and past state left outlier case (specimen12), and once per CM feature; AE, DIC1 and DIC2 features. Figures 7.3-7.5 presents the MLS estimations as calculated from Equation (4.2) at each time point for each specimen and each feature. DIC1 feature's transition time points from hidden state 1 to hidden state 2 are the closest to impact time points, comparing to DIC2 and AE transition times, see Table 7.3.

Table 7.3. Comparison between transition time points from hidden state 1 to hidden state 2 with impact time points.

	Specimen09	Specimen10	Specimen11
Impact time point	5000 sec	8300 sec	2400 sec
AE transition 1→2 time point	17500 sec	12000 sec	65500 sec
DIC1 transition 1→2 time point	7000 sec	8500 sec	5500 sec
DIC2 transition 1→2 time point	18000 sec	13000 sec	43000 sec

Therefore, DIC1 feature can be characterized as the best one in terms of diagnostics since MLS estimations are the closest to impact time points, something that was already observed in Figure 6.13.

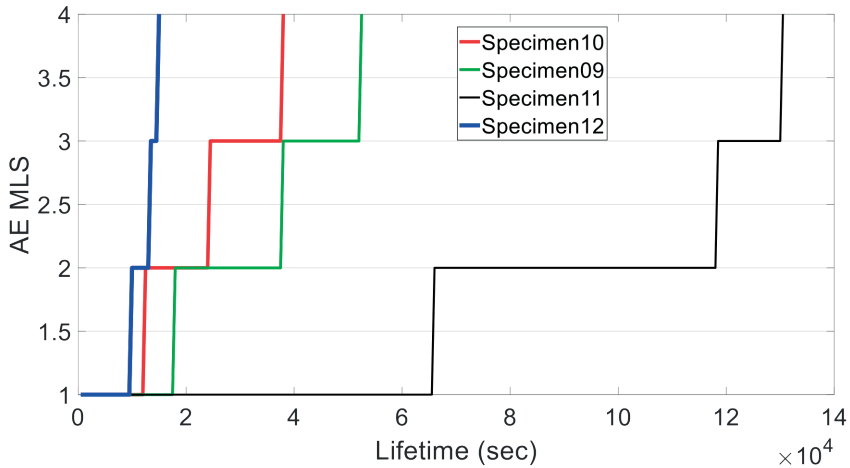


Figure 7.3. AE MLS diagnostic estimations of Specimen09-12.

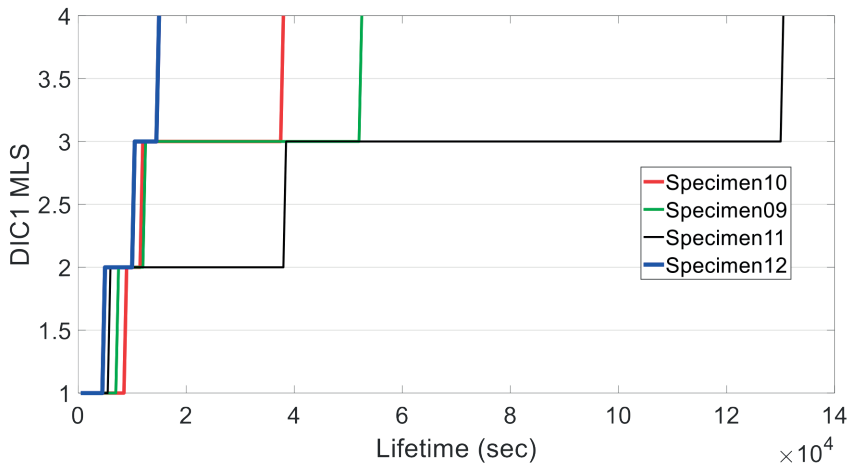


Figure 7.4. DIC1 MLS diagnostic estimations of Specimen09-12.

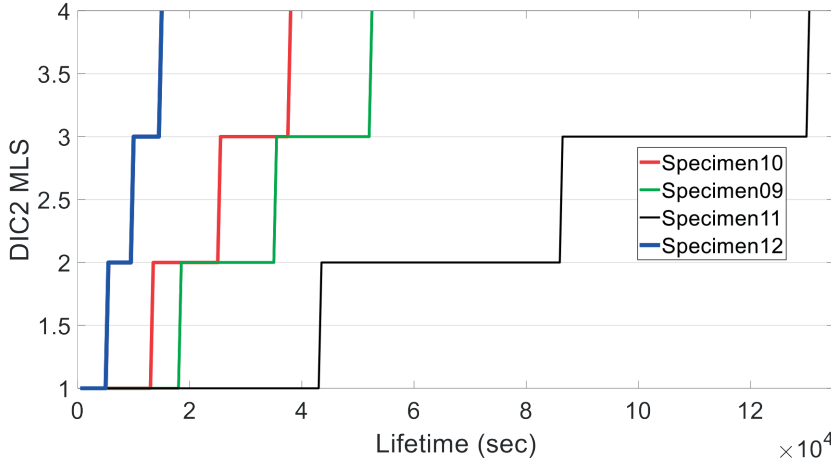


Figure 7.5. DIC2 MLS diagnostic estimations of Specimen09-12.

In Figures 7.6-7.8 the outcome (Weibull pdfs) of the ANHHSM (dashed lines) is presented and compared with the NHHSM's estimated parameters for each specimen and feature.

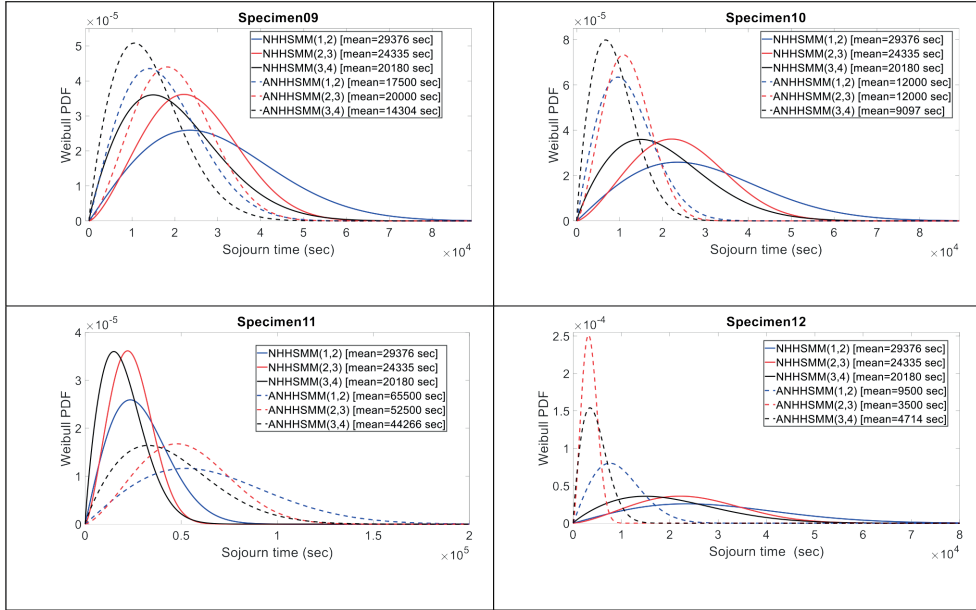


Figure 7.6. AE sojourn time Weibull distributions utilizing the Γ^* and Γ^{**} parameters.

Figures 7.3 and 7.6 reflects that specimen10 is an outlier since the sojourn time of the hidden state 1 based on MLS is just 12000 sec (see Figure 7.3) and based on the NHHSM is 29376 sec (Figure 7.6). Similar results were obtained for the sojourn time of the hidden state 2 since MLS sojourn time is 12000 sec and NHHSM sojourn time is 24335 sec. Utilizing the NHHSM estimated parameters θ_{AE}^* , the testing AE data and MLS estimations the

ANHHSMM is defined and dynamically adapts the parameters θ^*_{AE} to θ^{**}_{AE} , following the process which described in Section 4.3.

Based on Figure 7.6 (Specimen10) the ANHHSMM Weibull pdfs are shifted to the left side as it was desired since specimen10 is the left outlier, while the NHHSM Weibull pdfs don't manage to capture the swift properly. In this direction the ANHHSMM prognostic estimations are expected to be more accurate, comparing with the NHHSM estimations since the mean sojourn time values are getting shorter.

Figure 7.6 presents the adaptation output for the right outlier (Specimen11) and the inlier case (Specimen09) too. Based on Figure 7.6 (Specimen11) the ANHHSMM Weibull pdfs are shifted to the right side as it is desired since Specimen11 is a right outlier, while for the inlier case the Weibull pdfs are not shifted significantly as Figure 7.6 (Specimen09) presents.

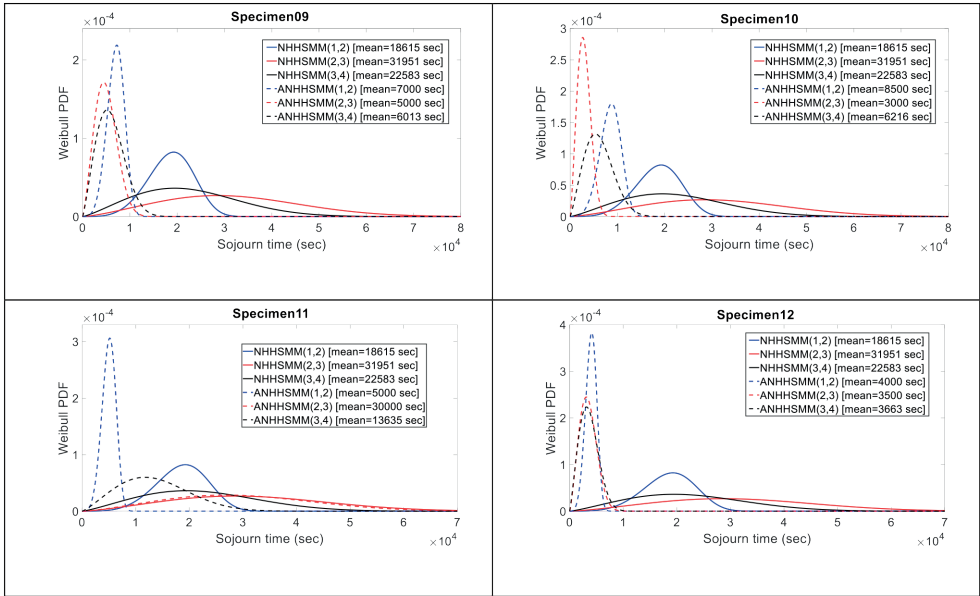


Figure 7.7. DIC1 sojourn time Weibull distributions utilizing the Γ^* and Γ^{**} parameters.

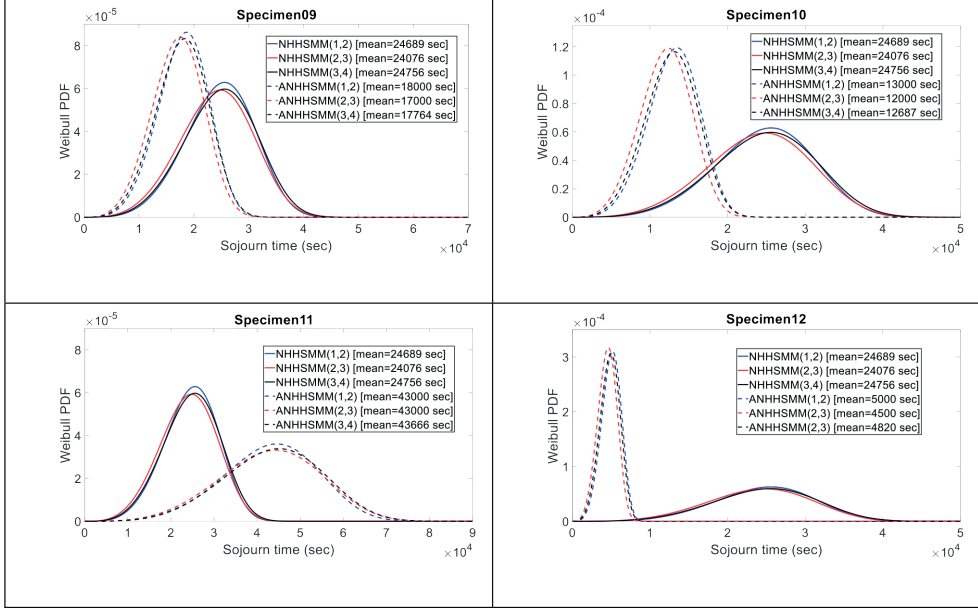


Figure 7.8. DIC2 sojourn time Weibull distributions utilizing the Γ^* and Γ^{**} parameters.

Figures 7.7 and 7.8 present the adaptation process utilizing DIC1 and DIC2 features accordingly. Based on these features the ANHSM Weibull pdfs are shifted to the desired side in almost all cases except DIC1 Specimen09 and DIC1 Specimen11. In these two cases the Weibull pdfs are shifted to the left side, however Specimen09 is an inlier and Specimen11 is a right outlier. Therefore, the prognostics of these two specimen is expected to be less accurate. This undesirable behaviour of the proposed adaptive approach has probably occurred due to the third ANHSM's extra assumption that dictates the ratios between the training and testing sojourn times of hidden states i and $i+1$ should be constant. This undesirable behaviour will be further discussed in the next chapter so as to identify the limitations of the proposed adaptive model.

7.4. Validation of the adaptive model

Following the aforementioned adaptive framework, three four-state ($N=4$) models, allowing soft and hard state transitions, were developed and $\theta^* = \{\theta_{AE}^*, \theta_{DIC1}^*, \theta_{DIC2}^*\}$, $\theta^{**} = \{\theta_{AE}^{**}, \theta_{DIC1}^{**}, \theta_{DIC2}^{**}\}$ parameters were estimated according to the training and testing AE, DIC1 and DIC2 features accordingly. Through Equation (4.4), the conditional RUL CDF is calculated at each time point and feature utilizing all the testing CM data up to that time point. The mean RUL and the 2.5% and 97.5% percentiles that define a 95% CI are also highlighted. Figures 7.9-7.11 present the prognostic results of the ANHSM and the NHHSM for all the testing specimen and features. As already mentioned previously, each testing degradation history was unseen, that is, they did not participate in the training process. For example in case of Specimen10, the minimum failure time of the training data set is 49000 sec, while the Specimen10's failure time is 38000 sec, see Table 6.1.

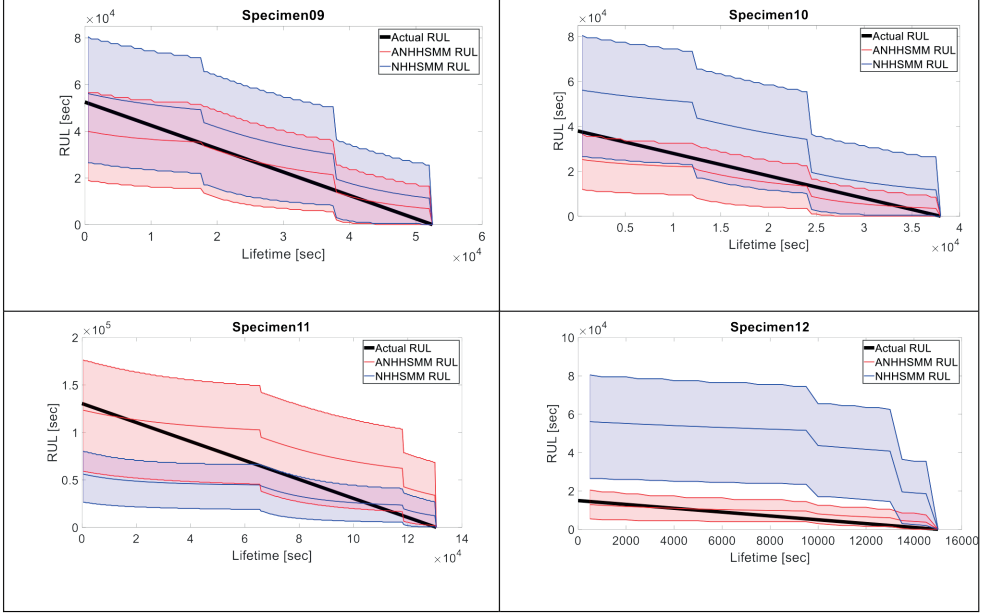
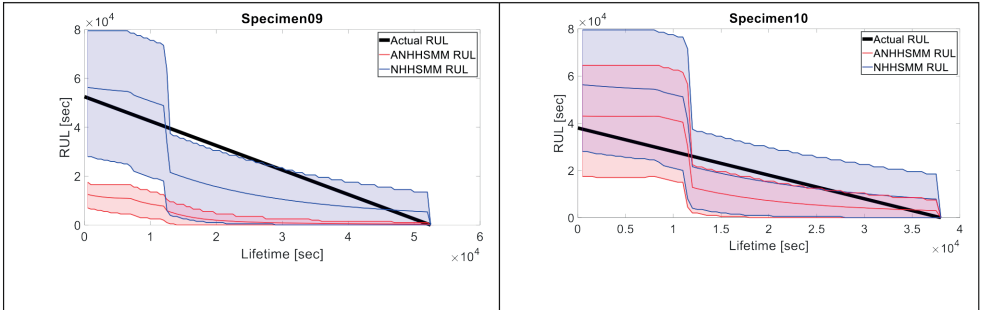


Figure 7.9. AE RUL predictions.

Based on Figure 7.9 the ANHHSM provides better prognostics in comparison with the NHHSM for left outliers (Specimen10 and Specimen12) and the inlier case (Specimen09), since the mean ANHHSM RUL predictions are able to approach more satisfactorily the actual RUL predictions. Furthermore, it can identify at the very early stage the right outlier, i.e. Specimen11, since the initial RUL predictions are closer to the actual ones, than the NHHSM's RUL predictions. However, the NHHSM provides more accurate RUL predictions towards the end of life for the right outlier. Probably, the main reason is that the fatigue life of the right outlier is relatively close to the maximum failure time of the training data set.



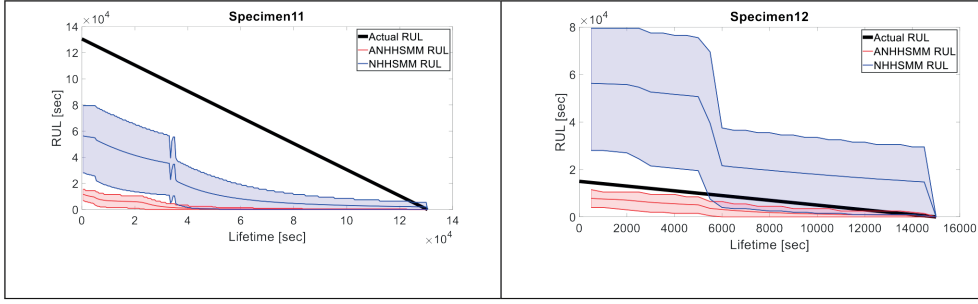


Figure 7.10. DIC1 RUL predictions.

As mentioned in Subsection 7.2, the DIC1 ANHHSMM prognostics of Specimen09 and Specimen11 are not accurate because their adapted Weibull pdfs (Figure 7.7) didn't shift towards the correct side. Regarding the left outlier cases, the performance of the proposed model can be accepted because RUL predictions can follow the trend of the actual RUL and they are conservative during the whole lifetime of these two specimens. However, based on Figure 7.10 the ANHHSMM cannot provide better prognostics than the NHHSM for all cases. But even the NHHSM's RUL predictions cannot be characterized as accurate enough. As a result the proposed feature, i.e. DIC1, has limited prognostic capabilities.

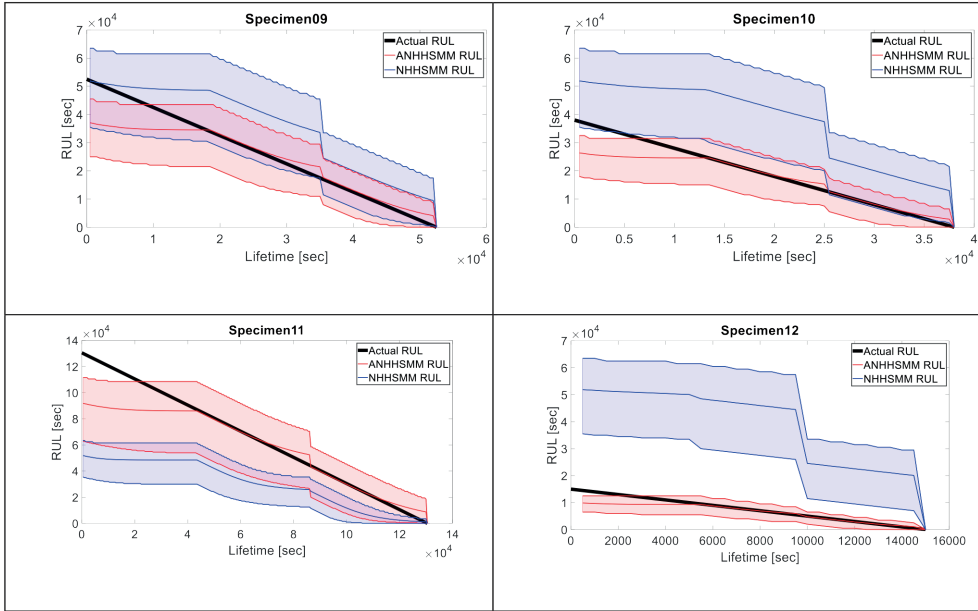


Figure 7.11. DIC2 RUL predictions.

Based on Figure 7.11 the ANHHSMM provides clearly better prognostics in comparison with the NHHSM for all cases.

The outstanding performance of the ANHHSMM utilizing the AE and DIC2 features demonstrates that the proposed adaptive framework has succeeded its objective; the mean ANHHSMM RUL predictions are satisfactorily close to the real RUL predictions and the

confidence intervals contain the real RUL curve during the entire lifetime of the testing specimens. Furthermore, the ANHHSMM can identify at a very early stage an outlier and adapt the RUL predictions in an efficient and accurate way since it succeeds the initial RUL predictions to be closer to the actual values than the NHHSMM's RUL predictions.

7.5. Prognostic performance metrics

Seven prognostic performance metric are utilized in order to conclude which feature can provide the best RUL predictions and to quantify the aforementioned observations. In Figures 7.12-7.19 the results of the performance metrics, defined in Subection 3.3.2, are presented. The optimum values of the prognostic performance metrics are following:

Table 7.4. Optimum values of the suggested prognostic performance metrics.

Precision: minimum value	Monotonicity: minimum value
MSE: minimum value	C_{Em} : minimum value
MAPE: minimum value	CIDC: minimum value
CRA: maximum value	

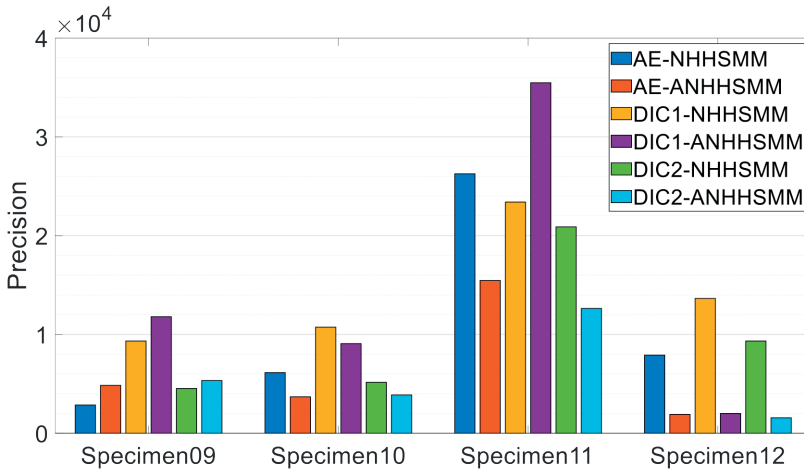


Figure 7.12. Precision prognostic performance metric of each specimen, feature and model.

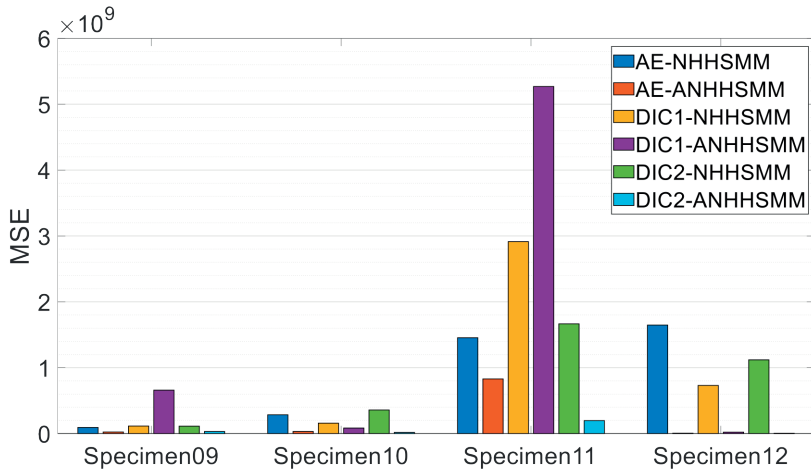


Figure 7.13. MSE prognostic performance metric of each specimen, feature and model.

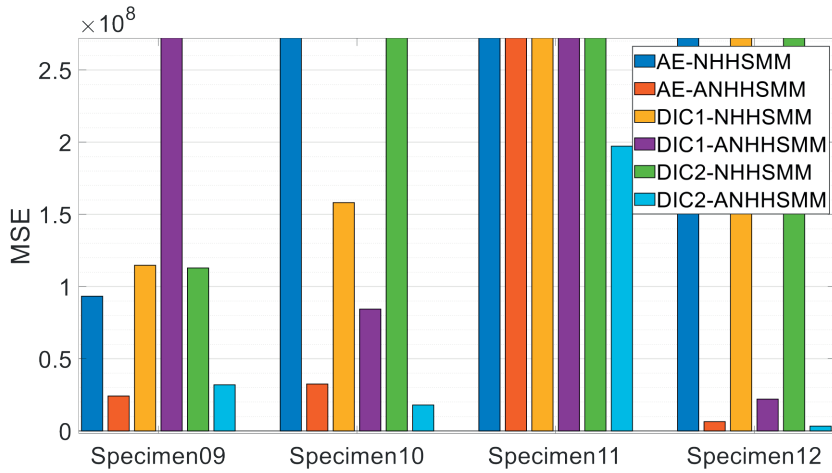


Figure 7.14. Zoomed MSE prognostic performance metric of each specimen, feature and model.

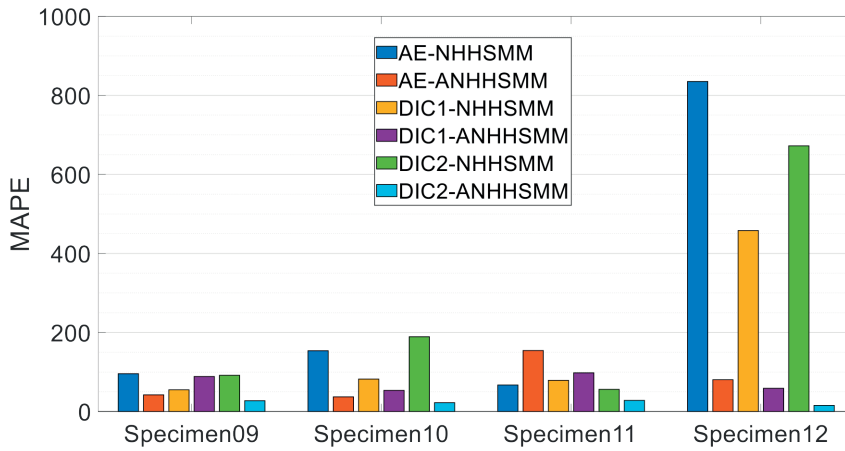


Figure 7.15. MAPE prognostic performance metric of each specimen, feature and model.

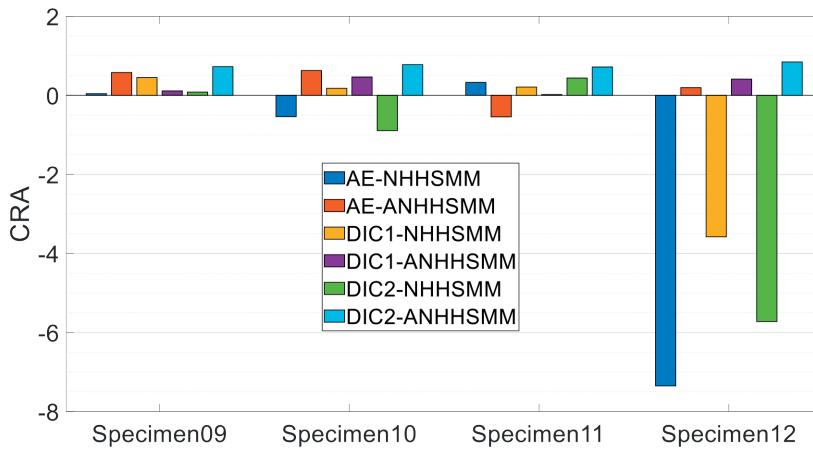


Figure 7.16. CRA prognostic performance metric of each specimen, feature and model.

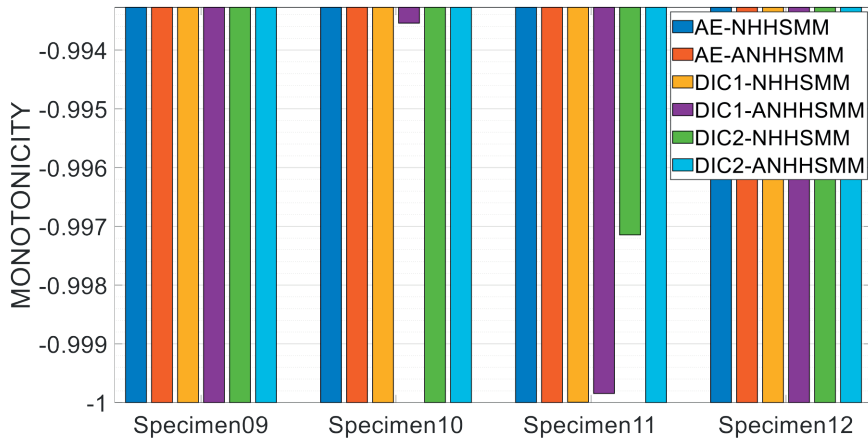


Figure 7.17. Monotonicity prognostic performance metric of each specimen, feature and model.

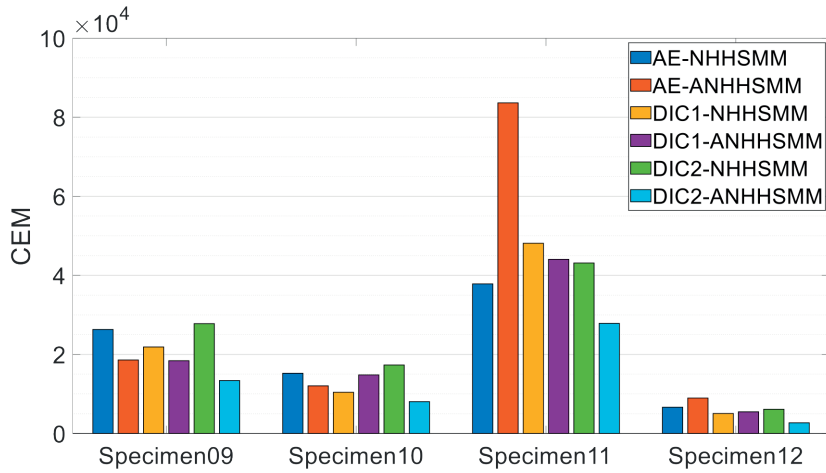


Figure 7.18. C_{EM} prognostic performance metric of each specimen, feature and model.

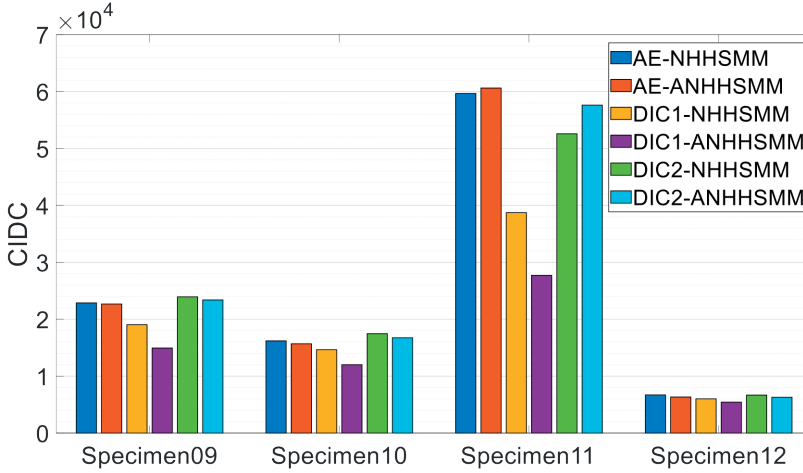


Figure 7.19. CIDC prognostic performance metric of each specimen, feature and model.

Based on these results, it is confirmed that:

- The ANHHSMM provides the best RUL estimations since ANHHSMM's RUL predictions score better than the NHHSMM's RUL predictions in the majority of the prognostic performance metrics.
- The DIC2 feature provides the best RUL predictions since DIC2 RUL predictions score better in prognostic performance metrics. A random example based on Figure 7.12 is given so as to illustrate the ascendance of DIC2 feature. DIC2-ANHHSMM predictions of Specimen12 excel at precision metric since the precision of the DIC2-ANHHSMM RUL predictions are lower than the precision of the AE and DIC1 RUL estimations, similar results can be obtained for the most of the available prognostic performance metrics.

References

- [1] R. Moghaddass and M. J. Zuo, "Multistate degradation and supervised estimation methods for a condition-monitored device," *IIE Trans. (Institute Ind. Eng., vol. 46, no. 2, pp. 131–148, 2014.*
- [2] N. Eleftheroglou and T. Loutas, "Fatigue damage diagnostics and prognostics of composites utilizing structural health monitoring data and stochastic processes," *Struct. Heal. Monit., vol. 15, no. 4, 2016.*

8

Conclusions and Recommendations

8.1. Introduction

This chapter summarises the main conclusions and contributions from each of the interconnected topics studied in this thesis. At the end, it provides some recommendations for further research regarding the topic of prognostics.

8.2. Conclusions

The aim of this thesis was to develop a new adaptive prognostic model that is able to predict more accurately than the current models the RUL of outliers; engineering systems which either under- or outperform. Based on the relevant literature this adaptive model has to be a frequentist DDM in case of composite structures. Furthermore, an adaptive extension of the NHHSMM seems to be very promising in order to predict more accurately the RUL of outlier composite structures.

The first step was to design the adaptive extension of the NHHSMM, i.e. ANHHSMM, and verified its correctness utilizing simulated MC data. Simulated MC data are needed so as to be sure that the model's algorithm does not contain computational bugs since the algorithm consists of thousands of code lines. Furthermore, a case-study was performed in order to validate the efficiency of the new adaptive data-driven model utilizing real data. Open-hole carbon/epoxy specimens were subjected to constant amplitude fatigue loading up to failure while in-situ impact and a drilling defect were used in order to demonstrate unexpected phenomena. AE and DIC techniques were employed so as to record CM data for the training and testing process. In addition, a new data fusion methodology, on a feature-level, was presented utilizing the CM features, i.e. AE, DIC1 and DIC2 features, and three design indexes i.e. monotonicity, prognosability and trendability. Eight specimens were used for training purposes, these specimens were subjected only to fatigue loading. Four specimens were used for testing the proposed adaptive model. Three of them were subjected to fatigue and in-situ impact, and created a left, a right outlier and an inlier case respectively to the training specimens. The last one was subjected just to fatigue loading but created one more left outlier case since it has an artificial drilling defect on it. Furthermore, five prognostic performance metrics, found in literature, were employed and two new were introduced, in order to compare the performance of the RUL predictions.

The main conclusions of the thesis can be listed as follows:

- Monotonicity, prognosability and trendability can be used as feature design properties for combining different CM features (data fusion) so as to involve a new hyper-feature with higher monotonicity, prognosability and trendability index than the initial CM features.
- Prognostic performance metrics should always be used in order to quantify the performance of different prognostic models, even when the difference is self-evident by just observing RUL figures, as in the case-study of this thesis.
- A new data fusion approach was developed. The main objective was to produce a hyper-feature with higher trendability than the trendability of AE and DIC2

features. The main reason for utilizing a data fusion approach was the expectation that a feature with higher trendability index can enhance the prognostic performance. In order to draw conclusions for the above expectation, quantitative and not just qualitative evidences have to be provided. Firstly, the trendability index of the four features are: $Trendability_{AE}=0.78247$, $Trendability_{DIC1}=0.92705$, $Trendability_{DIC2}=0.99971$ and $Trendability_{FUSION}=0.99971$. Secondly, based on the seven prognostic performance metrics the Fusion feature (same prognostics with DIC2 feature) provides better RUL predictions than the AE and DIC1 features, thus the aforementioned expectation seems to be valid. However, the AE feature provides better predictions than the DIC1 feature and at the same time the trendability index of DIC1 is higher than the trendability index of AE. These are two contrasting evidences and as a result it is not valid to conclude that higher trendability leads to more accurate prognostics.

- The AE and DIC2 RUL predictions demonstrate clearly that the ANHHSMM provides better prognostics than the state-of-the-art NHHSMM. Consequently, adapting the NHHSMM's parameters utilizing the MLS diagnostic measure has the potential to predict the RUL of outlier and inlier cases more efficiently and accurately. The above conclusion was verified via the seven proposed prognostic performance metrics. It was observed that the mean RUL predictions by NHHSMM converge to the actual RUL only towards the end of life. On the other hand, mean ANHHSMM RUL predictions converge to the actual RUL from the beginning of the composite specimen's lifetime. Moreover, in all cases as the composite specimen ages the percentile interval for the RUL becomes narrower, that is, the prediction uncertainty decreases since more data become available. Also, the provided ANHHSMM percentile intervals cover the actual RUL in almost all cases. Furthermore, the ANHHSMM RUL predictions are conservative regarding the actual failure time. This is generally better than the case in which the estimated RUL is higher than the actual RUL because underestimating the failure time can cause unexpected failures.
- The NHHSMM performed better than ANHHSMM when the DIC1 data were used. The DIC1 ANHHSMM RUL predictions are too conservative and as a result the estimated failure time is much earlier than the actual one. This undesirable behaviour of the proposed adaptive approach has probably occurred due to the XII ANHHSMM's assumption that dictates the ratios between the training and testing sojourn times of hidden states i and $i+1$ should be constant. This assumption holds for cases that one unexpected phenomenon occurs and it alters the sojourn times proportionally. However, this assumption is not valid in DIC1 case since the unexpected phenomenon has an impact only to the current hidden state. Therefore, the XII assumption is valid when an unexpected event has an impact to the forthcoming hidden states too, not only to the current one. In order to tackle this undesirable behaviour, the impact of an unexpected event to each hidden state has to be identified in real-time. But first it is mandatory to understand the physical meaning of each hidden state so as to identify the impact of an unexpected phenomenon. As a result, the main conclusion is that a hybrid version of the ANHHSMM should be involved so as to tackle the aforementioned limitation.

- The feature extraction process for the strain data was straightforward, as after the determination of the critical specimen's point, the axial strain data was extracted via the DIC technique. The well-established analytical model of Lekhnitskii enhanced the feature performance indicating that mechanics can play an informative role on the feature selection process. In contrast, extensive AE signal processing was performed in order to identify monotonic histories that could describe sufficiently the damage accumulation process, but a potential feature candidate could not be identified. As a result, the solution of normalized cumulative energy, as a feature, was selected, compromising the applicability of real-time implementation. Consequently, the DIC2 feature was characterized as the optimum prognostic performance feature, compare it with the AE and DIC1 feature.
- With reference to the DIC technique two different features, the DIC1 and DIC2, were utilized for prognostic purposes. It should be pointed out that the DIC1 feature can be characterized as the best one in terms of diagnostics performance, since MLS predictions are closer to impact time points than the AE and DIC2 MLS predictions. Also, the DIC1 and DIC2 features provided the worst and the best RUL estimations accordingly, based on the prognostic performance metrics. As a consequence, a feature that provides excellent diagnostic results, might fail to fulfil the prognostics requirements and vice versa. Therefore, a feature extraction process should be always designed based on case-study's requirements, should serve the case study goal and if the output is more than one (diagnostics and prognostics), more feature extraction processes can be designed and used.

8.3. Recommendations

Although this thesis addressed important challenges and limitations of the current prognostic models, there are still challenges and limitations that need to be further addressed.

8.3.1. ANHHSMM's assumptions

As already mentioned, the ANHHSMM provides better prognostics than the state-of-the-art NHHSM. Nevertheless, the applicability of the methodology should be further explored and future work should focus on the improvement of ANHHSMM's capabilities and the relaxation of the assumptions as presented in Chapter 4.

In particular, emphasis should be given in the XII assumption that dictates the ratios between the training and testing sojourn times of hidden states i and $i+1$ should be constant. This assumption holds for cases that one unexpected phenomenon occurs and it alters the sojourn times proportionally. However, this assumption is not valid for cases where this phenomenon is severe enough to force the model to overpass a hidden state and move to the next one, i.e. from hidden state i to $i+2$ or when multiple unexpected phenomena occur over the lifetime of the system where the ratio cannot be constant anymore. In that direction, a new version of the ANHHSMM should allow multi-step transitions too, so as to be possible for example to transit from hidden state i to $i+2$. In addition, as mentioned in the previous subsection, a hybrid version of the ANHHSMM can help to overcome the XII assumption's limitation.

Furthermore, the final state N is not hidden but self-announcing and always corresponds to the failure state. As a result, the last observation of the available training data should be unique dictating a common failure threshold in the training data. However, it is really difficult task to define in every case-study a common failure threshold for the whole training set without normalizing and/or accumulating the training data. Therefore, next ANHHSMM's versions should be capable of modeling the relationship between the failure state and CM data in an indirectly way such as a nonparametric discrete probability distribution. As a result the last row and column of the emission matrix B will not be predefined so as to fulfill the assumption II and the elements of the emission matrix will be estimated via the training CM data.

Finally, in the context of CBM (condition based maintenance) where the entire life cycle of a structure should be considered, when repair actions will be taking place, some engineering properties will be retrieved back –although not to 100%- and thus new versions of the ANHHSMM have to allow backward transitions (right-to-left transitions) too.

8.3.2. Condition monitoring data

In the case-study presented in this thesis, it was not possible to identify any AE feature with high monotonicity and prognosability index and as a result the proposed health indicator is the normalized cumulative energy feature. However, by normalizing the feature with the maximum value, compromises the RUL prediction in real-time, because prior knowledge of the maximum AE energy is not available. In general, extensive signal processing is required in order to identify features, which can describe sufficiently the damage evolution process of composite structures in real time. As a result, a really interesting research topic is to develop a feature extraction framework able to overcome the above challenges. In that direction, data fusion approaches can be used so as to design features that can enhance the prognostic performance and can be used in real-time. These data fusion approaches should take into consideration the studied engineering system, the selected RUL model and an expectation regarding how an ideal feature in terms of prognostics' accuracy should be.

Another issue is that the proposed prognostic approach in this thesis is applicable to a single CM feature. However, it has been long known that various CM techniques have different sensitivities to different composite structures' failure mechanisms. Therefore, it is extremely important to develop a prognostic approach, which can utilize more than one CM feature. In order to achieve that the likelihood function should be expanded so as to take into account more than one features.

Future work should also include data, which are extracted from more representative operating conditions, e.g. variable amplitude fatigue, generic element geometries, so as to get closer to real applications. Additional CM techniques such as distributed optical fiber sensors should be used, as this technique can provide axial strain data, which already has been proven to provide more accurate prognostics, but also this CM technique can be easier utilized in real applications.

8.3.3. Towards hybrid models

In this thesis the initialization process is a user-defined process except the parameter N (number of hidden states). The N is determined by using a simple enumerative approach, the BIC criterion, in order to compare several alternative N numbers and select the optimum

one. However, this initialization approach is subjected to several challenges. For instance, the number of alternative models can be very large, resulting to a very time-consuming process and at the same time there is no guarantee that the final initialization parameters will be the optimal in terms of prognostic performance. Additionally, the initialization approach requires a large amount of data for training and validation, which may not be available for real applications. In order to overcome the above limitations hybrid RUL models should be developed. Hybrid models are able to take into account the physical behaviour of the studied system and as a result it will be possible to define some model's parameters based on their physical meaning, not based on enumerative approaches.

Therefore the advantages of using a hybrid model can be withdrawn as follows:

- The required amount of CM data for training and validation can be reduced since some model's parameters will be defined based on their physical meaning.
- The computational time will be reduced since less parameters will be estimated via the MLE.
- It will enhance the process for selecting the initial prognostic performance parameters.
- Limitations such as the XII ANHHSMM's assumption can be tackled more efficiently.

Acknowledgments

In the beginning of my PhD my intention was to answer all the scientific questions relative to my research topic. However, the truth appears to be quite different. Not only I have more questions than answers but also, my career as researcher these last four years, provoked much more questions about myself. But is this a normal evolution? Probably, an answer can be that a PhD is a tough competition between you and yourself. During a PhD you are fully autonomous to choose how, when and by which means you will accomplish the final defined research objectives. As a result, you have to set some limits to yourself. But this is not a straightforward action. You have to fight with yourself sometimes. But fortunately, you are not alone in that fight; you have people around you, people that you chose and these people are there to help you to understand better your competitor and therefore to set easier these limits. Irony, how can someone else help you to understand better yourself? Therefore, I am feeling that I owe many thanks to these people who helped me to understand better who 'hopefully' Dr. Eleftheroglou was and is.

First of all, Dimitrios Zarouchas, my daily supervisor. Dimitri thank you for your support and interest not only in my professional, but also in my personal life and development. Thank you because you have always been there for me. Sometimes giving me answers or suggestions and sometimes just listen to me, even more important than the first one. Thank you for having a door that was always open. Thank you for the chilling moments. Thank you because you helped me to understand better who I am and ask myself a lot of challenging scientific and personal questions. Σ' ευχαριστώ!

Next, my promotor Professor Rinze Benedictus. Thank you for giving me the chance to do exactly what I was dreaming to realize in my scientific life without setting me any limitation. Thank you for your interest in my research. Thank you also for the trust you placed in me and gave me the freedom to take my own decisions, professional and personal, during the entire course of the PhD. Thank you for your understanding and finally thank you for having a door that was always open to me. Dank u wel!

I would like to thank my second-supervisor, Rene Alderliesten, who was always there when I need him providing me with plenty of constructive ideas. Thank you for your positive-critical influence on my research.

Gemma, thank you for everything. Thank you for all the paperwork you did for me. But not only for that, I owe you many more thanks for all the discussions, for your advices and understanding during the last four years. Thank you Gemmoula!

Special thanks goes of course to my former supervisor and a very good friend, Theodoros Loutas, with whom we shared many precious scientific and personal experiences. Thank you Teo!

My thesis involved a lot of experimental work, which would have been impossible without the help of the 'magicians' Berthil and Cees. Thank you. Also, Julian thank you for your help during the manufacturing process.

Many thanks goes to my colleagues or it is better to say friends that I met the last four years. Many thanks to my crazy office mates (boobs office as we used to call our office), Lucas, Leila, Eirini and Nicolas. Special thanks goes to Eirini since she used to be my partner in sushi-crime! Many thanks goes also to Pedro, Romina, Timo, Ilias and Nikos. Thank you for our discussions and interesting dinners. Thank you Chirag for the 'remote' help. Thank you Niels and Jesse for your help with the Dutch bureaucracy. Thank you John-Alan for helping me with the translation of propositions and this thesis summary.

Many thanks to my 'Dutch parents', Truus and Jaap. Thank you for your love and support.

Last, but most certainly not least, I would like to thank the people that my personal life is totally connected to. Thank you Aris for your endless support and encouragement. Thank you for your understanding during the difficult writing times. Thank you because your wide smile made this effort easier. Besides, I would like to thank Brioché, my dog, as he was always next to me during the writing process. He was always there trying to help me with his own unique way. Thank you Brioché! Finally, many thanks to my family, Thanos, Maria and Dimitris. Thank you for your unlimited love and support. Thank you because in that trip you were not fellow travelers but you were the vehicle that allowed me to travel, you have always my love. Σας ευχαριστώ για την απεριόριστη ανιδιοτελή αγάπη και υποστήριξη που μου παρέχετε απλόχερα σε κάθε βήμα της ζωής μου. Αυτό που ήμουν, είμαι και θα γίνω πηγάζει από εσάς τους τρεις. Σας αγαπώ!

Curriculum Vitae

Nikolaos Eleftheroglou

The author was born in Aspra Spitia, Greece, on the 14th of August of 1992. In June 2010 he graduated *cum laude* from the Aspra Spitia High School. In September that year, he enrolled in Department of Mechanical Engineering and Aeronautics, School of Engineering, University of Patras, where he obtained a Diploma in Mechanical Engineering and Aeronautics *cum laude* in 2015.

In September 2015 Delft University of Technology awarded the author a grant to fund the PhD project that resulted in this thesis. The author started this project at Delft University of Technology in February 2016, under supervision of Prof. Dr. Ir. R. Benedictus as promotor, Dr. D. Zarouchas as daily supervisor and Dr. Ir. R.C. Alderliesten as second supervisor.

List of publications

Journal papers

- [1] **N. Eleftheroglou**, and T. Loutas, “Fatigue damage diagnostics and prognostics of composites utilizing structural health monitoring data and stochastic processes,” *Struct. Heal. Monit.*, vol. 15, no. 4, 2016.
- [2] **N. Eleftheroglou**, D. S. Zarouchas, T. H. Loutas, R. C. Alderliesten, and R. Benedictus, “Online remaining fatigue life prognosis for composite materials based on strain data and stochastic modeling,” *Key Eng. Mater.*, vol. 713, 2016.
- [3] T. Loutas, **N. Eleftheroglou**, and D. Zarouchas, “A data-driven probabilistic framework towards the in-situ prognostics of fatigue life of composites based on acoustic emission data,” *Compos. Struct.*, vol. 161, 2017.
- [4] **N. Eleftheroglou**, D. Zarouchas, T. Loutas, R. Alderliesten, and R. Benedictus, “Structural health monitoring data fusion for in-situ life prognosis of composite structures,” *Reliab. Eng. Syst. Saf.*, vol. 178, 2018.
- [5] T. Loutas, **N. Eleftheroglou**, G. Georgoulas, P. Loukopoulos, D. Mba, and I. Bennett, “Valve Failure Prognostics In Reciprocating Compressors Utilizing Temperature Measurements, PCA-based Data Fusion And Probabilistic Algorithms,” *IEEE Trans. Ind. Electron.*, vol. PP, no. c, pp. 1–1, 2019.
- [6] **N. Eleftheroglou**, S.S. Mansouri, T.H. Loutas, P. Karvelis, G. Georgoulas, G. Nikolakopoulos, and D. Zarouchas, “Intelligent data-driven prognostic methodologies for the real-time remaining useful life until the end-of-discharge estimation of the Lithium-Polymer batteries of unmanned aerial vehicles with uncertainty quantification,” *Appl. Energy*, vol. 254, no. July, p. 113677, 2019.
- [7] **N. Eleftheroglou**, D. Zarouchas, and R. Benedictus “An adaptive probabilistic data-driven methodology for prognosis of the fatigue life of composite structures,” *Compos. Struct.*, vol. 245, 2020.

Conference papers

- [1] **N. Eleftheroglou**, and T.H. Loutas, “Utilizing AE data and Stochastic Modeling Towards Fatigue damage Diagnostics and Prognostics of composites,” *Acoustic Emission Working Group-58*, Drexel, Philadelphia, USA; 05/2016.
- [2] **N. Eleftheroglou**, D.S. Zarouchas, and T.H. Loutas, “In-situ fatigue damage assessment of carbon-fibre reinforced polymer structures using advanced experimental technique,” *17th European Conference on Composite Materials*, Munich, Germany; 06/2016.

[3] D.S. Zarouchas, and **N.Eleftheroglou**, “Experimental investigation on the effect of creep on the damage evolution of CFRP structures during fatigue loading,” 17th International Conference on Experimental Mechanics, Rhodes, Greece; 06/2016.

[4] T.H. Loutas, and **N. Eleftheroglou**, “A novel approach towards fatigue damage prognostics of composite materials utilizing SHM data and stochastic degradation modeling,” European Workshop 8th on Structural Health Monitoring, Bilbao, Spain; 07/2016.

[5] **N. Eleftheroglou**, D.S. Zarouchas, T.H. Loutas, R.C. Alderliesten, and R. Benedictus, “Online remaining fatigue life prognosis for composite materials based on strain data and stochastic modeling,” 15th International Conference on Fracture and Damage Mechanics, Alicante, Spain; 09/2016

[6] **N. Eleftheroglou**, D.S. Zarouchas, T.H. Loutas, R.C. Alderliesten, and R. Benedictus, “Online Remaining Useful Life Prognosis for Composite Materials Based on Acoustic Emission and Strain Data,” 11th International Workshop on Structural Health Monitoring 2017, Stanford, USA; 09/2017.

[7] **N. Eleftheroglou**, D.S. Zarouchas, T.H. Loutas, R.C. Alderliesten, and R. Benedictus, “Prognostics of composite structures utilizing structural health monitoring data fusion,” European Workshop 9th on Structural Health Monitoring, Manchester, UK; 07/2018.

[8] **N. Eleftheroglou**, D.S. Zarouchas, and R. Benedictus, “Extreme Prognostics for Remaining Useful Life Analysis of Composite Structures,” 10th Annual Conference of the Prognostics and Health Management Society, Philadelphia, USA; 09/2018.

[9] **N. Eleftheroglou**, D. Zarouchas, T.H. Loutas, S.S. Mansouri, G. Georgoulas, P. Karvelis, G. Nikolakopoulos, and R. Benedictus, “Real time Diagnostics and Prognostics of UAV Lithium-Polymer Batteries,” 11th Annual Conference of the Prognostics and Health Management Society, Scottsdale, USA; 09/2019.

Book chapters

[1] **N. Eleftheroglou**, T.H. Loutas, and S. Malefaki, “Stochastic modeling of fatigue damage in composite materials via Non Homogeneous Hidden Semi Markov Processes,” STATISTICAL, STOCHASTIC AND DATA ANALYSIS METHODS AND APPLICATIONS, ISAST; 2015.

[2] D. Zarouchas, and **N. Eleftheroglou**, “In-situ fatigue damage analysis and prognostics of composite structures based on health monitoring data,” FATIGUE LIFE PREDICTION OF COMPOSITES AND COMPOSITES STRUCTURES, SECOND EDITION, Matthew Deans; 2020.

Invited seminars

[1] **N. Eleftheroglou**, “Prognostics for Remaining Useful Life Analysis of Composite Structures,” Drexel, Philadelphia, USA; 09/2018.

